SAND99-1886J

Uncertainty and Sensitivity Analysis for Two-Phase Flow in the Vicinity of the Repository in the 1996 Performance Assessment for the Waste Isolation Pilot Plant: Disturbed Conditions

J.C. Helton[a], J.E. Bean[b], K. Economy[c], J.W. Garner[d], R.J. MacKinnon[e], J. Miller[e], J.D. Schreiber[d] and P. Vaughn[e]

[a]Department of Mathematics, Arizona State University, Tempe, AZ 85287; [b]New Mexico Engineering Research Institute, Albuquerque, NM 87106; [c]GRAM, Inc., Albuquerque, NM 87112; [d]Piru Associates, Albuquerque, NM 87106; [e]Sandia National Laboratories, Albuquerque, NM 87185

Abstract

Uncertainty and sensitivity analysis results obtained in the 1996 performance assessment (PA) for the Waste Isolation Pilot Plant (WIPP) are presented for two-phase flow in the vicinity of the repository under disturbed conditions resulting from drilling intrusions. Techniques based on Latin hypercube sampling, examination of scatterplots, stepwise regression analysis, partial correlation analysis and rank transformations are used to investigate brine inflow, gas generation, repository pressure, brine saturation, and brine and gas outflow. Of the variables under study, repository pressure and brine flow from the repository to the Culebra Dolomite are potentially the most important in PA for the WIPP. Subsequent to a drilling intrusion, repository pressure was dominated by borehole permeability and generally below the level (i.e., 8 MPa) that could potentially produce spallings and direct brine releases. Brine flow from the repository to the Culebra Dolomite tended to be small or nonexistent, with its occurrence and size also dominated by borehole permeability.

Key Words: BRAGFLO, compliance certification application, disturbed conditions, epistemic uncertainty, Latin hypercube sampling, performance assessment, radioactive waste, sensitivity analysis, subjective uncertainty, transuranic waste, two-phase flow, uncertainty analysis, Waste Isolation Pilot Plant.

Please send page proof to:

Jon C. Helton
Department 6848, MS 0779
Sandia National Laboratories
Albuquerque, NM 87185-0779, USA
Phone: 505-284-4808
Fax: 505-844-2348
email: jchelto@sandia.gov

DISCLAIMER

DISCLAIMER

Portions of this document may be illegible in electronic image products. Images are produced from the best available original document.

1. Introduction

Uncertainty and sensitivity analysis results for fluid flow in the vicinity of the repository under disturbed conditions obtained as part of the 1996 performance assessment (PA) for the Waste Isolation Pilot Plant (WIPP) are presented. A preceding paper presents results for undisturbed conditions.[1]

The results under study were calculated with the BRAGFLO program[2] for the three replicated samples (i.e., R1, R2, R3) indicated in Eq. (7) of Ref. 3. In particular, results for the following cases in Table 6 of Ref. 4 will be presented: an E1 intrusion at 1000 yr, an E2 intrusion at 1000 yr, and an E2E1 intrusion with the E2 intrusion at 800 yr and the E1 intrusion at 2000 yr. In the preceding, the designation E1 refers to a single drilling intrusion through the repository that penetrates pressurized brine in the Castile Formation (Fm); the designation E2 refers to a single drilling intrusion through the repository that does not penetrate pressurized brine in the Castile Fm; and the designation E2E1 refers to two drilling intrusions through the repository, with the first and second intrusions not penetrating and penetrating pressurized brine in the Castile Fm, respectively. Calculations were also performed for E1 and E2 intrusions at 350 yr (Table 6, Ref. 4). However, as the results for fluid flow in the vicinity of the repository for intrusions at 350 yr are similar to those for intrusions at 1000 yr, the results for intrusions at 350 yr will not be presented.

The following topics related to conditions in the repository are considered: brine inflow (Sect. 2), gas generation (Sect. 3), pressure (Sect. 4), saturation (Sect. 5), brine and gas flow in an intruding borehole (Sect. 6), behavior of brine pocket (Sect. 7), and behavior of E2E1 intrusions (Sect. 8). As in the presentation for undisturbed conditions,[1] a number of specific results calculated by BRAGFLO are examined with techniques based on examination of scatterplots, partial correlation coefficients, and stepwise regression analysis (Sect. 3.5, Ref. 5). The analyses were performed with the STEPWISE[6, 7] and PCCSRC[8, 9] programs with rank-transformed data.[10] The specific BRAGFLO results considered are listed in Table 1 of this presentation and Table 1 of Ref. 1, which can be used to obtain exact definitions of the individual variables under consideration.

As in the analyses for undisturbed conditions,[1] the sensitivity analysis results presented in this article are based on all 300 observations (i.e., replicates R1, R2 and R3 are pooled for the performance of sensitivity analyses with scatterplots, correlation coefficients and stepwise regression analysis; see Sect. 8, Ref 3. Similarly, summaries of uncertainty based on box plots also use all 300 observations. In contrast, distributions of time-dependent results are typically shown for only replicate R1 to avoid the presentation of plots with so many individual curves that they are unreadable. However, mean and percentile curves are obtained from all 300 observations. Descriptions of the individual independent (i.e., sampled) variables in the sensitivity analyses are given in Table 1 of Ref. 3. As in the sensitivity analyses for undisturbed conditions, the variables *ANHCOMP* and *HALCOMP* are not used in the

calculation of partial correlation coefficients and regression models due to the −0.99 rank correlations imposed on the variable pairs (*ANHCOMP*, *ANHPRM*) and (*HALCOMP*, *HALPRM*) (Sect. 7.2, Ref. 11).

The results contained in this presentation were obtained in support of the U.S. Department of Energy's (DOE's) compliance certification application (CCA) for the WIPP[12] and are based on material contained in Chapt. 8 of Ref. 11.

2. Disturbed Conditions: Brine Inflow for E1 and E2 Intrusions

For undisturbed (i.e., E0) conditions, the two main pathways by which brine enters the repository are flow from the Salado Fm through the anhydrite marker beds and drainage from the disturbed rock zone (DRZ) (Sect. 2, Ref. 1). For E2 intrusions, an additional pathway is provided by brine flow down the intruding borehole from overlying formations; for E1 intrusions, two additional pathways are provided by brine flow down the intruding borehole from overlying formations and brine flow up the borehole from a pressurized brine pocket in the Castile Fm.

For brine inflow from the marker beds, E0, E1 and E2 conditions produce similar results (Fig. 1, Ref. 1; Fig. 1), with the inflows for E1 and E2 intrusions tending to be somewhat larger than the inflows for E0 conditions (Fig. 2). This difference results because E1 and E2 intrusions result in lower repository pressures (Sect. 4), which in turn result in reduced resistance to brine flow toward the repository and hence greater brine flow out of the marker beds. As indicated by partial rank correlation coefficients (PRCCs), the dominant variables affecting brine flow from the marker beds are anhydrite permeability (*ANHPRM*), halite permeability (*HALPRM*), and microbial gas generation flag (*WMICDFLG*) (Fig. 1). The positive effects for *ANHPRM* and *HALPRM* result from reducing resistance to flow in the anhydrite and halite, respectively. The negative effect for *WMICDFLG* results from increasing pressure in the repository before the drilling intrusion at 1000 yr and thus increasing resistance to flow out of the marker beds. A positive effect is also indicated for borehole permeability (*BHPRM*) after the E2 intrusion, with this effect resulting from reduced pressure in the repository and hence reduced resistance to flow out of the marker beds (Sect. 4).

Stepwise regression provides another way to investigate the effects of uncertain variables on brine flow from the marker beds (Table 2). The first regression, E0: 0 - 1000 yr, in Table 2 is for cumulative brine flow out of the marker beds under undisturbed conditions in the first 1000 yr after repository closure, which is also the flow that occurs over this time period for E1 and E2 intrusions at 1000 yr. The dominant variable is *ANHPRM*, with brine flow out of the marker beds increasing as *ANHPRM* increases because of reduced resistance to flow. In addition, positive effects are indicated for *HALPRM* and initial Salado pressure (*SALPRES*), with increasing values for *HALPRM* decreasing resistance to brine flow out of the halite into the marker beds and increasing values for *SALPRES* increasing the pressure gradient towards the repository. Negative effects are indicated for *WMICDFLG*, increase in brine saturation of waste due to capillary forces (*WASTWICK*), gas generation rate due to corrosion under inundated conditions (*WGRCOR*), and gas generation rate due to microbial degradation of cellulose under inundated

conditions (*WGRMICI*) due to the role that these variables play in increasing gas generation and hence pressure in the repository (Sect. 4, Ref. 1).

Regression results for cumulative brine inflow from 1000 to 10,000 yr after a drilling intrusion at 1000 yr are presented under the headings E2: 1000 - 10,000 yr and E1: 1000 - 10,000 yr for E2 and E1 intrusions, respectively. For both intrusion types, *ANHPRM, SALPRES* and *HALPRM* have similar effects to those observed for undisturbed conditions, although *ANHPRM* can now account for more of the uncertainty (i.e., $R^2 = 0.81$, 0.80 for E2, E1: 1000 - 10,000 yr versus $R^2 = 0.58$ for E0: 0 - 1000 yr) in brine inflow due to the reduction in repository pressure resulting from the venting of gas through the borehole. Consistent with this, *BHPRM* has a positive effect on brine inflow from the marker beds for both intrusion types because increasing *BHPRM* tends to increase gas flow up the borehole and thus reduce repository pressure. Small negative effects are indicated for *WMICDFLG* and brine pocket compressibility (*BPCOMP*) for the E2 and E1 intrusions, respectively, with both variables tending to increase pressure in the repository and thus reduce brine inflow from the marker beds.

Results for the entire 10,000 yr period (i.e., E2: 0 - 10,000 yr, E1: 0 - 10,000 yr in Table 2) are consistent with those previously observed for the periods 0 - 1000 yr and 1000 - 10,000 yr. In particular, the dominant variable is *ANHPRM*, with small positive effects indicated for *BHPRM, HALPRM* and *SALPRES*, and small negative effects indicated for *WMICDFLG, WGRCOR* and *BPCOMP*.

The last three regressions in Table 2 are for the differences between brine inflow for E2 and E0, E1 and E0, and E2 and E1 intrusions (see Fig. 2 for scatterplots of the flows associated with E0, E1 and E2 intrusions). The differences in brine inflows between E2 and E1 intrusions and undisturbed (i.e., E0) conditions are dominated by *ANHPRM*, with the difference between flows for disturbed and undisturbed conditions tending to increase as *ANHPRM* increases. This effect occurs because the potential of higher values of *ANHPRM* to allow more brine inflow to the repository is realized to a greater extent under the lower repository pressure conditions associated with E1 and E2 intrusions. Additional small effects are indicated for a number of variables. The difference between E2 and E1 flows is dominated by *BPCOMP*, with this difference tending to increase as *BPCOMP* increases. This behavior occurs because increasing *BPCOMP* increases brine inflow from the brine pocket to the repository and thus pressure in the repository, with the result that brine inflow from the marker beds is reduced. Smaller effects are indicated for several additional variables. However, the differences between brine inflows from the marker beds for E1 and E2 intrusions are rather small (Fig. 2).

A more detailed summary of brine inflow can be obtained by examining the flows associated with individual marker beds. The flows from the individual marker beds are similar as suggested by the comparison of total flow in Fig. 2, with the flows for E2 intrusions shown in Fig. 3 and the corresponding flows for E1 intrusions shown in Fig. 8.2.3 of Ref. 11. The largest brine inflows from the anhydrite marker beds tend to come from Marker Bed 139. In general, the patterns for E1 and E2 intrusion are similar to those already observed for E0 conditions (Fig. 2, Ref. 1),

although the flows for disturbed conditions tend to be somewhat higher due to reduced repository pressures as previously discussed. The regression analyses for brine flows out of the individual marker beds are consistent with previously presented results (Table 2, Ref. 1; Table 2) and indicate that the uncertainty in these flows is dominated by *ANHPRM*, *HALPRM*, *WMICDFLG* and *BHPRM* (Tables 8.2.2, 8.2.3, Ref. 11).

Unlike brine flow from the marker beds, there is often considerable difference in cumulative brine flow into the repository for E0, E1 and E2 conditions (Fig. 1, Ref. 1; Fig. 4). For the E2 intrusion, the cumulative brine inflow increases relative to that observed for undisturbed conditions due to brine flow down the intruding borehole (Fig. 5). Due to the assumption of a borehole plug at the Rustler/Salado interface with a 200 yr life expectancy (Table 8, Ref. 2), this flow does not begin until 200 yr after the drilling intrusion. For the E1 intrusion, the cumulative brine inflow increases relative to that observed for undisturbed conditions due to both brine flow down the intruding borehole (Fig. 5) and brine flow up the intruding borehole from the brine pocket (Fig. 6). The sharp increases in cumulative brine flow for E1 intrusions (Figs. 4, 6) take place during the 200 yr period (i.e., from 1000 to 1200 yr) during which an open borehole is assumed to exist between the brine pocket and the repository (Table 8, Ref. 2). In the computational implementation of the analysis, this section of the borehole is assigned a permeability of 10^{-9} m^2. After 1200 yr, the effects of flow down the borehole are also apparent for E1 intrusions (Figs. 4, 5).

Prior to 1000 yr, the sensitivity analysis results for cumulative brine flow into the repository for E0, E1 and E2 conditions are the same (Fig. 3, Ref. 1; Fig. 4), with halite porosity (*HALPOR*) being the dominant variable. After 1000 yr, *HALPOR* is gradually exceeded by *BHPRM* in importance for disturbed conditions due to the role of *BHPRM* in controlling brine flow in the borehole. This flow takes place both down the borehole from overlying formations (Fig. 5) and, for the E1 intrusion, up the borehole from the brine pocket (Fig. 6). For flow down the borehole into the repository, *BHPRM* is the dominant variable for both E1 and E2 intrusions (Fig. 5), with this effect resulting because increasing *BHPRM* reduces resistance to flow in the borehole. A brief negative effect is indicated for *WMICDFLG* shortly after 1200 yr (Fig. 5) due to the obstruction of brine inflow by the rapid venting of gas when the repository is at high pressure. As a reminder, *WMICDFLG* is the dominant variable with respect to the uncertainty in repository pressure under undisturbed conditions (Fig. 18, Table 6, Ref. 1).

The variable *WMICDFLG* also shows a negative effect on total brine inflow to the repository after 1200 yr for the E1 intrusion that is not present for the E2 intrusion (Fig. 4). This behavior results because large flows of brine can take place from the brine pocket to the repository for an E1 intrusion from 1000 to 1200 yr, during which period an open borehole is assumed to connect the brine pocket and the repository (Fig. 4). However, this flow will not take place when the repository pressure is too high (Fig. 7). Thus, the negative effect for *WMICDFLG* again results from its dominant role in determining the uncertainty in repository pressure. This effect results in the negative PRCC for *WMICDFLG* for cumulative brine flow from the brine pocket (Fig. 6) and thus in the negative PRCC for cumulative brine flow into the repository (Fig. 4). In addition to the negative effect of *WMICDFLG*, the variables *BPCOMP* and *BHPRM* have positive effects on cumulative brine flow from the brine pocket to the repository.

Specifically, increasing *BPCOMP* increases the amount of brine that leaves the brine pocket for each unit drop in pressure, and increasing *BHPRM* both reduces the pressure in the repository and reduces resistance to flow between the brine pocket and the repository.

Stepwise regression analysis provides an alternative to the sensitivity analysis based on PRCCs in Figs. 4 - 5 (Table 3). Under undisturbed conditions from 0 to 1000 yr, brine inflow to the repository is dominated by *HALPOR*. After an E2 intrusion at 1000 yr, the dominant variable is *BHPRM*, with cumulative brine inflow increasing as *BHPRM* increases. This effect happens for two reasons. First, increasing *BHPRM* reduces repository pressure and thus allows more brine inflow from the marker beds. Second, increasing *BHPRM* allows more brine to flow down the borehole and into the repository. After *BHPRM*, positive effects are indicated for *ANHPRM*, *HALPOR* and *HALPRM*, with these variables increasing brine flow from the marker beds, DRZ and Salado halite, respectively. Finally, a small negative effect is indicated for the residual brine saturation of the waste (*WRBRNSAT*) and results because increasing *WRBRNSAT* decreases brine mobility within the repository and thus decreases the inflow of brine to the repository to replace brine that has moved to a new location. The E2 results for 0 to 10,000 yr are similar to those for 1000 to 10,000 yr with the exception that *HALPOR* is more important from 0 to 10,000 yr than from 1000 to 10,000 yr due to its influence on brine drainage from the DRZ at early times.

After an E1 intrusion at 1000 yr, the dominant variable is again *BHPRM* for reasons similar to those for the E2 intrusion. Further, brine can also flow into the repository from the brine pocket after an E1 intrusion, with the result that *BPCOMP*, brine pocket volume (*BPVOL*) and brine pocket initial pressure (*BPINTPRS*) appear in the regression model with positive coefficients. Of these, *BPCOMP* is the most important. A positive effect is also indicated for *ANHPRM* because of its role in controlling brine flow from the marker beds, and negative effects are indicated for *WMICDFLG* and *WGRCOR* because of their role in controlling repository pressure. As for the E2 intrusion, the results for 0 to 10,000 yr for the E1 intrusion are similar to those for 1000 to 10,000 yr, with the same exception that *HALPOR* is more important from 0 to 10,000 yr than from 1000 to 10,000 yr.

The final regressions in Table 3 are for the differences between brine inflow to the repository for E2 and E0, E1 and E0, and E1 and E2 intrusions. The differences between E2 and E1 intrusions and undisturbed (i.e., E0) conditions are dominated by *BHPRM* because increasing *BHPRM* reduces pressure in the repository and resistance to brine flow in the borehole. For the E2 intrusion, the difference also increases as *ANHPRM*, *WMICDFLG*, *HALPRM*, *WGRCOR* and *WASTWICK* increase. The positive effects for *ANHPRM* and *HALPRM* result from increasing flow into the repository from the marker beds after the intrusion. The positive effects for *WMICDFLG*, *WGRCOR* and *WASTWICK* result from increasing repository pressure and thus reducing brine inflow from the marker beds under undisturbed conditions. For the E1 intrusion, the difference also increases as *BPCOMP*, *BPVOL*, *BPINTPRS* and *ANHPRM* increase and decreases as *WMICDFLG* increases. The positive effects for *BPCOMP*, *BPVOL* and *BPINTPRS* result from increasing brine flow from the brine pocket, and the negative effect for *WMICDFLG* results from decreasing flow from the brine pocket between 1000 and 1200 yr when an open borehole

exists beneath the repository (Fig. 7). The positive effect for *ANHPRM* results from increased flow out of the marker beds due to reduced pressure in the repository after an E1 pressure.

The dominant variable in determining the difference in brine flow into the repository for E1 and E2 intrusions is *BPCOMP*, with this difference tending to increase as *BPCOMP* increases. In addition, negative effects are indicated for *WMICDFLG*, *BHPRM* and *WASTWICK*, and positive effects are indicated for *BPINTPRS* and *BPVOL*. The negative effects for *WMICDFLG* and *WASTWICK* result from increasing repository pressure and thus reducing flow from the brine pocket between 1000 and 1200 yr (Fig. 7). The negative effect for *BHPRM* results because little brine flow down the borehole occurs for small values of *BHPRM*, in which case brine flow from the brine pocket dominates the difference in flows between E1 and E2 intrusions; at large values of *BHPRM*, so much brine flows down the borehole that the repository saturates and rises to hydrostatic pressure, which reduces brine inflow from the brine pocket (see Sect. 4 for additional discussion). The positive effects for *BPINTPRS* and *BPVOL* result from their role in increasing flow from the brine pocket. However, the final regression model has an R^2 value of only 0.39. Thus, the examination of scatterplots is advisable to obtain a better feeling for the processes involved in determining this difference (Fig. 8). The dominant roles played by *BPCOMP* and *BHPRM* are clearly indicated by the scatterplots in Fig. 8. The primary differences in brine inflow to the repository for undisturbed (i.e., E0) and disturbed (i.e., E1, E2) conditions derive from brine flow in the intruding borehole. For the E2 intrusion, flow down the borehole into the repository is dominated by *BHPRM* (Table 4, Fig. 9). Similarly, brine flow down the borehole for an E1 intrusion is also dominated by *BHPRM*, although increasing values for *BPCOMP* tend to decrease the amount of flow down the borehole (Table 4; Fig. 8.2.10, Ref. 11) by increasing the amount of repository pore volume that will be filled by brine from the brine pocket.

The difference in flow down the borehole for E2 and E1 intrusions is dominated by *BHPRM* and *BPCOMP* (Table 4, Fig. 10). In general, E2 intrusions tend to have more flow down the borehole than E1 intrusions due to the absence of flow from the brine pocket. The most important variable with respect to flow from the brine pocket is *BPCOMP*, with the flow tending to increase as *BPCOMP* increases (Table 4, Fig. 11). As a result, increasing *BPCOMP* tends to increase the difference between brine flow down the borehole for E2 and E1 intrusions.

3. Disturbed Conditions: Gas Generation for E1 and E2 Intrusions

As most of the cellulose is consumed by microbial action by 1000 yr for undisturbed conditions (Fig. 8, Ref. 1), there is not a significant difference between gas generation due to microbial degradation under disturbed and undisturbed conditions. However, disturbed conditions result in greater gas generation from corrosion due to the increased amount of brine entering the repository (Figs. 12, 13).

Gas generation due to corrosion for E1 and E2 intrusions is dominated by *WGRCOR*, *WASTWICK*, *HALPOR* and *BHPRM*, with gas generation tending to increase as each of these variables increases (Fig. 12). The positive

effect for *WGRCOR* results from increasing the rate at which steel is consumed by corrosion, and the positive effects for *WASTWICK*, *HALPOR* and *BHPRM* result from increasing the amount of brine available for the corrosion process. Similar results were obtained in the PRCC analysis for gas generation under undisturbed conditions except that *BHPRM* was not a relevant variable (Fig. 11, Ref. 1).

Similar results were also obtained in stepwise regression analyses for total gas generation due to corrosion over 10,000 yr for E1 and E2 intrusions (Table 5). For both intrusion modes, the three dominant variables are *HALPOR*, *WGRCOR* and *BHPRM*, with smaller effects indicated for several additional variables. For perspective, scatterplots for *HALPOR* and *WGRCOR* for the E2 intrusion are shown in Fig. 14.

More gas is produced by E1 and E2 intrusions than for E0 (i.e., undisturbed) conditions; further, sometimes the amount of gas produced under E1 conditions exceeds that produced under E2 conditions and sometimes the reverse is true (Fig. 13). The dominant variables in determining the difference in the amount of gas produced under E1 or E2 conditions and the amount of gas produced under E0 conditions are *BHPRM* and *WGRCOR*, with this difference tending to increase as each of these variables increases. The positive effect for *BHPRM* results from increasing the amount of brine entering the repository, and the positive effect for *WGRCOR* results from increasing the rate at which this brine is consumed by corrosion. Smaller effects are also indicated for several additional variables. For the E2 intrusions, the difference also tends to increase as *ANHPRM* and *WMICDFLG* increase because increasing *ANHPRM* allows more brine to flow into the repository under the decreased pressures associated with the E2 intrusion and increasing *WMICDFLG* elevates repository pressure under E0 conditions and thus tends to reduce the amount of brine flowing into the repository. For the E1 intrusion, increasing *BPCOMP* and *BPINTPRS* increases the amount of brine flowing into the repository from the brine pocket, increasing *HALPOR* makes it less likely that corrosion will be brine limited under E0 conditions, and increasing *WMICDFLG* tends to exclude brine under E0 conditions.

The first three variables selected in the regression analysis for the difference between gas generation due to corrosion for E1 and E2 intrusions are *BPCOMP*, *BHPRM* and *WMICDFLG*, with this difference tending to increase as *BPCOMP* increases and tending to decrease as *BHPRM* and *WMICDFLG* increase (Table 5). The positive effect for *BPCOMP* results from allowing more brine flow from the brine pocket to the repository for E1 intrusions; the negative effect for *BHPRM* results from allowing more brine flow into the repository from overlying formations for E2 intrusions, and the negative effect for *WMICDFLG* results from reducing brine flow from the brine pocket to the repository during the 200 yr period immediately following an E1 intrusion in which an open borehole is assumed to exist between the brine pocket and the repository (Fig. 7). After *BPCOMP*, *BHPRM* and *WMICDFLG*, the regression model selects an additional 6 variables. However, the final regression model has an R^2 of only 0.36, which indicates a rather poor fit to the data. In such cases, an examination of scatterplots is often informative (Fig. 15).

The scatterplots in Fig. 15 show patterns involving *BPCOMP* and *BHPRM* are consistent with the signs of the regression coefficients in Table 5. In particular, the difference in gas generation for E1 and E2 conditions tends to increase as *BPCOMP* increases and to decrease as *BHPRM* increases. However, *BHPRM* shows a complex pattern with the difference only being affected by the largest values of *BHPRM*. This pattern cannot be captured by the linear regression techniques in use, which results in a low R^2 value for the final regression model. As discussed in Sect. 4, the indicated effect for *BHPRM* results from the tendency of the intruded waste panel to fill with brine for large values of *BHPRM*.

Due to the effects of corrosion, total gas generation for E1 and E2 intrusions is also elevated relative to that observed for undisturbed conditions (Fig. 10, Ref. 1; Figs. 16, 17). Now, *WMICDFLG* appears as an important variable (Fig. 16, Table 5) in addition to *WGRCOR*, *WASTWICK*, *HALPOR* and *BHPRM*, which were also identified when only gas generation due to corrosion was considered (Fig. 12, Table 5). As previously discussed, *WMICDFLG* controls the amount of gas generated by the microbial degradation of cellulose.

The effects of the drilling intrusion are more apparent when gas generation in the intruded panel and the rest of the repository are compared. Specifically, the intruded panel often has its entire steel inventory consumed by corrosion (Fig. 18), which does not occur for the remainder of the repository in intrusion scenarios (Fig. 18) or for the unintruded repository (Fig. 15, Ref. 1).

There is a linear relationship between the amount of steel consumed by corrosion and the amount of gas generated (Fig. 14, Ref. 1). As a result, the same variables that are identified as affecting the amount of gas generated by corrosion (i.e., *WGRCOR*, *WASTWICK*, *HALPOR*, *BHPRM* in Fig. 12) are also identified as affecting the amount of steel remaining in the upper and lower waste panels (Fig. 18). Because the fraction of steel remaining rather than the fraction of steel consumed by corrosion appears in Fig. 18, the signs on the PRCCs in this figure are reversed from the signs in Fig. 12.

Stepwise regression analysis provides a supplement to the sensitivity results based on PRCCs in Figs. 18 (Table 6). The dependent variables in Table 6 are fractions of steel consumed by corrosion under different sets of conditions; regressions for amounts of gas generated by corrosion would produce the same results. For the first 1000 yr in both the upper and lower waste panels, the dominant variable is *WGRCOR*, with the fraction of steel consumed tending to increase as *WGRCOR* increases. In addition, positive effects are indicated for *WASTWICK*, *HALPOR* and residual gas saturation in the shaft (*SHRGSSAT*) for the first 1000 yr in both the upper and lower waste panels and a negative effect is indicated for *WMICDFLG*, with increasing values for *WASTWICK* and *HALPOR* tending to increase the amount of brine available to the corrosion process, increasing values for *WMICDFLG* tending to decrease the amount of brine available to the corrosion process, and increasing values of *SHRGSSAT* tending to alter patterns of gas and brine flow across the part of the computational grid corresponding to the shaft within the

repository and DRZ (i.e., Regions 10 and 11, Fig. 1, Ref. 2). Also, a small positive effect for *ANHPRM* is indicated in the lower panel due to its role in enhancing brine flow from the marker beds.

For E2 intrusions between 1000 and 10,000 yr, *HALPOR* is the most important variable for the upper waste panels and *WGRCOR* is the most important variable for the lower waste panel (Table 6). For both upper and lower panels, *BHPRM* is the second variable selected in the regression analysis. The upper panels receive less of the brine flowing down the borehole than the lower panel. As a result, the amount of brine entering by drainage from the DRZ, which is determined by *HALPOR*, is the most important variable in determining the amount of steel that will be consumed by corrosion. In contrast, the lower panel receives more brine inflow on a unit volume basis than the upper panels and the amount of steel consumed is dominated by how fast this brine can be used in the corrosion process, with this rate dominated by *WGRCOR*. The variable *BHPRM* has a positive effect due to its role in increasing both brine flow down the borehole and out of the marker beds. The variable *ANHPRM* also has a positive effect in both regressions due to its role in increasing brine flow out of the marker beds. The appearance of *WASTWICK* with a negative regression coefficient for the lower waste panel results because increasing *WASTWICK* increases steel consumption in the first 1000 yr and thus reduces the amount of steel that can be consumed between 1000 and 10,000 yr. Several other variables (i.e., *HALPRM*, *SHRGSSAT*, *SHPRMCON*, *BPVOL*) are indicated as having small effects. Increasing *HALPRM* tends to increase brine flow out of the marker beds (Table 2). The variables *SHRGSSAT* and permeability of concrete in the shaft (*SHPRMCON*) affect gas and brine flow across the part of the computational grid corresponding to the shaft within the repository and DRZ (i.e., Regions 10 and 11, Fig. 1, Ref. 2). The appearance of *BPVOL* is spurious.

The regressions for E2 intrusions between 1000 and 10,000 yr have relatively low R^2 values (i.e., 0.63, 0.56) due to patterns of the form shown by the scatterplots in Fig. 19. Specifically, the left and right columns in Fig. 19 display scatterplots for the first three variables selected in the regression analyses in Table 6 for steel consumption between 1000 and 10,000 yr in the upper and lower waste panels, respectively. For the upper waste panels, the positive trends indicated in the scatterplots for *HALPOR*, *BHPRM* and *WGRCOR* are consistent with the positive regression coefficients in Table 6. However, the patterns are fairly diffuse, and the fact that corrosion ceases in the absence of brine is producing patterns that are difficult to capture with a linear regression model. In particular, a well-defined relationship between steel consumption and *WGRCOR* can be seen for small values of *WGRCOR*, with this pattern then becoming very diffuse for larger values of *WGRCOR* due to brine exhaustion. For the lower waste panel, a much stronger relationship between gas generation and *WGRCOR* can be seen because the extensive brine flow into the lower waste panel makes it unlikely that corrosion will cease due to brine exhaustion. The leveling off and actual decrease in the fraction of steel consumed for larger values of *WGRCOR* occurs because large values of *WGRCOR* result in more steel consumption in the first 1000 yr and hence in less steel being available for consumption between 1000 and 10,000 yr. For small values of *WGRCOR*, corrosion is not limited by the steel inventory and so the loss of steel during the first 1000 yr has no effect on the fraction of steel consumed by corrosion

between 1000 and 10,000 yr. As for the upper waste panels, the relationships between the fraction of steel consumed by corrosion and the sampled variables are too complex to be captured by a linear regression model.

When the entire 10,000 yr period is considered for E2 intrusions, *HALPOR* is the dominant variable with respect to fraction of steel consumed in the upper panels (Table 6), and *WGRCOR* is the dominant variable with respect to the fraction of steel consumed in the lower panel (Table 6, Fig. 20). The greater availability of brine in the lower waste panel results in the fraction of steel consumed by corrosion being dominated by the rate at which corrosion takes place (Fig. 20). The larger values for *WGRCOR* result in a complete consumption of the steel if adequate brine is present (Fig. 20). Overall, the patterns of variable influence are consistent with those previously observed and discussed for the 0 - 1000 yr and 1000 - 10,000 yr time periods.

The 0 - 1000 yr results are identical for E1 and E2 intrusions at 1000 yr (Table 6). For the upper waste panels over the interval 1000 - 10,000 yr, the analyses for E1 and E2 intrusions both select *HALPOR*, *BHPRM* and *WGRCOR* as the first three variables in the regression model (Table 6) for reasons previously discussed. The analysis for the E1 intrusion then selects *WMICDFLG*, *BPPRM* and *BPINTPRS*. The selection of *WMICDFLG* with a negative regression coefficient results because of the role that *WMICDFLG* plays in reducing and/or stopping brine flow from the brine pocket to the repository in the 200 yr period between the occurrence of the drilling intrusion and the failure of the plug at the Rustler/Salado interface (Fig. 7). The appearance of brine pocket permeability (*BPPRM*) with a negative regression coefficient is counterintuitive; however, *BPCOMP* and *BPPRM* were sampled with a rank correlation of -0.75, which can cause unanticipated patterns in a regression analysis. The variable *BPINTPRS* appears with a positive regression coefficient because increasing its value tends to increase brine flow from the brine pocket to the repository.

For the lower waste panel over the interval 1000 - 10,000 yr, the regression analysis for the E1 intrusion selects *WGRCOR*, *BHPRM* and *WASTWICK* and produces a model with an R^2 value of only 0.45 (Table 6). This poor fit is resulting from patterns that cannot be captured by the regression model in use (Fig. 21). Specifically, the linear relationship for small values of *WGRCOR* followed by an asymptote for larger values is too complex for a simple linear regression model to duplicate.

The variable *BPCOMP* was identified as being important with respect to the amount of brine that flows from the brine pocket to the repository for an E1 intrusion (Table 4, Fig. 11). However, *BPCOMP* does not appear in the sensitivity analyses for the amount of steel consumed by corrosion subsequent to an E1 intrusion (Fig. 18, Table 6). Given the large amount of brine that typically enters the repository for an E1 intrusion, the importance of *BPCOMP* with respect to the amount of brine entering the repository is lost due to the dominant effect of *WGRCOR* in determining the rate at which this brine is consumed (Fig. 21; see Fig. 8.3.12, Ref. 11, for scatterplots of *BPCOMP* and fractions of steel consumed in upper and lower waste panels). A similar pattern occurs for E2 intrusions, where

BHPRM controls the amount of brine flowing down a borehole into the repository (Table 3, Fig. 9) and the amount of steel consumed by corrosion subsequent to an intrusion is dominated by *WGRCOR* (Fig. 19).

For steel consumption in the upper waste panels over the entire 10,000 yr period with an E1 intrusion at 1000 yr, the same variables are identified as for steel consumption from 1000 to 10,000 yr (Table 6), which is consistent with the result that most steel consumption occurs after 1000 yr (Fig. 18). For steel consumption in the upper waste panels, the analyses for both E1 and E2 intrusions identify *HALPOR*, *WGRCOR* and *BHPRM* as the top three variables. Interestingly, the regression analysis for steel consumption in the lower waste panel over the entire 10,000 yr period with an E1 intrusion at 1000 yr is considerably more successful than the corresponding analysis for steel consumption between 1000 and 10,000 yr (i.e., a model with 8 variables and an R^2 of 0.76 versus a model with 3 variables and an R^2 of 0.45). This difference arises from the difficulty of capturing the effects of a complete consumption of the remaining steel inventory between 1000 and 10,000 yr (Figs. 18, 21). The dominant variable for steel consumption in the lower waste panel with an E1 intrusion at 1000 yr is *WGRCOR*, which is consistent with the corresponding scatterplot in Fig. 20. The remaining 7 variables in the regression model (i.e., *BHPRM*, *WASTWICK*, *HALPOR*, *SHRGSSAT*, *BPINTPRS* and *ANHPRM* with positive regression coefficients and *WMICDFLG* with a negative regression coefficient) have considerably smaller effects than *WGRCOR* and have been discussed previously for results in the 0 - 1000 yr and 1000 - 10,000 yr time intervals.

Regression analyses were also performed for the upper and lower waste panels for the difference between fraction of steel consumed for E1 and E2 intrusions at 1000 yr (Table 6). However, neither regression was very successful in identifying the variables that determine these differences (i.e., R^2 values of 0.28 and 0.46). For perspective, scatterplots of the variables used to define the indicated differences for the upper and lower waste panels are shown in Fig. 22. The basic problem is that the underlying patterns are too complicated to be captured by a simple regression model. For the upper waste panels, *BPCOMP*, *BHPRM*, *WMICDFLG* and *HALPOR* interact to determine the difference between steel consumption for E1 and E2 intrusions (Fig. 8.3.14, Ref. 11). Large values for *BPCOMP* tend to increase the difference because of increased brine flow from the brine pocket. Similarly, large values of *WMICDFLG* tend to decrease the difference because of decreased flow from the brine pocket. Small values for *HALPOR* tend to increase the difference because drainage from the DRZ is a more important brine source for the E2 than the E1 intrusion. Finally, the cases where steel consumption for the E2 intrusion exceeds steel consumption for the E1 intrusion are associated exclusively with the largest values for *BHPRM*.

For the lower waste panel, *BPCOMP*, *BHPRM*, *WMICDFLG* and *HALPOR* again determine the difference between steel consumption for E1 and E2 intrusions (Fig. 8.3.15, Ref. 11). In contrast to the upper waste panels where positive and negative differences occur over the entire range of steel consumption (Fig. 22), steel consumption under E1 conditions always equals or exceeds the consumption under E2 conditions for the lower waste panel (Fig. 22). Further, the largest differences are strongly concentrated near a consumption fraction of 1 for the E1 intrusion (Fig. 22). When corrosion rates are small, E1 and E2 intrusions result in corrosion of similar amounts of

steel (Fig. 20) because there is no exhaustion of the available brine. At higher corrosion rates, the amount of steel that can be consumed by corrosion becomes limited by the amount of available brine, which is why the E1 intrusion often results in the consumption of more steel in the lower waste panel than does the E2 intrusion (Fig. 22). Specifically, increasing *BPCOMP* increases the difference between the fraction of steel consumed under E1 and E2 conditions because it increases the amount of brine present under E1 conditions. Similarly, increasing each of *BHPRM* and *HALPOR* tends to increase the amount of brine present under E2 conditions and thus reduce the difference between the fraction of steel consumed under E1 and E2 conditions. Finally, increasing *WMICDFLG* tends to reduce the amount of brine present under E1 conditions and thus reduce the difference between the fraction of steel consumed under E1 and E2 conditions. However, the large number of observations for which steel consumption in the lower waste panel is the same for E1 and E2 intrusions creates a pattern that cannot be captured by a simple regression model, which is why the corresponding regression in Table 6 has an R^2 value of only 0.46.

The increased brine inflow, and hence increased corrosion, results in the increased gas generation observed for E1 and E2 intrusions relative to that observed for undisturbed conditions (Figs. 13, 17). Due to the different patterns of brine inflow, and hence corrosion, in the upper and lower waste panels, there are also different patterns of gas generation (Fig. 23). In particular, gas generation in the lower waste panel ceases for some sample elements due to a complete consumption of the steel inventory (Fig. 18). In contrast, the steel inventory is not depleted in the upper waste panels (Fig. 18) and so gas generation continues over the entire 10,000 yr period unless there is no brine in the upper waste panels.

The PRCCs in Fig. 23 for cumulative gas generation consistently show *WMICDFLG* to be the dominant variable due to its role in determining the amount of gas generated by microbial degradation of cellulose. After *WMICDFLG*, the selected variables are consistent with those obtained in Fig. 18 for fraction of steel remaining, with the appropriate reversal in sign. For completeness, Table 7 presents the same regression analyses for total gas generation as presented in Table 6 for amount of steel consumed. The results in Tables 6 and 7 are generally the same with the appropriate addition of *WMICDFLG* due to its role in influencing microbial gas generation.

4. Disturbed Conditions: Pressure for E1 and E2 Intrusions

Pressure in the repository under undisturbed conditions tends to increase monotonically towards an asymptote for each sample element (Fig. 18, Ref. 1), with the value of this asymptote determined primarily by the amount of gas generated by corrosion and microbial degradation (Fig. 20, Ref. 1). A very different pattern is exhibited under disturbed conditions, with pressure tending to decrease rapidly after a drilling intrusion (Fig. 24). The results in Fig. 24 are for pressure in the lower waste panel; the pressure histories for the upper waste panels are very similar (Fig. 25).

Due to the assumption of a borehole plug with a life expectancy of 200 yr at the Rustler/Salado interface (Table 8, Ref. 2), the E2 intrusion at 1000 yr has no effect on repository pressure until 1200 yr. In contrast, the E1 intrusion is modeled with an open borehole (i.e., with a permeability of 10^{-9} m^2) between the plug and the brine pocket during this 200 yr period, with the result that the potential for flow between the brine pocket and the repository exists. The effects of this flow can be seen in the rapidly changing pressures between 1000 and 1200 yr for some sample elements for the E1 intrusion (Fig. 26). However, the highest repository pressures show little change from 1000 to 1200 yr because these pressures are sufficiently high to prevent brine flow from the brine pocket to the repository (Fig. 7). These high repository pressures tend to be associated with large values for *WMICDFLG* (Fig. 27). Sample elements with low pressures at 1000 yr often undergo a sudden increase in pressure immediately after the drilling intrusion, with this pressure then decreasing over the next 200 yr (Fig. 26) due to brine and gas flow through the DRZ and the panel closures to the remainder of the repository. The effect of the DRZ and panel closures in spreading out the pressure pulse due to penetration of a brine pocket can be seen in the slow monotonic increase in pressure in the rest of the repository in contrast with the sharp increase in pressure in the waste panel associated with the intrusion into the brine pocket (Fig. 26). Repository pressure undergoes a rapid decrease after failure of the plug at the Rustler/Salado interface at 1200 yr due to gas outflow (Fig. 24).

The PRCCs in Fig. 24 prior to 1000 yr are the same as those in Fig. 18 of Ref. 1 for undisturbed conditions. At 1000 yr, pressure in the repository is dominated by *WMICDFLG* and other variables (i.e., *WGRCOR*, *WASTWICK*, *HALPOR*, *ANHPRM*, *WGRMICI*) that influence gas generation under undisturbed conditions (Figs. 24, 27, Table 8). Immediately after 1200 yr, *BHPRM* shows a negative effect on pressure because gas flow up the borehole increases with increasing values for *BHPRM*. However, the PRCCs in Fig. 24 and regression analyses in Table 8 are not very successful in identifying the variables dominating the uncertainty in pressure after 1200 yr (e.g., the two regressions in Table 8 for pressure at 10,000 yr have R^2 values of only 0.20 and 0.25).

The poor performance of the sensitivity measures after 1200 yr is due to patterns that cannot be identified by the regression-based procedures in use. In particular, repository pressure is dominated by *BHPRM* after 1200 yr (Fig. 28). Pressure tends to decrease as *BHPRM* increases until a value of approximately $10^{-11.6}$ m^2 (2.5×10^{-12} m^2) is reached; at this point, pressure jumps to approximately 6×10^6 Pa, which is hydrostatic pressure at repository depth. The patterns in Fig. 28 result from an interplay of gas and brine flow in the borehole. At low permeabilities, little gas can flow out the borehole and so pressures remain high. As *BHPRM* increases, more gas can flow out the borehole and so pressure decreases. In particular, pressure stays relatively low (i.e., ~ 1.5 to 3.0×10^6 Pa) at intermediate values for *BHPRM* because a continuous brine column is not established between the repository and overlying formations. As *BHPRM* increases, more brine flows down the borehole and the repository fills with brine at higher values of *BHPRM*. When this occurs, a continuous brine column is established between the repository and overlying formation, with the result that repository pressure then jumps to hydrostatic pressure.

Total pore volume in the repository is shown in Fig. 29. Pore volume tracks pressure very closely (Fig. 20, Ref. 1). As a result, pore volume is influenced by the same variables as repository pressure, with *BHPRM* being the dominant variable (Fig. 28). Due to the lower pressures, pore volume under disturbed conditions is lower than pore volume under undisturbed conditions (Fig. 20, Ref. 1; Fig. 29).

5. Disturbed Conditions: Saturation for E1 and E2 Intrusions

The occurrence of a drilling intrusion can have a significant effect on the brine saturation in both the upper and lower waste panels (Fig. 30). In particular, the tendency is to increase the saturation due to (i) increased flow from the marker beds (Fig. 2), (ii) flow down the borehole from overlying formations (Fig. 6), and (iii) flow up from the brine pocket in the event of an E1 intrusion (Fig. 6). Although saturation tends to increase throughout the repository, the effect is particularly pronounced in the intruded panel (Fig. 30), which is the lower waste panel in the calculations performed for the 1996 WIPP PA. As indicated by the horizontal brine saturation curves in Fig. 30, the intruded panel often becomes fully brine saturated subject to the limitations imposed by the residual gas saturation (*WGRSSAT*). Due to the brine flow from the brine pocket, the intruded panel is more likely to become fully brine saturated for an E1 intrusion than for an E2 intrusion (Fig. 31).

As indicated by the PRCCs in Fig. 30, the uncertainty in the brine saturation in the unintruded (i.e., upper) waste panels is determined by *HALPOR*, *BHPRM*, *WGRCOR* and *WASTWICK*, with saturation tending to increase as *HALPOR* and *BHPRM* increase and tending to decrease as *WGRCOR* and *WASTWICK* increase. The positive effects for *HALPOR* and *BHPRM* result because increasing each of these variables allows more brine to enter the waste panels. The negative effects for *WGRCOR* and *WASTWICK* result because increasing each of these variables increases the rate at which brine is consumed by corrosion, which in turn has two effects on saturation. First, the direct loss of brine reduces saturation. Second, the generation of gas by corrosion increases repository pressure, which in turn tends to increase repository porosity due to pore space expansion and thus reduce brine saturation. Together, these two effects result in a reduced amount of brine occupying an increased pore volume. Pore space expansion due to increased pressure is also why *WMICDFLG* appears as an important variable prior to the intrusion and then drops to having no effect as the gas generated by microbial degradation is vented after the drilling intrusion. As a reminder, most microbial gas generation ends by 1000 yr (Figs. 7, 8, Ref. 1).

As an alternative analysis for brine saturation in the upper waste panels, regression results for saturation at 10,000 yr are presented in Table 9. As in the PRCC analysis (Fig. 30), positive effects are indicated for *BHPRM* and *HALPOR* and negative effects are indicated for *WGRCOR* and *WASTWICK*. In addition, small positive effects are indicated for *ANHPRM* and *HALPRM* because increasing each of these variables tends to increase brine flow out of the anhydrite marker beds (Table 2). Small values for *BHPRM* and *HALPOR* often result in a complete consumption of the brine in the upper waste panels (i.e., a brine saturation of zero); a similar pattern also occurs for large values of

WGRCOR (Fig. 8.5.3, Ref. 11). A similar but less pronounced pattern also occurs for *ANHPRM*, with smaller values tending to be associated with zero brine saturations. A small negative effect is indicated for *SHRGSSAT* (Table 9), probably due to its role in affecting gas and brine flow across the part of the computational grid in the repository and DRZ that corresponds to the shaft.

For brine saturation in the lower (i.e., intruded) waste panel, the PRCCs in Fig. 30 indicate positive effects for *BHPRM* and *HALPOR*, negative effects for *WGRCOR* and *WRGSSAT*, and negative, rapidly decreasing effects for *WMICDFLG* and *WASTWICK*. The corresponding regression analysis for brine saturation at 10,000 yr indicates positive effects for *BHPRM*, *ANHPRM* and *HALPOR*, and negative effects for *WRGSSAT*, permeability of halite in shaft (*SHPRMHAL*) and *WGRCOR* (Table 9). The effects associated with *BHPRM*, *ANHPRM* and *HALPOR* result because increasing each of these variables increases brine inflow to the intruded panel. Of these variables, *BHPRM* has the largest effect (Fig. 32) because of its role in both reducing pressure in the repository, which increases brine flow out of the marker beds, and allowing brine flow down the intruding borehole. However, due to the large amount of brine inflow, the panel tends to completely fill with brine, with the result that the primary determinant of brine saturation is the residual gas saturation *WRGSSAT*. The dominant role played by *WRGSSAT* in determining brine saturation can be seen in the straight line of points in the corresponding scatterplot (Fig. 32).

A result closely related to brine saturation is the volume of brine contained in the repository. As indicated by PRCCs, brine volume in the upper (i.e., unintruded) waste panels subsequent to an E2 intrusion tends to increase as *BHPRM* and *HALPOR* increase and tends to decrease as *WGRCOR* and *WASTWICK* increase (Fig. 33). Increasing each of *HALPOR* and *BHPRM* tends to increase the amount of brine entering the upper waste panels, and increasing each of *WGRCOR* and *WASTWICK* tends to increase the amount of brine being consumed by corrosion. In addition to *BHPRM*, *HALPOR*, *WGRCOR* and *WASTWICK*, the regression analysis for brine volume at 10,000 yr also indicates small positive effects for *ANHPRM* and *HALPRM* and a small negative effect for *WRBRNSAT* (Table 10). The positive effects for *ANHPRM* and *HALPRM* result from their role in influencing the amount of brine that flows from the marker beds to the repository (Table 2). The negative effect for *WRBRNSAT* probably results from its role in influencing brine flow patterns within the repository. The scatterplot for *BHPRM* shows a well-defined pattern, with a sudden jump in brine volume at $10^x \doteq 10^{-11.6}$ m^2, x = *BHPRM* (Fig. 34; see Fig. 8.5.7, Ref. 11, for scatterplots for *WGRCOR* and *HALPOR*). As discussed in Sect. 4, this jump corresponds to the lower waste panel becoming fully brine saturated.

For the lower (i.e., intruded) waste panel after an E2 intrusion at 1000 yr, PRCCs indicate small positive effects for *BHPRM*, *ANHPRM* and *HALPOR* and a small negative effect for *WGRCOR* (Fig. 33). However, the PRCCs tend to be small (e.g., all PRCCs are less than 0.5 in absolute value by 10,000 yr). The corresponding regression model in Table 10 has an R^2 value of only 0.44 and thus is also not very successful in accounting for the uncertainty in brine volume. As examination of Fig. 34 shows, the poor performance of regression-based results derives from a complex pattern of behavior involving *BHPRM*. In particular, three distinct regimes of behavior can be seen. Above

$10^x \doteq 10^{-11.6}$ m^2, x = *BHPRM*, brine volumes are clustered around 5×10^3 m^3; as discussed in Sect. 4 and illustrated in Fig. 28, these volumes are associated with the repository being at hydrostatic pressure. Between $10^x \doteq 10^{-12.6}$ m^2 and $10^x \doteq 10^{-11.6}$ m^2, x = *BHPRM*, volumes are clustered around 2.4×10^3 m^3; as shown in Fig. 28, these volumes are associated with low pressures in the repository. Below $10^x \doteq 10^{-12.6}$ m^2, x = *BHPRM*, these volumes show a wide range of possible values, with this wide range corresponding to the similarly wide range of values for repository pressure (Fig. 28). Thus, there is a close, but complex, link between repository pressure and volume of brine contained in the intruded waste panel (Fig. 35). In particular, *BHPRM* is the dominant variable in determining both pressure and brine volume in the intruded panel (Figs. 28, 34) after an E2 intrusion.

Brine volume in the upper (i.e., unintruded) waste panels subsequent to an E1 intrusion behaves in a similar manner to that observed subsequent to an E2 intrusion (Figs. 33, 36). As for the E2 intrusion, (i) brine volume tends to decrease with time but may show an increase at very late times, (ii) positive effects are indicated for *BHPRM* and *HALPOR*, and (iii) negative effects are indicated for *WGRCOR* and *WASTWICK*. The regression models for brine volume in the upper waste panels after E1 and E2 intrusions are also similar (Table 10), although the model for the E1 intrusion shows the effects of variables that affect the brine pocket (i.e., positive effects for *BPCOMP* and *BPVOL*). The scatterplot for *BHPRM* and brine volume in the upper waste panels subsequent to an E1 intrusion is similar to the corresponding scatterplot in Fig. 34 for brine volume subsequent to an E2 intrusion.

Brine volume in the lower (i.e., intruded) waste panel subsequent to an E1 intrusion also behaves similarly to brine volume subsequent to an E2 intrusion (Figs. 33, 36). Specifically, brine volume tends to cluster around values of 5×10^3 m^3 and 2.5×10^3 m^3 (Fig. 36); the corresponding values for the E2 intrusion are 5×10^3 m^3 and 2.4×10^3 m^3 (Fig. 33). For the E1 intrusion, the PRCC analysis is poor, with all variables having PRCCs less than 0.3 in absolute value after the drilling intrusion at 1000 yr (Fig. 36). The regression analysis is also poor, with an R^2 value of only 0.37 (Table 10). This poor performance occurs because a complex relationship exist between brine volume and *BHPRM*. Thus, as for the E2 intrusion, brine volume and repository pressure are being controlled by *BHPRM* (Figs. 28, 35, 37).

6. Disturbed Conditions: Brine and Gas Flow in Borehole for E1 and E2 Intrusions

The defining characteristics of disturbed conditions result from brine and gas flow in the intruding borehole. A borehole plug at the Rustler/Salado interface is assumed to be effective for 200 yr after a drilling intrusion through the repository (Table 8, Ref. 2). After the failure of this plug, repository pressure drops rapidly (Fig. 24) due to gas flow up the intruding borehole (Fig. 38). After an initial rapid venting of gas, the flow rate tends to continue at a slower rate as additional gas is generated by the corrosion of steel.

Prior to the drilling intrusion, a very small amount of gas moves into the undisturbed halite at the edge of the DRZ in the computational cell that will become part of the borehole (i.e., Cell 575 in Fig. 3 of Ref. 2). The amount of movement that takes place is dominated by the indicator variable for the relative permeability model (*ANHBCVGP*), with less gas movement taking place into Cell 575 when the van Genuchten-Parker model (*ANHBCVGP* = 1) is used (Fig. 38). The preceding statement is made because of the negative PRCC shown for *ANHBCVGP* (Fig. 38) between 0 and 1000 yr. However, the actual magnitude of this movement is very small and of no consequence to the analysis and is mentioned only because of the appearance of the PRCC for *ANHBCVGP* prior to 1000 yr in Fig. 38.

The amount of gas vented within a few hundred years of the plug failure is dominated by *WMICDFLG*, *BHPRM*, *WGRCOR* and *WASTWICK*, with the amount of gas moving up the borehole tending to increase as each of these variables increases (Fig. 38). The positive effects for *WMICDFLG*, *WGRCOR* and *WASTWICK* result from increasing the amount of gas in the repository at the time of the intrusion, and the positive effect for *BHPRM* results from reducing the resistance to gas flow in the borehole.

After the first few hundred years, *WMICDFLG*, *BHPRM* and *WGRCOR* continue to show positive effects on the cumulative gas release (Fig. 38). For *WMICDFLG*, this continuing importance to cumulative gas release is indicative of the large gas release that takes place immediately after the drilling intrusion (Fig. 38) and the importance of *WMICDFLG* in determining the size of this release. As a reminder, *WMICDFLG* only affects microbial gas generation, which is often completed by 1000 yr and almost always completed by 2000 yr (Fig. 5, Ref. 1). At later times, a positive effect is also indicated for *HALPOR* due to its role in influencing gas generation due to corrosion (Fig. 38, also see Figs. 12, 14, 16, 23).

Similar results are also obtained in a stepwise regression analysis for cumulative gas flow up the borehole (Table 11). Specifically, gas flow up the borehole tends to increase as each of *WMICDFLG*, *BHPRM*, *HALPOR*, *WGRCOR*, *ANHPRM* and *SHRGSSAT* increases. The roles of these variables have been discussed previously. Specifically, increasing *WMICDFLG* increases microbial gas generation; increasing *BHPRM* both reduces resistance to gas flow up the borehole and allows more brine to enter the repository by flow down the borehole and out of the marker beds; increasing *HALPOR* and *ANHPRM* increases brine flow into the repository by increasing brine flow out of the DRZ and the marker beds, respectively; increasing *WGRCOR* increases gas generation; and increasing *SHRGSSAT* alters brine and gas flow patterns within the repository (see Fig. 8.6.2, Ref. 11, for scatterplots for *WMICDFLG*, *BHPRM*, *HALPOR* and *WGRCOR*.)

The regression analysis results for cumulative gas flow up the borehole subsequent to an E1 intrusion are similar to those obtained for an E2 intrusion (Table 11), although the final R^2 value tends to be somewhat lower (i.e., 0.63 versus 0.75). The same top four variables are picked in both analyses (i.e., *WMICDFLG*, *WGRCOR*, *BHPRM* and *HALPOR*). The selection of *BPPRM* with a negative regression coefficient is counterintuitive but may result from

the rank correlation of −0.75 assigned to *BPCOMP* and *BPPRM*; in any event, the effect indicated for *BPPRM* is small (i.e., the inclusion of *BPPRM* in the regression model changes the R^2 value from 0.61 to 0.62).

Unlike the extensive gas flows up an intruding borehole (Fig. 38), most sample elements result in no brine flow up the intruding borehole (Fig. 39). Due to flow from the brine pocket (Fig. 6), the E1 intrusion usually results in more brine flow up the borehole than the E2 intrusion when such flow occurs; however, the typical case is no flow for both E1 and E2 intrusions. In contrast to the general importance of the E1 intrusion with respect to brine flow up the borehole, the largest such flow for replicate R1 actually results from brine inflow from the marker beds (i.e., compare the largest cumulative flow curves for E1 and E2 intrusions in Fig. 39).

The PRCCs in Fig. 39 and also the regression analyses in Table 11 are probably not very good indicators of variable importance for brine flow up the intruding borehole due to the large number of zero flows. In particular, the regression analyses for E2 and E1 intrusions have R^2 values of only 0.50 and 0.63. Due to the large number of zero flows, examination of scatterplots provides a more reliable indication of variable importance. For the E2 intrusion, brine flow up the intruding borehole tends to be associated with large values for *BHPRM* and *ANHPRM* and small values for *WGRCOR* (Fig. 8.6.4, Ref. 11). The positive effect for *BHPRM* results because increasing *BHPRM* permits more brine to enter the repository due to flow both down the borehole and out of the marker beds and also reduces resistance to flow up the borehole should the intruded waste panel fill with brine. The positive effect for *ANHPRM* results because increasing *ANHPRM* results in more brine flow out of the marker beds. Finally, the negative effect for *WGRCOR* results because increasing *WGRCOR* causes more brine to be removed by corrosion and thus reduces the amount of brine available for flow up the borehole; also, flow up the borehole of the additional gas produced for large values of *WGRCOR* may impede brine flow in the borehole.

For the E1 intrusion, brine flow up the intruding borehole tends to be associated with large values for *BHPRM* and *BPCOMP* and with small values for *WMICDFLG* (Fig. 8.6.5, Ref. 11). The positive effects for *BHPRM* result for the reasons just indicated for the E2 intrusion and also because increasing *BHPRM* reduces resistance to brine flow in the borehole between the brine pocket and the repository (Fig. 8.2.12, Ref. 11). The positive effect for *BPCOMP* results because increasing *BPCOMP* increases the amount of brine that leaves the brine pocket for each unit drop in pressure (Fig. 11). Finally, the negative effect for *WMICDFLG* results because large values for *WMICDFLG* prevent brine movement from the brine pocket to the repository during the 200 yr period that an open borehole exists between these two locations (Fig. 7), which in turn means more brine from other sources is required to fill the intruded panel before brine flow up the borehole can begin.

7. Disturbed Conditions: Behavior of Brine Pocket for E1 Intrusions

As discussed in Sect. 2, brine flow from a region of pressurized brine (i.e., a brine pocket) is an important potential source of brine to the repository for E1 intrusions. The behavior of a brine pocket subsequent to a drilling intrusion is now considered in more detail.

The pressure behavior of the brine pocket is quite dynamic subsequent to a drilling intrusion (Fig. 40). For 200 yr after the intrusion, an open borehole (i.e., permeability of 10^{-9} m^2) is assumed to exist between the brine pocket and the repository and an impermeable plug is assumed to exist at the Rustler/Salado interface (Table 8, Ref. 2). This results in rapid changes of pressure in both the brine pocket and the repository (Figs. 24, 40). During this period, the pressure in the repository typically increases (Fig. 26) and the pressure in the brine pocket decreases (Fig. 40). These changes in pressure tend to be accompanied by a surge of brine from the brine pocket to the repository (Fig. 6), with these surges resulting in a corresponding decrease in the volume of brine contained in the brine pocket (Fig. 40). Typically, most of the brine flow out of the brine pocket takes place during these initial surges (Figs. 6, 40). However, brine flow from the brine pocket to the repository will not take place when the pressure in the repository is sufficiently high relative to the pressure in the brine pocket (Fig. 7). This behavior can be seen in the higher repository pressure curves in Fig. 26, which are essentially unaffected by the penetration of the brine pocket. This stoppage of flow due to high repository pressures is why the largest brine pocket volumes in Fig. 40 show little change after penetration by a drilling intrusion.

After 200 yr, the plug at the Rustler/Salado interface is assumed to fail and the entire borehole is assigned a permeability of 10^x, $x = BHPRM$. At this point, gas can escape from the repository to overlying formations, which causes a rapid drop in repository pressure (Figs. 24, 26). From this point on, there is no longer an open borehole between the repository and the brine pocket (Table 8, Ref. 2). Rather, this portion of the borehole is assumed to have a permeability of 10^x, $x = BHPRM$, for the next 1000 yr. This change in permeability produces a complex pattern of pressure behavior in the brine pocket, with pressure sometimes continuing to decrease as more brine flows out of the brine pocket and at other times increasing towards hydrostatic pressure due to the filling of the repository with brine and the resultant formation of a continuous brine-filled connection with overlying formations. Some sample elements that experienced no brine outflow from the brine pocket during the first 200 yr after the intrusion due to high pressures in the repository now show such outflow as a result of reduced repository pressure (Fig. 40).

After 1000 yr (i.e., 1200 yr after the drilling intrusion), the permeability in the borehole between the repository and the brine pocket is reduced from 10^x, $x = BHPRM$, to 10^x, $x = BHPRM - 1$ (i.e., permeability is reduced by an order of magnitude), which tends to reduce brine flow from the brine pocket to the repository (Table 8, Ref. 2). This effect can be seen in the decreased slope of some of the brine pocket volume curves at 2200 yr (Fig. 40). However, many sample elements show little, if any, change in brine pocket volume after the initial brine outflow immediately after the drilling intrusion.

Before the intrusion at 1000 yr, brine pressure is completely dominated by *BPINTPRS*, which has a PRCC of 1 (Fig. 40). Immediately after the intrusion, positive effects are indicated for *WMICDFLG* and *WGRCOR*. Both of these variables tend to increase repository pressure at 1000 yr (Fig. 28, Table 8) and thus reduce brine flow from, and thus pressure change in, the brine pocket. After 1000 yr, the initial pressure *BPINTPRS* has little effect on brine pocket pressure; thus, the brine pocket tends to rapidly "forget" its initial pressure conditions. The importance of *WMICDFLG* and *WGRCOR* also rapidly decreases after failure of the plug at the Rustler/Salado interface allows gas to flow out of the repository. The variable with the largest PRCC at later times is *BHPRM*. The negative effect indicated for *BHPRM* indicates that brine pocket pressure tends to decrease as *BHPRM* increases. However, the effect is rather weak as the PRCC is mostly less than 0.5 in absolute value. As will be discussed later, the underlying relationship between *BHPRM* and brine pocket pressure is too complex to be adequately captured by a PRCC.

The stepwise regression analysis in Table 12 for pressure at 10,000 yr provides an alternate analysis of the variables affecting brine pocket pressure subsequent to a drilling intrusion. The first variable selected in the regression analysis is *BPCOMP*, with pressure tending to increase as *BPCOMP* increases. This positive relationship between *BPCOMP* and pressure results because increasing *BPCOMP* increases the amount of brine that will leave the brine pocket for a unit drop in pressure. As a result, larger values for *BPCOMP* produce more brine for a given drop in brine pocket pressure than is the case for smaller values for *BPCOMP*. Although *BPCOMP* by itself produces a regression model with an R^2 value of only 0.20, the positive relationship between *BPCOMP* and pressure can be clearly seen in the corresponding scatterplot (Fig. 41). However, this effect is not large enough to meet the screening criteria to appear in Fig. 40 (i.e., a PRCC with an absolute value of at least 0.5 at some point in time). After *BPCOMP*, the regression analysis selects *WMICDFLG* with a positive regression coefficient. As previously discussed, this effect results from the role of *WMICDFLG* in suppressing flow from the brine pocket in the first 200 yr after the drilling intrusion. The positive effect associated with *WMICDFLG* can be seen in the corresponding scatterplot (Fig. 8.8.3, Ref. 11). The next variable selected in the regression analysis is *BHPRM*, with the pressure tending to decrease as *BHPRM* increases. This is consistent with the general pattern shown by the scatterplot in Fig. 41. However, the overall pattern is more complex than simply some noise around an overall linear trend. In particular, the largest values of *BHPRM* have brine pocket pressures in the vicinity of 1×10^7 Pa, which corresponds to hydrostatic pressure. Analogous behavior was observed for repository pressure, with this pressure tending to hydrostatic pressure for the largest values of *BHPRM* due to the establishment of a continuous brine connection with overlying formations (Fig. 28). This complex pattern of behavior is why *BHPRM* appears in Fig. 40 with a negative but rather small PRCC. The last two variables selected in the regression analysis are *BPVOL* and *HALPRM*, with pressure tending to increase as each of these variables increases. The positive effect for *BPVOL* results because larger brine pockets will tend to depressurize more slowly than smaller brine pockets and can be barely discerned in the corresponding scatterplot (Fig. 8.8.3, Ref. 11). The reason for the positive effect associated with *HALPRM* is not apparent and cannot be discerned in the corresponding scatterplot.

Overall, neither the PRCC analysis in Fig. 40 nor the stepwise regression analysis in Table 12 for brine pocket pressure is particularly good. The underlying reason is that the relationships between pressure and the sampled variables are too complex to be captured by the linear models that underlie these techniques. In particular, a complex, nonmonotonic relationship exists between pressure and *BHPRM* (Fig. 41). Similar relationships were encountered in the analysis of repository pressure subsequent to E1 and E2 intrusions (Fig. 28).

The dominant variable with respect to brine volume in the brine pocket is *BPVOL* (Fig. 40), which is consistent with the rather small changes in brine pocket volume subsequent to a drilling intrusion. Specifically, the changes in volume due to brine outflow are typically smaller than the differences in initial volumes defined by *BPVOL*. A positive effect is indicated for *WMICDFLG*, which results from its previously discussed role in suppressing outflow from the brine pocket in the first 200 yr after the drilling intrusion. A negative effect is also indicated for *BPCOMP* and results because increasing *BPCOMP* increases the amount of brine that flows out of the brine pocket for a given drop in pressure. The regression analysis for brine volume is quite successful (Table 12). The initial volume *BPVOL* produces a regression model with an R^2 value of 0.82, which is consistent with its large PRCC (Fig. 40). Next, *BPCOMP* is selected with a negative regression coefficient, which is again consistent with the PRCC analysis (Fig. 40). Together, *BPVOL* and *BPCOMP* produce a regression model with an R^2 value of 0.90 and thus can account for most of the uncertainty in volume. After *BPVOL* and *BPCOMP*, the regression analysis selects *WMICDFLG*, *WASTWICK* and *ANHPRM* with positive regression coefficients and *BHPRM* and *BPINTPRS* with negative regression coefficients. The positive effects for *WMICDFLG*, *WASTWICK* and *ANHPRM* result from increasing pressure in the repository in the first 200 yr after the drilling intrusion and thus reducing brine flow from the brine pocket to the repository. The negative effects for *BHPRM* and *BPINTPRS* result from reducing resistance to flow in the borehole and increasing the pressure gradient between the brine pocket and the repository, respectively. However, the effects of *WMICDFLG*, *BHPRM*, *BPINTPRS*, *WASTWICK* and *ANHPRM* are small and only increase the R^2 value for the regression model from 0.90 to 0.93. For perspective, the scatterplots for *BPVOL* and *BPCOMP* are given in Fig. 42.

8. Disturbed Conditions: E2E1 Intrusions

Thus far, this presentation has focused on E1 and E2 intrusions. Calculations were also performed for E2E1 intrusions, with the E2 intrusion occurring at 800 yr and the E1 intrusion occurring at 2000 yr. This calculation was performed with the same computational grid used for E1 and E2 intrusions (Figs. 1-3, Ref. 2), which required use of the same computational cells to represent both drilling intrusions (i.e., region 1 in Fig. 1, Ref. 2). This dual usage was accomplished through the definition of appropriate time-dependent borehole permeabilities (Table 13).

Overall, the results obtained for the E2E1 intrusion are similar to the results obtained for E1 and E2 intrusions. For example, total brine flow into the repository for the E2E1 intrusion (Fig. 43) shows a pattern that is a composite of the patterns shown for E1 and E2 intrusions (Fig. 4). Specifically, the E2 intrusion results in substantial brine

flows down the intruding borehole for a few sample elements, which can be seen in the increased flows between 1000 and 2000 yr in Fig. 43 for those sample elements; a similar pattern can be seen in Fig. 4 for the E2 intrusion. Then, a sharp jump in cumulative inflow for the E2E1 intrusion occurs at 2000 yr due to flow from the brine pocket; again, the same pattern can be seen in Fig. 4 for the E1 intrusion. Overall, the surge in inflow at the time of the E1 intrusion for an E2E1 event is somewhat larger than the surge for an isolated E1 (Figs. 4, 6, 43). This behavior occurs because the initial E2 intrusion reduces pressure in the repository and thus results in less resistance to flow from the brine pocket to the repository during the 200 yr period that an open borehole (i.e., permeability of 1×10^{-9} m^2) connects the repository and the brine pocket. Most brine flow from the brine pocket to the repository takes place during this 200 yr interval (Figs. 4, 6, 43). Brine flow down the intruding borehole and into the repository is similar for E1, E2 and E2E1 intrusions (Figs. 5, 43).

Total gas generation is similar for E1, E2 and E2E1 intrusions (Figs. 16, 44). The microbial gas generation is essentially the same for all cases, with most of the cellulose inventory being consumed in the first 1000 yr (Figs. 6, 7). The E2E1 intrusion produces somewhat more gas due to corrosion (Figs. 16, 44) owing to the slightly greater inflows of brine from the brine pocket as discussed in the preceding paragraph.

Due to its influence on spallings and direct brine releases,[15, 16] repository pressure is one of the most important results calculated by BRAGFLO. As might be anticipated, repository pressure for E2E1 intrusions displays a pattern similar to that already observed for E1 and E2 intrusions (Figs. 28, 45). Specifically, pressure drops rapidly at the time of failure for the borehole plugs associated with the initial E2 intrusion (i.e., at 1000 yr); then, a sudden rise in pressure occurs at the time of the subsequent E1 intrusion (i.e., at 2000 yr). After the E1 intrusion, repository pressure is controlled almost entirely by borehole permeability (i.e., $k = 10^x$, $x = BHPRM$) (Fig. 28).

Due to its influence on direct brine releases, repository brine saturation is another important result calculated by BRAGFLO. Again, the brine saturation results for E2E1 intrusions are similar to those observed for E1 and E2 intrusions (Figs. 30, 31, 46). In particular, brine saturation starts rising after the E2 intrusion and then shows a sharp jump after the E1 intrusion (Fig. 46). This behavior is particularly pronounced in the lower (i.e., intruded) waste panel, which often reaches full brine saturation as indicated by the horizontal brine saturation curves. In contrast, the upper (i.e., unintruded) waste panels typically remain substantially below full brine saturation.

Brine volume in the repository is a potentially important variable because it influences the amount of radionuclides that can be dissolved in brine. Again, E1, E2 and E2E1 intrusions display similar brine volume patterns (Figs. 33, 36, 47). The brine volume tends to increase after an intrusion, with this effect being more pronounced in the lower (i.e., intruded) waste panel than in the upper (i.e., unintruded) waste panels and also more pronounced subsequent to an E1 intrusion. The brine volumes subsequent to an isolated E1 intrusion (Fig. 36) are very similar to those subsequent to an E1 intrusion associated with an E2E1 intrusion (Fig. 47). The brine volumes

in the intruded waste panel are almost entirely controlled by borehole permeability (i.e., $k = 10^x$, $x = BHPRM$) (Figs. 34, 37) and are very closed linked to repository pressure (Fig. 35), which is also controlled by *BHPRM* (Fig. 28).

Brine flow up an intruding borehole is the primary mechanism by which radionuclides can be released from the repository to the Culebra Dolomite. These releases are similar for an isolated E1 intrusion and an E1 intrusion subsequent to an E2 intrusion in the same waste panel (Figs. 39, 48), although the degree of similarity will be at least partially influenced by the timing of the individual intrusions. However, the preceding E2 intrusion does not radically change the character of the brine flows associated with a subsequent E1 intrusion. In particular, most of the modeled E2E1 intrusions result in no meaningful brine flows from the repository to the Culebra, as is also the case for E1 intrusions (Figs. 39, 48). Several of the larger brine releases are actually coming from brine outflow from the anhydrite marker beds (Fig. 39).

The behavior of the brine pocket for an E1 intrusion and an E2E1 intrusion are similar, although there are some observable differences (Figs. 40, 49). For the E2E1 intrusion, the repository is at lower pressure at the time of the E1 intrusion than is the case for an isolated E1 intrusion, with the result that there is less resistance to brine flow from the brine pocket to the repository. This lessened resistance results in more rapid and greater decreases in brine pocket pressure for the E2E1 intrusion than is the case for an isolated E1 intrusion (Figs. 40, 49). Also, the lessened resistance results in greater decreases in brine pocket volume for E2E1 intrusions than for isolated E1 intrusions (Figs. 40, 49). In particular, some sample elements that show little or no decrease in brine pocket volume for an isolated E1 intrusion show a substantial decrease for an E2E1 intrusion (Figs. 40, 49).

9. Discussion

As in the corresponding analysis for undisturbed conditions,[1] uncertainty and sensitivity analysis procedures based on Latin hypercube sampling, examination of scatterplots, stepwise regression analysis, partial correlation analysis, and rank transformations were used to investigate brine inflow, gas generation, repository pressure, brine saturation, and brine and gas outflow in the vicinity of the repository under disturbed conditions. The same general observations made with respect to the techniques in use as part of the discussion of the analysis for undisturbed conditions also apply to the analysis for disturbed conditions (Sect. 7, Ref. 1).

Of the results under study, repository pressure and brine flow up an intruding borehole are potentially the most important in determining radionuclide releases from the repository, with repository pressure influencing spallings[15, 17, 18] and direct brine[16] releases and brine flow up an intruding borehole influencing releases to the Culebra Dolomite.[19]

Repository pressure subsequent to a drilling intrusion is dominated by borehole permeability (*BHPRM*; see Fig. 28), with repository pressure ultimately determined by the competing effects of gas flow up the borehole and

brine flow down the borehole. In particular, three regimes of behavior were observed for the effects of borehole permeability (Fig. 28), with repository pressures tending to remain high for low values of *BHPRM* (i.e., $10^x < 10^{-13}$ m^2, $x = BHPRM$), to drop to low values for intermediate values of permeability (i.e., $10^{-13} < 10^x < 2.5 \times 10^{-12}$ m^2, $x = BHPRM$) and to rise to hydrostatic pressure for large values of permeability (i.e., 2.5×10^{-12} $m^2 < 10^x$, $x = BHPRM$). The preceding effects result because low values for *BHPRM* inhibit both gas flow up the borehole and brine flow down the borehole, intermediate values for *BHPRM* permit gas flow up the borehole but inhibit brine flow down the borehole, and high values for *BHPRM* permit both gas flow up the borehole and brine flow down the borehole. In the latter case, sufficient brine flows down the borehole to saturate the repository, with the result that repository pressure rises to hydrostatic pressure due to the continuous brine-filled connection that is formed with overlying units.

Brine flow from the repository to the Culebra Dolomite is also dominated by *BHPRM*. In particular, the intruded waste panel must become brine saturated before brine can flow from the repository to the Culebra, with such saturation typically only occurring for large values of *BHPRM* due to brine flow down the borehole. Further, once the potential for brine flow up the borehole exists, such flow tends to increase as *BHPRM* increases. However, the assessed uncertainty in *BHPRM* and other variables indicated a substantial degree of belief (i.e., > 0.5) that there would be no brine flow from the repository to the Culebra in an intruding borehole.

Partial correlation coefficients and stepwise regression analysis were not very effective in identifying the effects of *BHPRM* on repository pressure and brine flow from the repository to the Culebra. Ultimately, these effects were identified by the examination of scatterplots. This difficulty motivated an examination of procedures for identifying patterns in scatterplots and recognition that the chi-square test provides an effective means of identifying such patterns in a sampling-based sensitivity analysis.[20-22]

The analysis considered drilling intrusions that penetrated pressurized brine in the Castile Fm (i.e., E1 intrusions) and also intrusions that did not penetrate pressurized brine in the Castile Fm (i.e., E2 intrusions). However, the pressure and brine flow results subsequent to E1 and E2 intrusions were similar, as was also the case for results obtained for E2E1 intrusions (i.e., and E2 intrusion followed by an E1 intrusion). This behavior is different from that predicted in previous PAs for the WIPP, where E1 intrusions resulted in larger brine flows from the repository to the Culebra than was the case for E2 intrusions.[23-25]

The low pressure in the repository subsequent to E1, E2 and E2E1 intrusions typically resulted in no spallings and direct brine releases for second and subsequent drilling intrusions into the repository.[15, 16] In particular, repository pressure had to be above the pressure of brine-saturated drilling fluid at the depth of the repository (i.e., 8 MPa) for the potential to have a spallings or direct brine release to exist,[26] with such pressures rarely predicted to exist subsequent to a drilling intrusion (Figs. 24, 45). Due to the low resistance to gas flow in the DRZ, pressure was essentially constant throughout the repository subsequent to a drilling intrusion (Fig. 26). The smaller brine flows to

the Culebra than in previous PAs for the WIPP and also reduced radionuclide solubilities[19] resulted in smaller radionuclide releases to the Culebra than predicted in previous PAs.[19, 23-25]

Acknowledgment

Work performed for Sandia National Laboratories (SNL), which is a multiprogram laboratory operated by Sandia Corporation, a Lockheed Martin Company, for the United States Department of Energy under contract DE-AC04-94AL85000. Review provided at SNL by M. Chavez, C. Crawford and M.S. Tierney. Editorial support provided by L. Harrison, T. Allen and H. Radke of Tech Reps, Inc.

References

1. Helton, J.C., Bean, J.E., Economy, K., Garner, J.W., MacKinnon, R.J., Miller, J., Schreiber, J.D., & Vaughn, P., Uncertainty and Sensitivity Analysis for Two-Phase Flow in the Vicinity of the Repository in the 1996 Performance Assessment for the Waste Isolation Pilot Plant: Undisturbed Conditions, *Reliability Engineering and System Safety* (in this issue).

2. Vaughn, P., Bean, J.E., Helton, J.C., Lord, M.E., MacKinnon, R.J., & Schreiber, J.D., Representation of Two-Phase Flow in the Vicinity of the Repository in the 1996 Performance Assessment for the Waste Isolation Pilot Plant, *Reliability Engineering and System Safety* (in this issue).

3. Helton, J.C., Martell, M.-A., & Tierney, M.S., Characterization of Subjective Uncertainty in the 1996 Performance Assessment for the Waste Isolation Pilot Plant, *Reliability Engineering and System Safety* (in this issue).

4. Helton, J.C., Davis, F.J., & Johnson, J.D., Characterization of Stochastic Uncertainty in the 1996 Performance Assessment for the Waste Isolation Pilot Plant, *Reliability Engineering and System Safety* (in this issue).

5. Helton, J.C., Uncertainty and Sensitivity Analysis Techniques for Use in Performance Assessment for Radioactive Waste Disposal, *Reliability Engineering and System Safety*, 1993, **42**(2-3), 327-367.

6. Iman, R.L., Davenport, J.M., Frost, E.L., & Shortencarier, M.J., *Stepwise Regression with PRESS and Rank Regression (Program User's Guide)*, SAND79-1472, Sandia National Laboratories, Albuquerque, NM, 1980.

7. WIPP PA (Performance Assessment), WIPP PA User's Manual for *STEPWISE, Version 2.20, Document Version 1.00*, Sandia WIPP Central Files WPO #27768, Sandia National Laboratories, Albuquerque, NM, 1995.

8. Iman, R.L., Shortencarier, M.J., & Johnson, J.D., *A FORTRAN 77 Program and User's Guide for the Calculation of Partial Correlation and Standardized Regression Coefficients*, NUREG/CR-4122, SAND85-0044, Sandia National Laboratories, Albuquerque, NM, 1985.

9. Gilkey, A.P., *PCCSRC, Version 2.21, User's Manual, [Document Version 1.0]*, Sandia WIPP Central Files WPO #27773, Sandia National Laboratories, Albuquerque, NM, 1995.

10. Iman, R.L., & Conover, W.J., The Use of the Rank Transform in Regression, *Technometrics*, 1979, **21**(4), 499-509.

11. Helton, J.C., Bean, J.E., Berglund, J.W., Davis, F.J., Economy, K., Garner, J.W., Johnson, J.D., MacKinnon, R.J., Miller, J., O'Brien, D.G., Ramsey, J.L., Schreiber, J.D., Shinta, A., Smith, L.N., Stoelzel, D.M., Stockman, C., & Vaughn, P., *Uncertainty and Sensitivity Analysis Results Obtained in the 1996 Performance Assessment for the Waste Isolation Pilot Plant*, SAND98-0365, Sandia National Laboratories, Albuquerque, NM, 1998.

12. U.S. Department of Energy, *Title 40 CFR Part 191 Compliance Certification Application for the Waste Isolation Pilot Plant*, DOE/CAO-1996-2184, Volumes I-XXI, Carlsbad, NM: U.S. Department of Energy, Carlsbad Area Office, 1996.

13. U.S. Department of Energy, *Waste Isolation Pilot Plant Sealing System Design Report*, DOE/WIPP-95-3117, Office of Scientific and Technical Information, Oak Ridge, TN, 1995. Sandia WIPP Central Files WPO # 29062, Sandia National Laboratories, Albuquerque, NM, 1996.

14. Thompson, T.W., Coons, W.E., Krumhansl, J.L., & Hansen, F.D., *Inadvertent Intrusion Borehole Permeability, Final Draft*, Sandia WIPP Central Files WPO # 41131, Sandia National Laboratories, Albuquerque, NM, 1996.

15. Berglund, J.W., Garner, J.W., Helton, J.C., Johnson, J.D., & Smith, L.N, Direct Releases to the Surface and Associated Complementary Cumulative Distribution Functions in the 1996 Performance Assessment for the Waste Isolation Pilot Plant: Cuttings, Cavings and Spallings, *Reliability Engineering and System Safety* (in this issue).

16. Stoelzel, D.M., O'Brien, D.G., Garner, J.W., Helton, J.C., Johnson, J. D., & Smith, L.N., Direct Releases to the Surface and Associated Complementary Cumulative Distribution Functions in the 1996 Performance Assessment for the Waste Isolation Pilot Plant: Direct Brine Release, *Reliability Engineering and System Safety* (in this issue).

17. Hansen, F.D., Knowles, M.K., Thompson, T.W., Gross, M., McLennan, J.D. & Schatz, J.F. *Description and Evaluation of a Mechanistically Based Conceptual Model for Spall*, SAND97-1369, Sandia National Laboratories, Albuquerque, NM, 1997.

18. Knowles, M.K., Hansen, F.D., Thompson, T.W., Gross, M.B., & Schatz, J.F., Review and Perspectives on Spallings Releases in the 1996 Performance Assessment for the Waste Isolation Pilot Plant, *Reliability Engineering and System Safety* (in this issue).

19. Stockman, C.T., Garner, J.W., Helton, J.C., Johnson, J. D., Shinta, A., & Smith, L.N., Radionuclide Transport in the Vicinity of the Repository and Associated Complementary Cumulative Distribution Functions in the 1996 Performance Assessment for the Waste Isolation Pilot Plant, *Reliability Engineering and System Safety* (in this issue).

20. Kleijnen, J.P.C., & Helton, J.C., Statistical Analyses of Scatterplots to Identify Important Factors in Large-Scale Simulations, 1: Review and Comparison of Techniques, *Reliability Engineering and System Safety*, 1999, **65**, 147-185.

21. Kleijnen, J.P.C., & Helton, J.C., Statistical Analyses of Scatterplots to Identify Important Factors in Large-Scale Simulations, 2: Robustness of Techniques, *Reliability Engineering and System Safety*, 1999, **65**, 187-197.

22. Shortencarier, M.J., & Helton, J.C., *User's Manual for PATTRN, a FORTRAN Program for Identifying Patterns in Scatterplots*, SAND99-1058, Sandia National Laboratories, Albuquerque, NM, 1999.

23. Helton, J.C., Garner, J.W., Marietta, M.G., Rechard, R.P., Rudeen, D.K., & Swift, P.N., Uncertainty and Sensitivity Analysis Results Obtained in a Preliminary Performance Assessment for the Waste Isolation Pilot Plant, *Nuclear Science and Engineering*, 1993, **114**(4), 286-331.

24. Helton, J.C., Anderson, D.R., Baker, B.L., Bean, J.E., Berglund, J.W., Beyeler, W., Garner, J.W., Iuzzolino, H.J., Marietta, M.G., Rechard, R.P., Roache, P.J., Rudeen, D.K., Schreiber, J.D., Swift, P.N., Tierney, M.S., & Vaughn, P., Effect of Alternative Conceptual Models in a Preliminary Performance Assessment for the Waste Isolation Pilot Plant, *Nuclear Engineering and Design*, 1995, **154**(3), 251-344.

25. Helton, J.C., Anderson, D.R., Baker, B.L., Bean, J.E., Berglund, J.W., Beyeler, W., Economy, K., Garner, J.W., Hora, S.C., Iuzzolino, H.J., Knupp, P., Marietta, M.G., Rath, J., Rechard, R.P., Roache, P.J., Rudeen, D.K., Salari, K., Schreiber, J.D., Swift, P.N., Tierney, M.S., & Vaughn, P., Uncertainty and Sensitivity Analysis Results Obtained in the 1992 Performance Assessment for the Waste Isolation Pilot Plant, *Reliability Engineering and System Safety*, 1996, **51**(1), 53-100.

26. Stoelzel, D.M., & O'Brien, D.G., *Analysis Package for the BRAGFLO Direct Release Calculations (Task 4) of the Performance Assessment Analyses Supporting the Compliance Certification Application*, Sandia WIPP Central Files WPO #40520, Sandia National Laboratories, Albuquerque, NM, 1996.

Figure Captions

Fig. 1. Uncertainty and sensitivity analysis results for cumulative brine flow from anhydrite marker beds (*BRAALIC*) for an intrusion at 1000 yr into lower waste panel; similar results are obtained for an E1 intrusion (Fig. 8.2.1, Ref. 11).

Fig. 2. Scatterplots for cumulative brine flow from anhydrite marker beds (*BRAALIC*) over 10,000 yr for E0 conditions, an E1 intrusion at 1000 yr into lower waste panel, and an E2 intrusion at 1000 yr into lower waste panel.

Fig. 3. Cumulative brine flow over 10,000 yr into DRZ (*BRM38NIC*, *BRM38SIC*, *BRAABNIC*, *BRAABSIC*, *BRM39NIC*, *BRM39SIC*) and into repository (*BRNREPTC*) for an E2 intrusion at 1000 yr into lower waste panel.

Fig. 4. Uncertainty and sensitivity analysis results for cumulative brine flow into repository (*BRNREPTC*) for E1 and E2 intrusions at 1000 yr into lower waste panel.

Fig. 5. Uncertainty and sensitivity analysis results for cumulative brine flow down borehole (*BNBHDNUZ*) for E1 and E2 intrusions at 1000 yr into lower waste panel.

Fig. 6. Uncertainty and sensitivity analysis results for cumulative brine flow up borehole from brine pocket into bottom of lower DRZ (*BNBHLDRZ*) for E1 intrusion at 1000 yr into lower waste panel.

Fig. 7. Scatterplots for brine flow out of the brine pocket between 1000 and 1200 yr (*BHLDRZD* = *BNBHLDRZ* at 1200 yr – *BNBHLDRZ* at 1000 yr) versus *WMICDFLG* and repository pressure at 1000 yr (*WAS_PRES* at 1000 yr) for an E1 intrusion into lower waste panel at 1000 yr.

Fig. 8. Scatterplots for cumulative brine inflow into the repository (*BRNREPTC*) over 10,000 yr for an E1 intrusion at 1000 yr into lower waste panel minus cumulative brine inflow into the repository over 10,000 yr for an E2 intrusion at 1000 yr into lower waste panel (i.e., (E1: 0 - 10,000 yr) – (E2: 0 - 10,000 yr) in Table 3) versus *BPCOMP* and *BHPRM*.

Fig. 9. Scatterplots for cumulative brine flow through borehole into upper DRZ (*BNBHDNUZ*) over 10,000 yr for E1 and E2 intrusions at 1000 yr into lower waste panel versus *BHPRM*.

Fig. 10. Scatterplots for cumulative brine flow down a borehole into the upper DRZ (*BNBHDNUZ*) over 10,000 yr for an E2 intrusion at 1000 yr into lower waste panel minus cumulative brine flow down a borehole into the upper DRZ over 10,000 yr for an E1 at 1000 yr into lower waste panel (i.e., (E2: Upper DRZ) – (E1: Upper DRZ) in Table 4) versus *BHPRM* and *BPCOMP*.

Fig. 11. Scatterplots for cumulative brine flow from borehole into lower DRZ (*BNBHLDRZ*) over 10,000 yr for an E1 intrusion at 1000 yr into lower waste panel versus *BPCOMP*. (see Fig. 8.2.12, Ref. 11, for *BHPRM* and *WMICDFLG*.

Fig. 12. Uncertainty and sensitivity analysis results for cumulative gas generation due to corrosion (*FE_MOLE*) for an intrusion at 1000 yr into lower waste panel; similar results are obtained for an E1 intrusion (Fig. 8.3.1, Ref. 11).

Fig. 13. Scatterplots for cumulative gas generation over 10,000 yr due to corrosion (*FE_MOLE*) for E0 conditions, an E1 intrusion at 1000 yr into lower waste panel, and an E2 intrusion at 1000 yr into lower waste panel.

Fig. 14. Scatterplots for cumulative gas generation due to corrosion (*FE_MOLE*) at 10,000 yr for an E2 intrusion at 1000 yr into lower waste panel versus *HALPOR* and *WGRCOR*.

Fig. 15. Scatterplots for difference between cumulative gas generation due to corrosion (*FE_MOLE*) over 10,000 yr for E1 and E2 intrusions at 1000 yr into lower waste panel (i.e., (E1: 0 - 10,000 yr) - (E2: 0 -10,000 yr) in Table 5) versus *BPCOMP*, *BHPRM* and *WMICDFLG*.

Fig. 16. Uncertainty and sensitivity analysis results for cumulative gas generation due to corrosion and microbial degradation (*GAS_MOLE*) for an intrusion at 1000 yr into lower waste panel; similar results are obtained for an E1 intrusion (Fig. 8.3.5, Ref. 11).

Fig. 17. Scatterplots for cumulative gas generation due to corrosion and microbial degradation (*GAS_MOLE*) at 10,000 yr for E0 conditions, an E1 intrusion at 1000 yr into lower waste panel, and an E2 intrusion at 1000 yr into lower waste panel.

Fig. 18. Uncertainty and sensitivity analysis results for fraction of steel remaining in upper waste panels (*FEREM_R*) (upper frames) and lower waste panel (*FEREM_W*) (lower frames) for an E2 intrusion at 1000 yr into lower waste panel; similar results are obtained for an E1 intrusion (Fig. 8.3.8, Ref. 11).

Fig. 19. Scatterplots for fraction of steel consumed in upper waste panels (1–*FEREM_R*) (left frames) and lower waste panel (1–*FEREM_W*) (right frames) between 1000 and 10,000 yr for an E2 intrusion at 1000 yr into lower waste panel versus *HALPOR*, *WGRCOR*, *BHPRM*, and *ANHPRM*.

Fig. 20. Scatterplots for fraction of steel in lower waste panel consumed by corrosion (1–*FEREM_W*) over 10,000 yr for E1 and E2 intrusions at 1000 yr into lower waste panel versus *WGRCOR*.

Fig. 21. Scatterplots for fraction of steel in upper waste panels (1–*FEREM_R*) (left frames) and lower waste panel (1–*FEREM_W*) (right frames) consumed by corrosion between 1000 and 10,000 yr for an E1 intrusion at 1000 yr into lower waste panel versus *HALPOR*, *WGRCOR*, *BHPRM* and *WASTWICK*.

Fig. 22. Scatterplots for fraction of steel in upper (1–*FEREM_R*) and lower (1–*FEREM_W*) waste panels consumed by corrosion for E1 and E2 intrusions at 1000 yr into lower waste panel.

Fig. 23. Uncertainty and sensitivity analysis results for cumulative gas generation due to corrosion and microbial degradation in upper waste panels (*GSMOL_R*) (upper frames) and lower waste panel (*GASMOL_W*) (lower frames) for an E2 intrusion at 1000 yr into lower waste panel; similar results are obtained for an E1 intrusion (Fig. 8.3.17, Ref. 11).

Fig. 24. Uncertainty and sensitivity analysis results for repository pressure (*WAS_PRES*) for an E1 intrusion into lower waste panel at 1000 yr; similar results are obtained for an E2 intrusion (Fig. 8.4.1, Ref. 11).

Fig. 25. Scatterplots for repository pressure in upper (*REP_PRES*) and lower (*WAS_PRES*) waste panels at 10,000 yr for an E1 intrusion into lower waste panel at 1000 yr; similar results are obtained for an E2 intrusion (Fig. 8.4.2, Ref. 11).

Fig. 26. Pressure in waste panel (*WAS_PRES*) penetrated by an E1 intrusion at 1000 yr (i.e., the lower waste panel) and in rest of repository (*REP_PRES*) (i.e., the upper waste panels).

Fig. 27. Scatterplot for repository pressure (*WAS_PRES*) at 1000 yr under undisturbed conditions versus *WMICDFLG*.

Fig. 28. Scatterplots for repository pressure (*WAS_PRES*) at 10,000 yr versus *BHPRM* for an E1 intrusion at 1000 yr into lower waste panel; similar results are obtained for an E2 intrusion (Fig. 8.4.5, Ref. 11).

Fig. 29. Uncertainty analysis results for total pore volume in repository (*PORVOL_T*) for an E1 intrusion into lower waste panel at 1000 yr; similar results are obtained for an E2 intrusion (Fig. 8.4.6, Ref. 11).

Fig. 30. Uncertainty and sensitivity analysis results for brine saturation in upper (*REP_SATB*) and lower (*WAS_SATB*) waste panels for an E2 intrusion at 1000 yr into lower waste panel (Note: Plots for PRCCs show all variables that have a PRCC that exceeds 0.5 in absolute value at some point in time, with the PRCCs for the variables with the five largest, in absolute value, PRCCs being plotted and the maximum, in absolute value, PRCCs being shown for the remaining variables together with the intervals over which the PRCCs exceed 0.5 in absolute value); similar results are obtained for an E1 intrusion (Fig. 8.5.2, Ref. 11).

Fig. 31. Uncertainty analysis results for brine saturation in lower (*WAS_SATB*) waste panel for an E1 intrusion at 1000 yr into lower waste panel.

Fig. 32. Scatterplots for brine saturation in lower waste panel (*WAS_SATB*) at 10,000 yr for an E2 intrusion at 1000 yr into lower waste panel versus *BHPRM* and *WRGSSAT*.

Fig. 33. Uncertainty and sensitivity analysis results for brine volume in upper (*BRNVOL_R*) and lower (*BRNVOL_W*) waste panels for an E2 intrusion at 1000 yr into lower waste panel (See Note, Fig. 30).

Fig. 34. Uncertainty and sensitivity analysis results for brine volume in upper (*BRNVOL_R*) and lower (*BRNVOL_W*) waste panels for an E1 intrusion at 1000 yr into lower waste panel.

Fig. 35. Scatterplots for brine volume in upper (*BRNVOL_R*) and lower (*BRNVOL_W*) waste panels versus *BHPRM* at 10,000 yr for an E2 intrusion at 1000 yr into lower waste panel.

Fig. 36. Scatterplot for repository pressure (*WAS_PRES*) at 10,000 yr versus brine volume in lower waste panel (*BRNVOL_W*) for an E2 intrusion at 1000 yr into lower waste panel; similar results are obtained for an E1 intrusion (Fig. 8.5.8, Ref. 11).

Fig. 37. Scatterplot for brine volume in lower waste panel (*BRNVOL_W*) at 10,000 yr for an E1 intrusion at 1000 yr into lower waste panel versus *BHPRM*.

Fig. 38. Uncertainty and sensitivity analysis results for cumulative gas flow up borehole at top of DRZ (*GSMBHUDZ*) for an E2 intrusion at 1000 yr into lower waste panel (See Note, Fig. 30); similar results are obtained for an E1 intrusion (Fig. 8.61, Ref. 11).

Fig. 39. Uncertainty and sensitivity analysis results for cumulative brine flow up borehole at top of DRZ (*BNBHUDRZ*) for E1 and E2 intrusions at 1000 yr into lower waste panel.

Fig. 40. Uncertainty and sensitivity analysis results for pressure (*B_P_PRES*) and brine volume (*BRNVOL_B*) in brine pocket for an E1 intrusion at 1000 yr into lower waste panel.

Fig. 41. Scatterplots for brine pocket pressure (*B_P_PRES*) at 10,000 yr versus *BPCOMP* and *BHPRM* for an E1 intrusion at 1000 yr into lower waste panel.

Fig. 42. Scatterplots for brine volume in pressurized brine pocket (*BRNVOL_B*) at 10,000 yr versus *BPVOL* and *BPCOMP* for an E1 intrusion at 1000 yr into lower waste panel.

Fig. 43. Cumulative brine flow into repository (*BRNREPTC*), cumulative brine flow down intruding boreholes (*BNBHDNUZ*), and cumulative brine flow into bottom of DRZ from brine pocket (*BNBHLDRZ*) for an E2E1 intrusion into lower waste panel with the E2 intrusion at 800 yr and the E1 intrusion at 2000 yr.

Fig. 44. Cumulative gas generation due to corrosion and microbial degradation (*GAS_MOLE*) for an E2E1 intrusion into lower waste panel with the E2 intrusion at 800 yr and the E1 intrusion at 2000 yr.

Fig. 45. Repository pressure (*WAS_PRES*) for an E2E1 intrusion into lower waste panel with the E2 intrusion at 800 yr and the E1 intrusion at 2000 yr.

Fig. 46. Brine saturation in upper (*REP_SATB*) and lower (*WAS_SATB*) waste panels for an E2E1 intrusion into lower waste panel with the E2 intrusion at 800 yr and the E1 intrusion at 2000 yr.

Fig. 47. Brine volume in upper (*BRNVOL_R*) and lower (*BRNVOL_W*) waste panels for an E2E1 intrusion into lower waste panel with the E2 intrusion at 800 yr and the E1 intrusion at 2000 yr.

Fig. 48. Cumulative brine flow up borehole at top of DRZ (*BNBHUDRZ*) for an E2E1 intrusion into lower waste panel with the E2 intrusion at 800 yr and the E1 intrusion at 2000 yr.

Fig. 49. Pressure (*B_P_PRES*) and brine volume (*BRNVOL_B*) in brine pocket for an E2E1 intrusion into lower waste panel with the E2 intrusion at 800 yr and the E1 intrusion at 2000 yr.

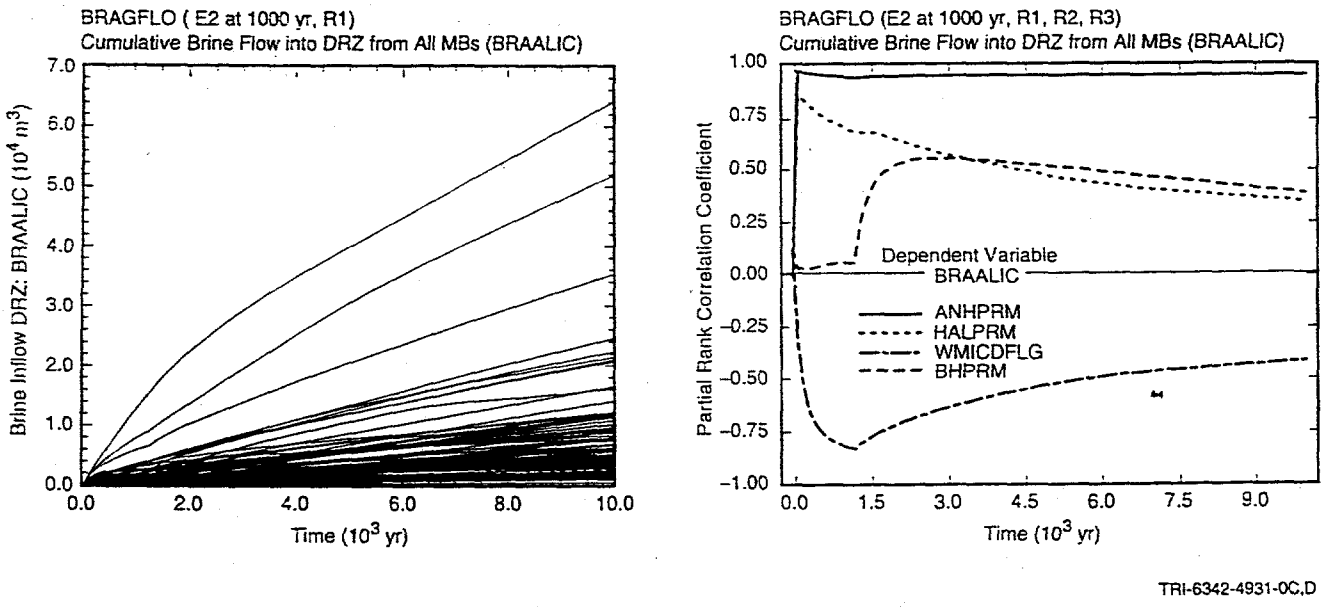

Fig. 1. Uncertainty and sensitivity analysis results for cumulative brine flow from anhydrite marker beds (*BRAALIC*) for an E2 intrusion at 1000 yr into lower waste panel; similar results are obtained for an E1 intrusion (Fig. 8.2.1, Ref. 11).

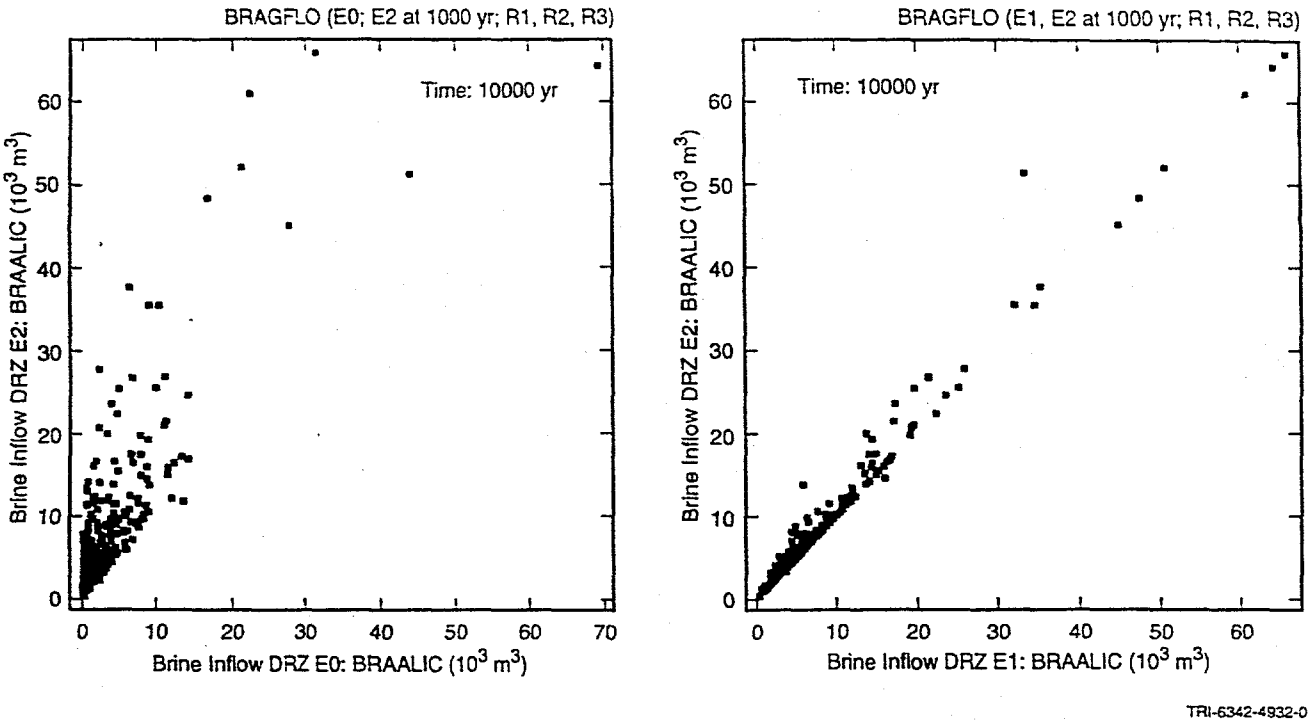

Fig. 2. Scatterplots for cumulative brine flow from anhydrite marker beds (*BRAALIC*) over 10,000 yr for E0 conditions, an E1 intrusion at 1000 yr into lower waste panel, and an E2 intrusion at 1000 yr into lower waste panel.

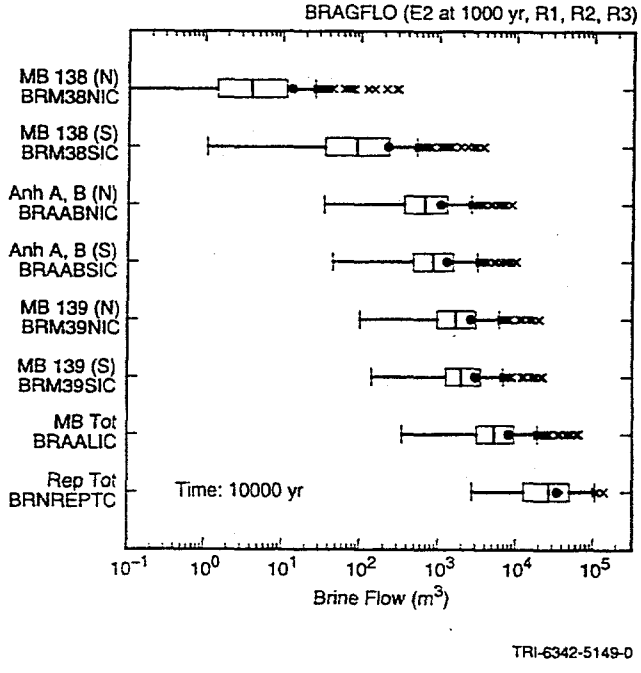

Fig. 3. Cumulative brine flow over 10,000 yr into DRZ (*BRM38NIC*, *BRM38SIC*, *BRAABNIC*, *BRAABSIC*, *BRM39NIC*, *BRM39SIC*) and into repository (*BRNREPTC*) for an E2 intrusion at 1000 yr into lower waste panel.

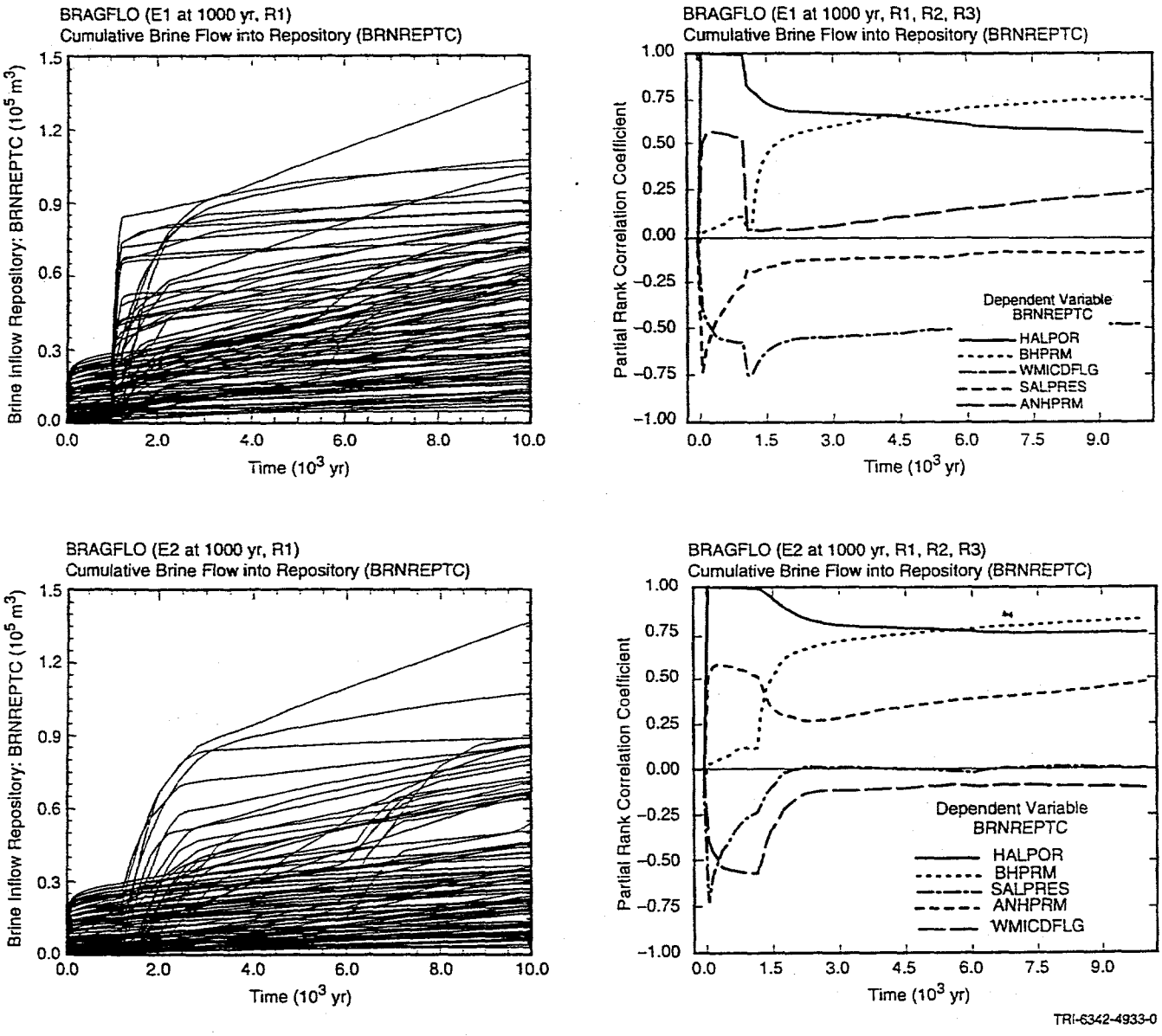

Fig. 4. Uncertainty and sensitivity analysis results for cumulative brine flow into repository (*BRNREPTC*) for E1 and E2 intrusions at 1000 yr into lower waste panel.

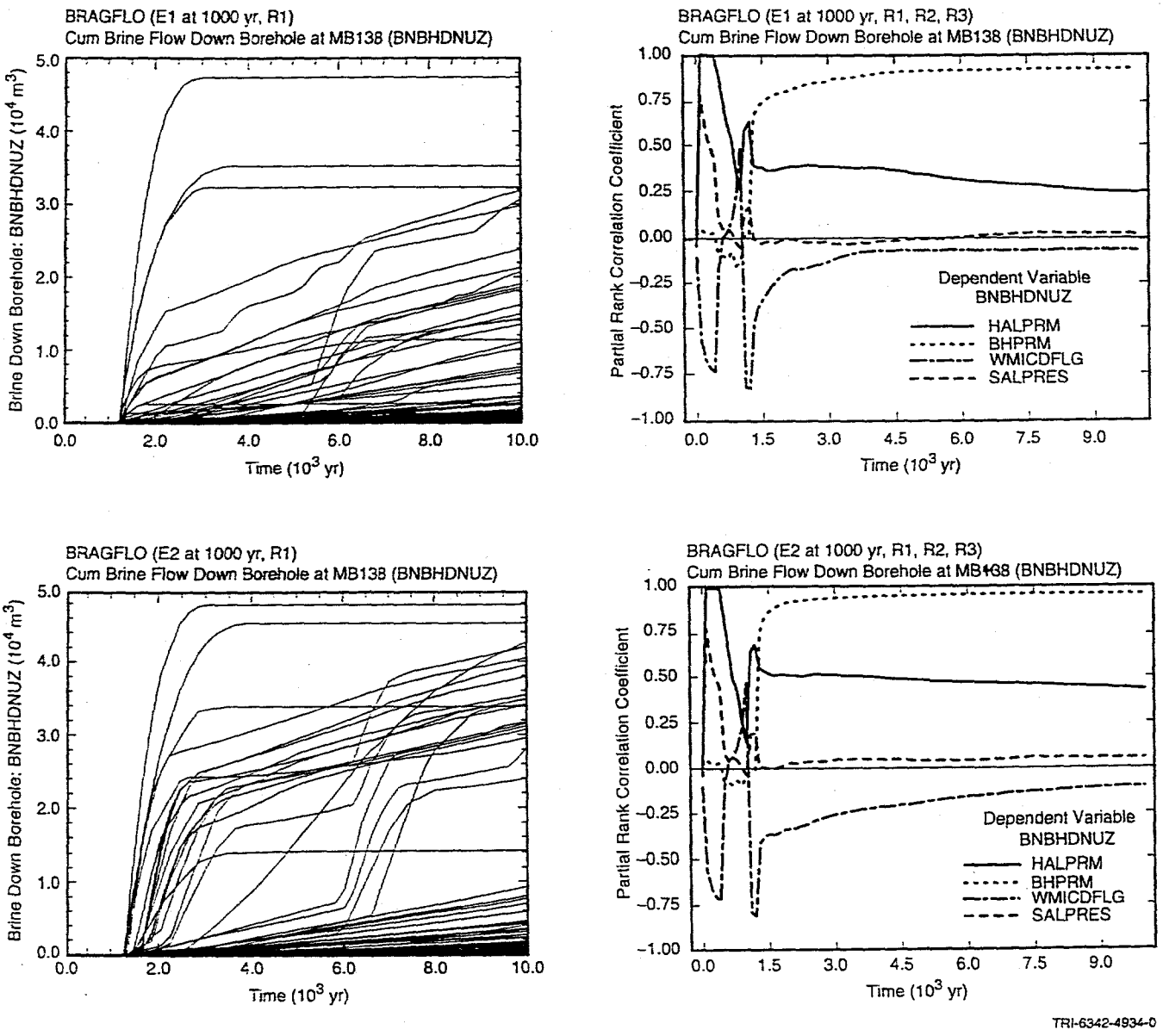

Fig. 5. Uncertainty and sensitivity analysis results for cumulative brine flow down borehole (*BNBHDNUZ*) for E1 and E2 intrusions at 1000 yr into lower waste panel.

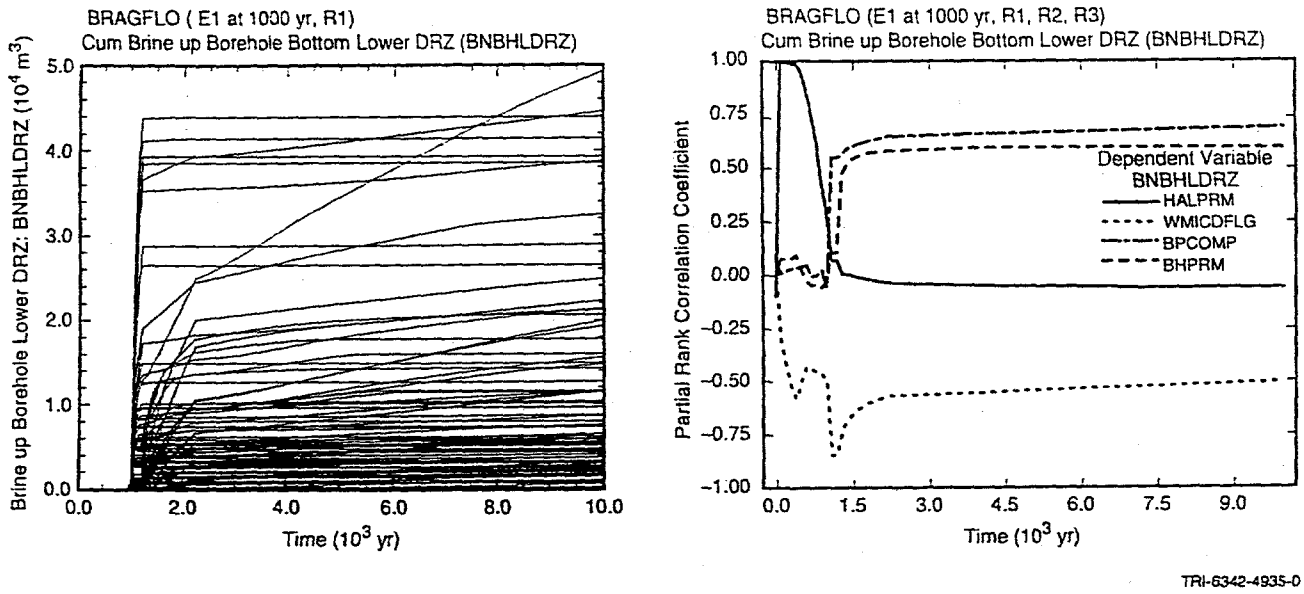

Fig. 6. Uncertainty and sensitivity analysis results for cumulative brine flow up borehole from brine pocket into bottom of lower DRZ (*BNBHLDRZ*) for E1 intrusion at 1000 yr into lower waste panel.

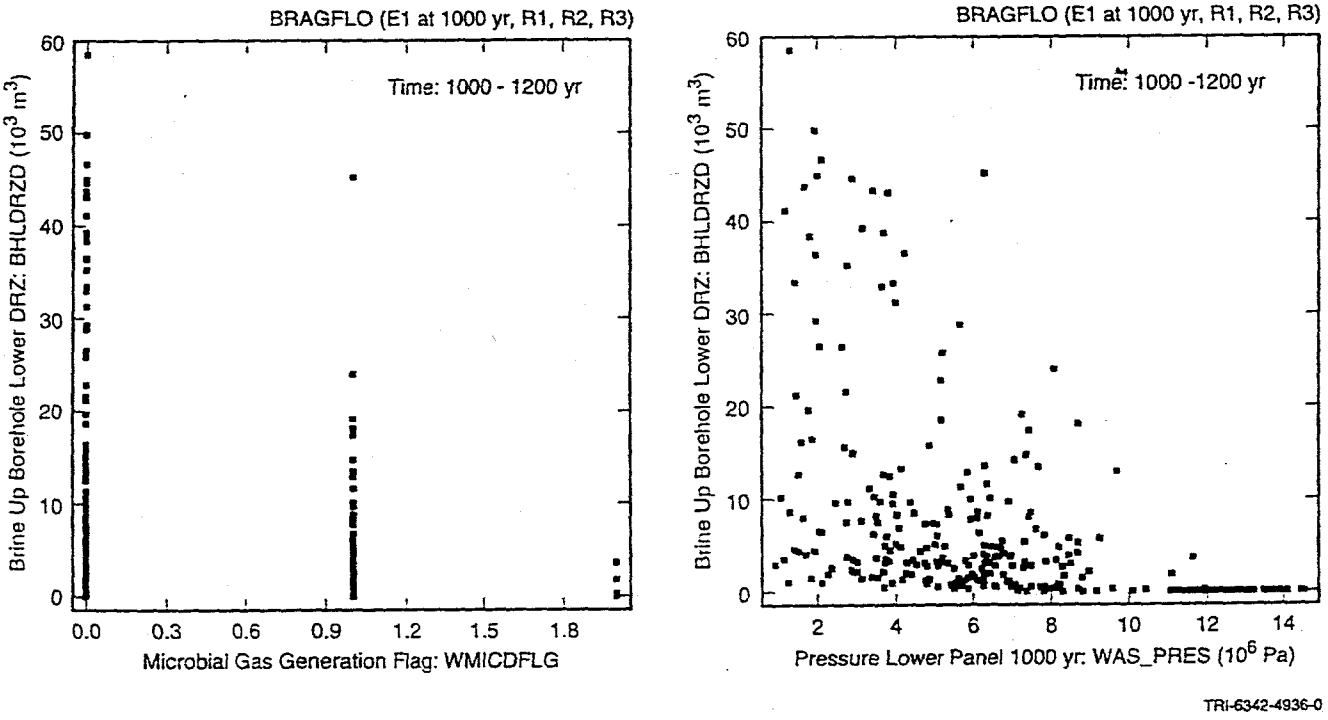

Fig. 7. Scatterplots for brine flow out of the brine pocket between 1000 and 1200 yr (*BHLDRZD* = *BNBHLDRZ* at 1200 yr – *BNBHLDRZ* at 1000 yr) versus *WMICDFLG* and repository pressure at 1000 yr (*WAS_PRES* at 1000 yr) for an E1 intrusion into lower waste panel at 1000 yr.

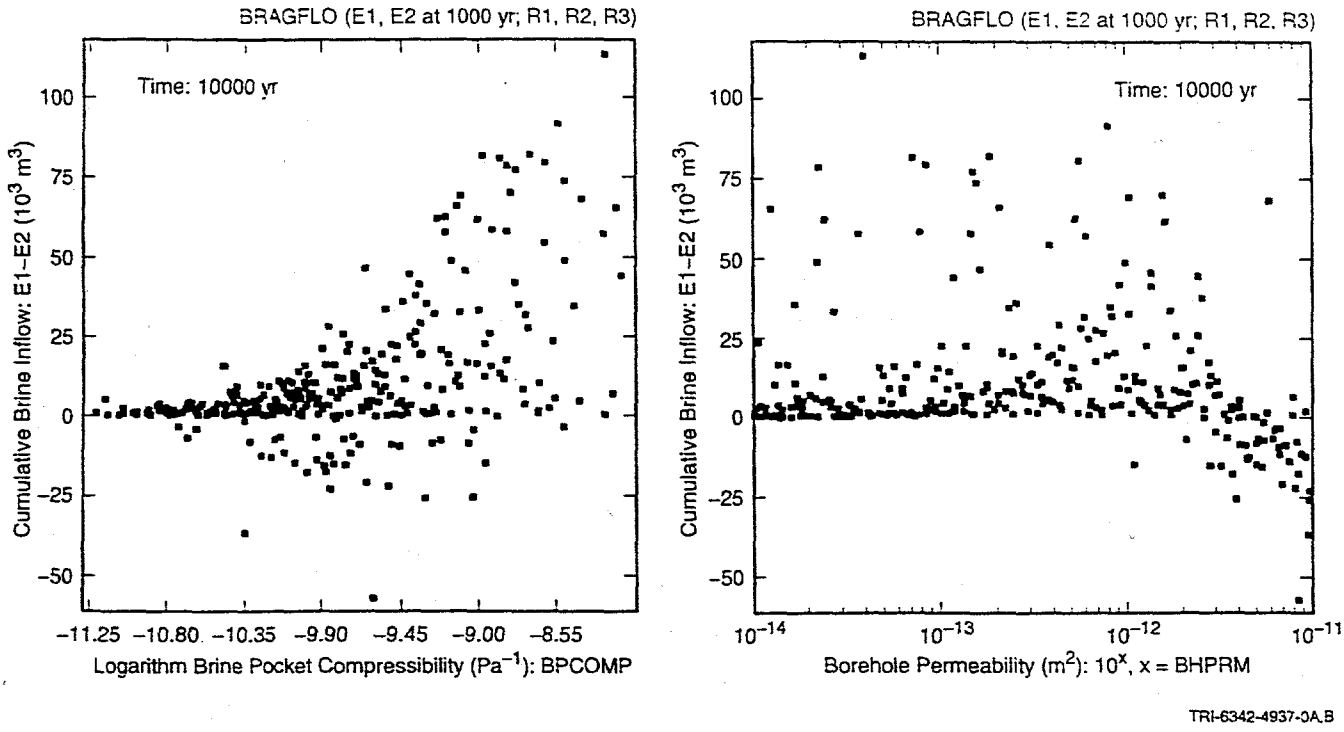

Fig. 8. Scatterplots for cumulative brine inflow into the repository (*BRNREPTC*) over 10,000 yr for an E1 intrusion at 1000 yr into lower waste panel minus cumulative brine inflow into the repository over 10,000 yr for an E2 intrusion at 1000 yr into lower waste panel (i.e., (E1: 0 - 10,000 yr) – (E2: 0 - 10,000 yr) in Table 3) versus *BPCOMP* and *BHPRM*.

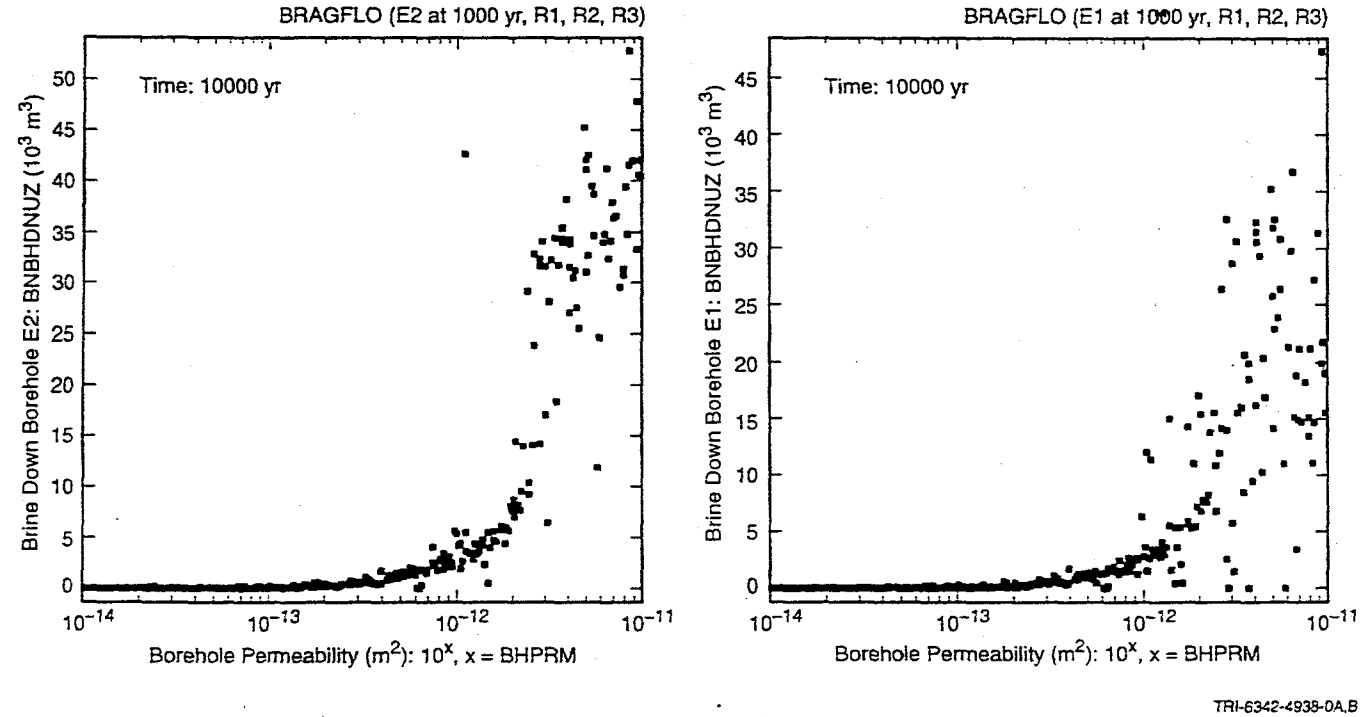

Fig. 9. Scatterplots for cumulative brine flow through borehole into upper DRZ (*BNBHDNUZ*) over 10,000 yr for E1 and E2 intrusions at 1000 yr into lower waste panel versus *BHPRM*.

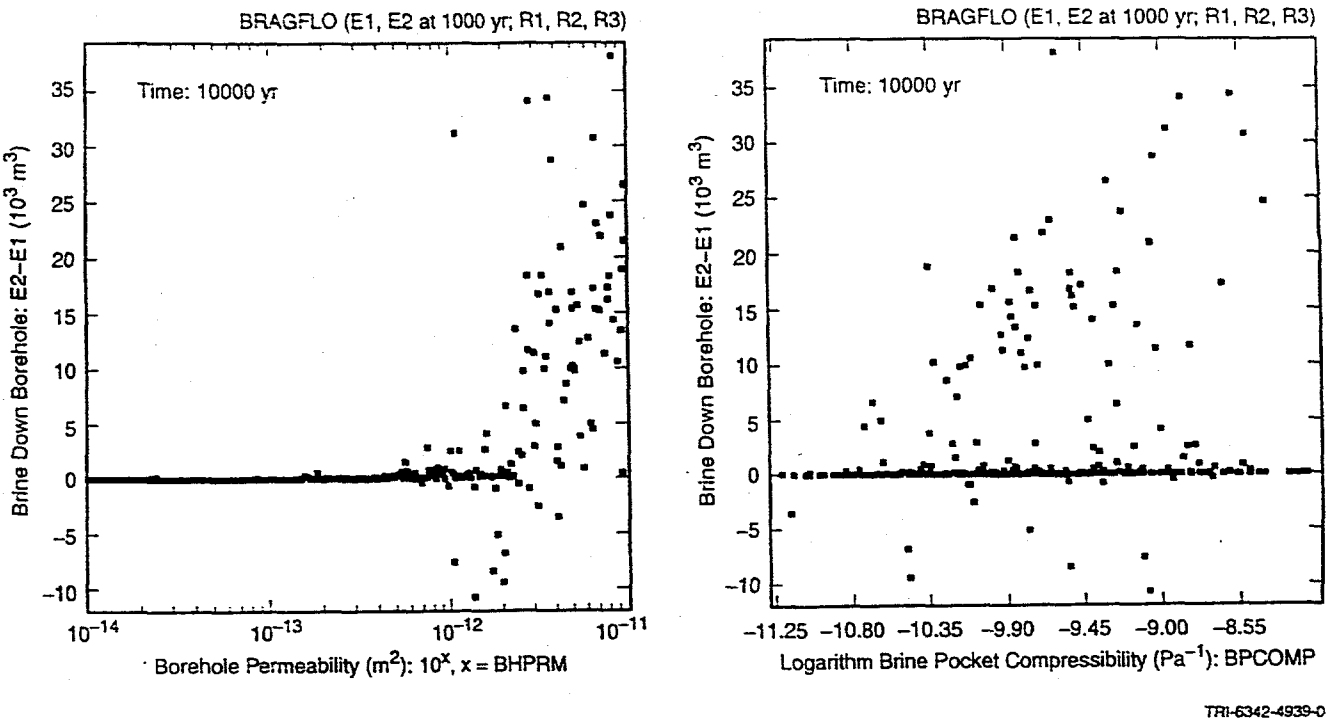

Fig. 10. Scatterplots for cumulative brine flow down a borehole into the upper DRZ (*BNBHDNUZ*) over 10,000 yr for an E2 intrusion at 1000 yr into lower waste panel minus cumulative brine flow down a borehole into the upper DRZ over 10,000 yr for an E1 at 1000 yr into lower waste panel (i.e., (E2: Upper DRZ) – (E1: Upper DRZ) in Table 4) versus *BHPRM* and *BPCOMP*.

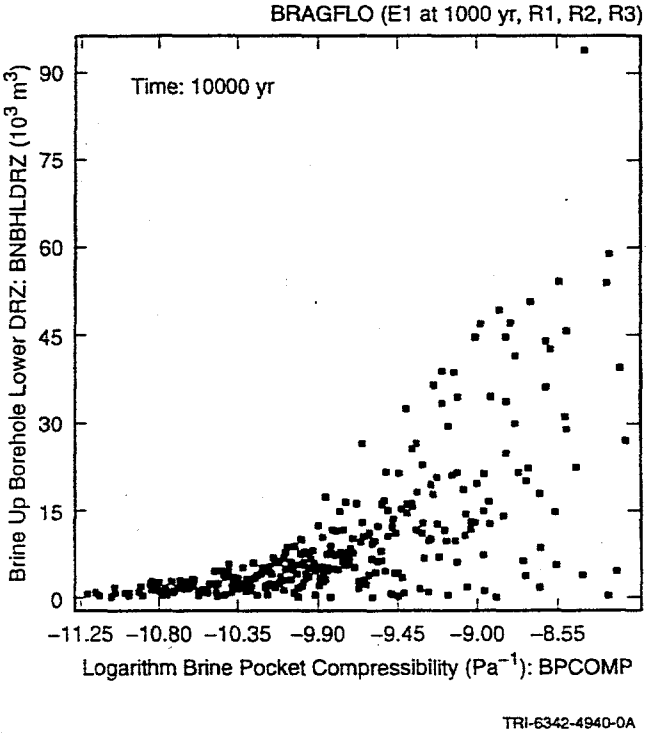

Fig. 11. Scatterplots for cumulative brine flow from borehole into lower DRZ (*BNBHLDRZ*) over 10,000 yr for an E1 intrusion at 1000 yr into lower waste panel versus *BPCOMP*. (see Fig. 8.2.12, Ref. 11, for scatterplots for *BHPRM* and *WMICDFLG*).

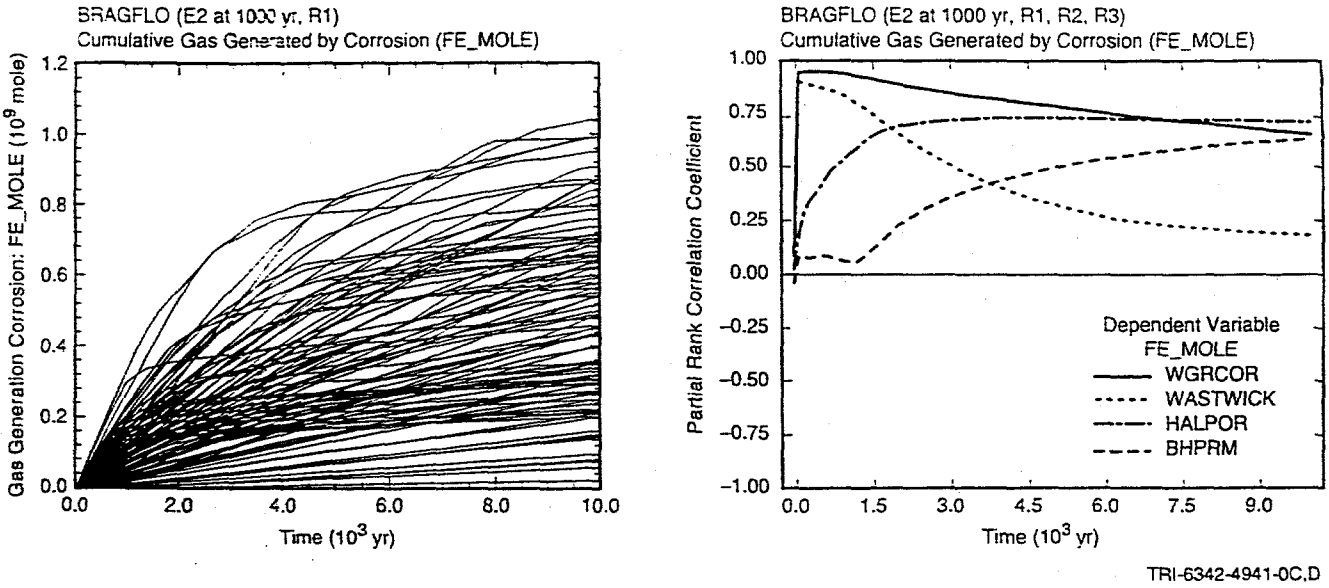

Fig. 12. Uncertainty and sensitivity analysis results for cumulative gas generation due to corrosion (*FE_MOLE*) for an E2 intrusion at 1000 yr into lower waste panel; similar results are obtained for an E1 intrusion (Fig. 8.3.1, Ref. 11).

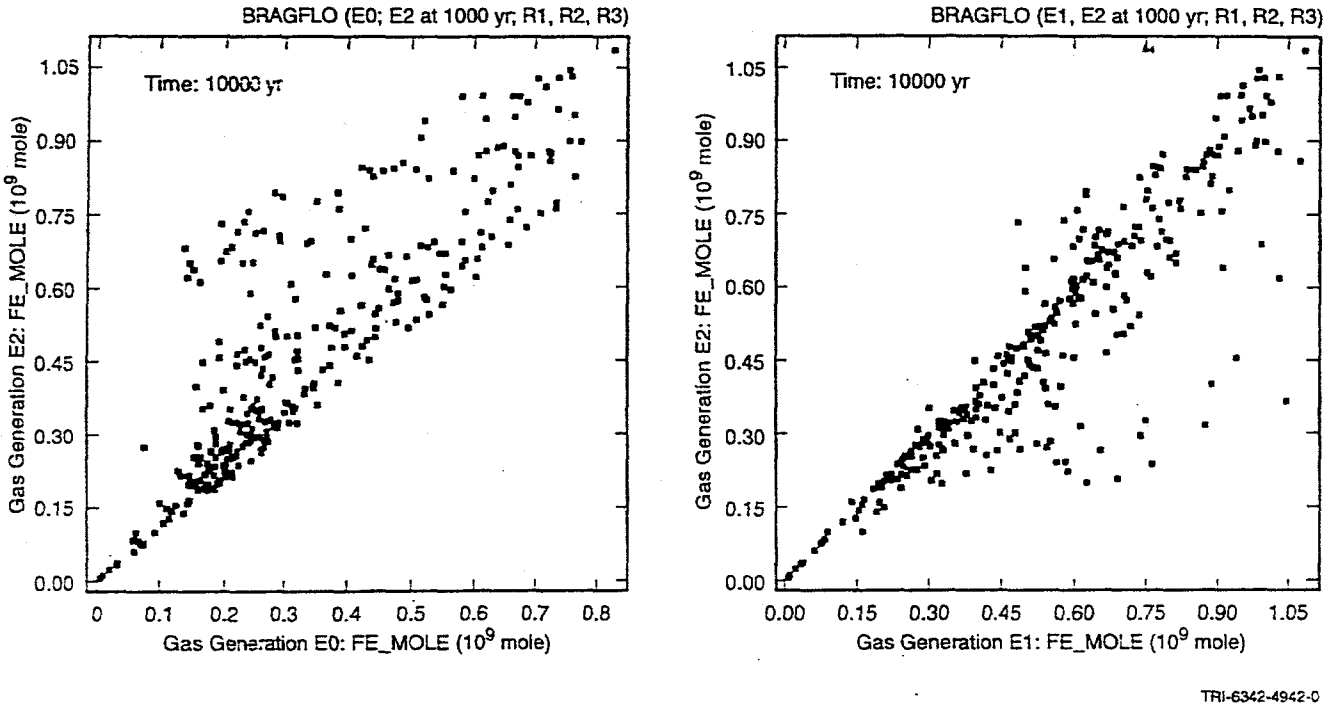

Fig. 13. Scatterplots for cumulative gas generation over 10,000 yr due to corrosion (*FE_MOLE*) for E0 conditions, an E1 intrusion at 1000 yr into lower waste panel, and an E2 intrusion at 1000 yr into lower waste panel.

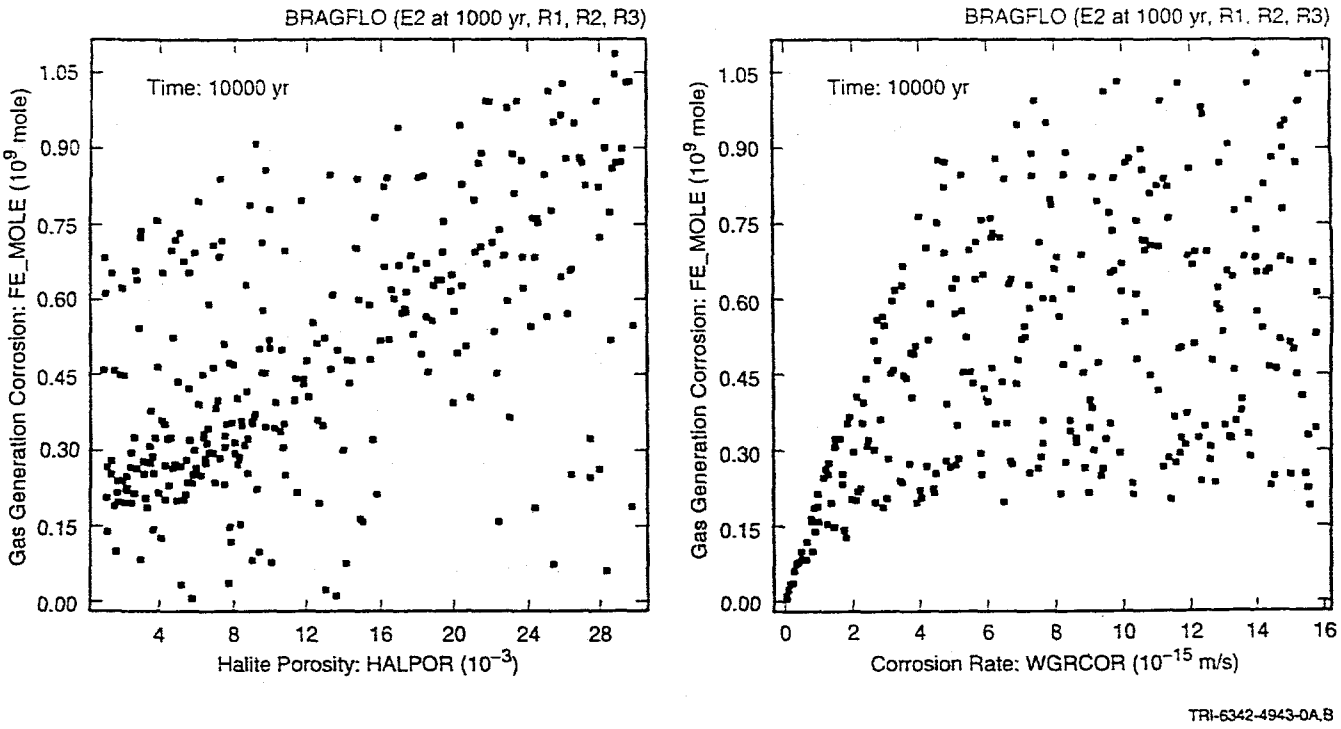

Fig. 14. Scatterplots for cumulative gas generation due to corrosion (*FE_MOLE*) at 10,000 yr for an E2 intrusion at 1000 yr into lower waste panel versus *HALPOR* and *WGRCOR*.

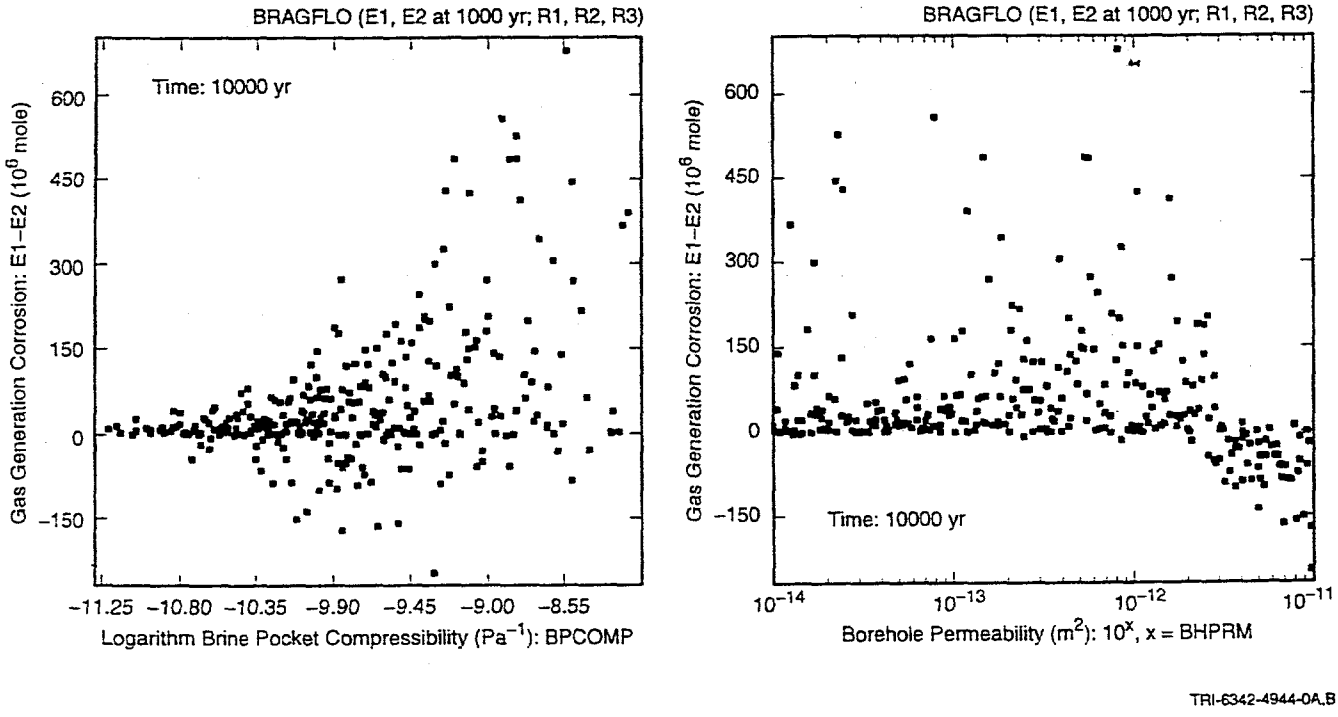

Fig. 15. Scatterplots for difference between cumulative gas generation due to corrosion (*FE_MOLE*) over 10,000 yr for E1 and E2 intrusions at 1000 yr into lower waste panel (i.e., (E1: 0 - 10,000 yr) - (E2: 0 - 10,000 yr) in Table 5) versus *BPCOMP*, *BHPRM* and *WMICDFLG*.

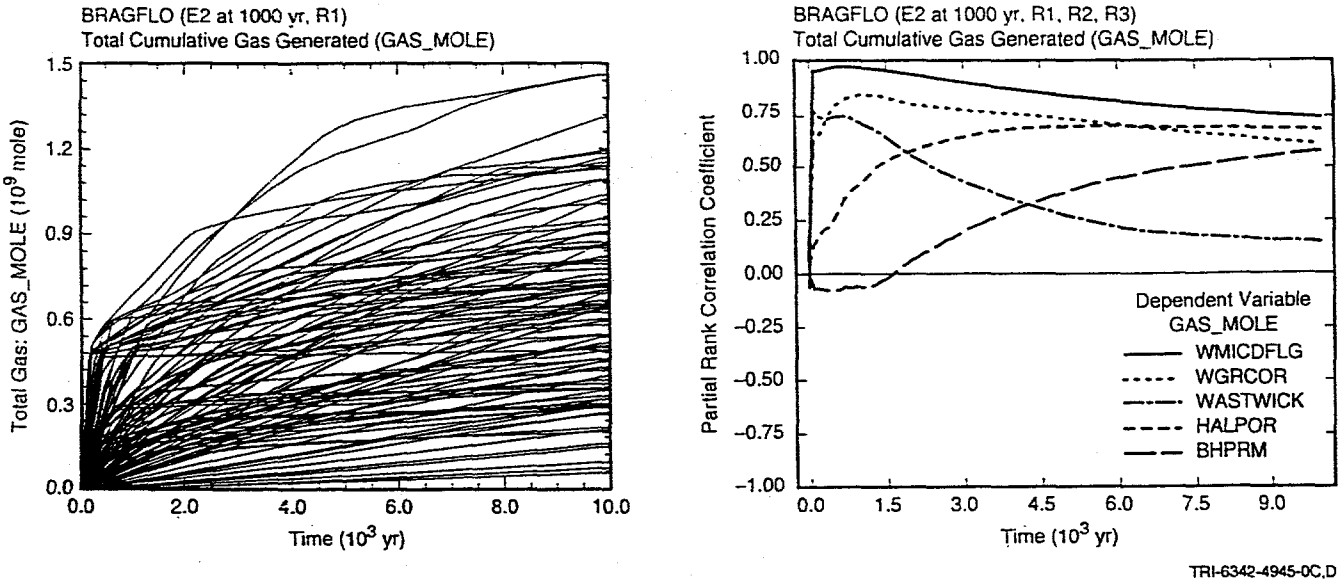

Fig. 16. Uncertainty and sensitivity analysis results for cumulative gas generation due to corrosion and microbial degradation (*GAS_MOLE*) for an E2 intrusion at 1000 yr into lower waste panel; similar results are obtained for an E1 intrusion (Fig. 8.3.5, Ref. 11).

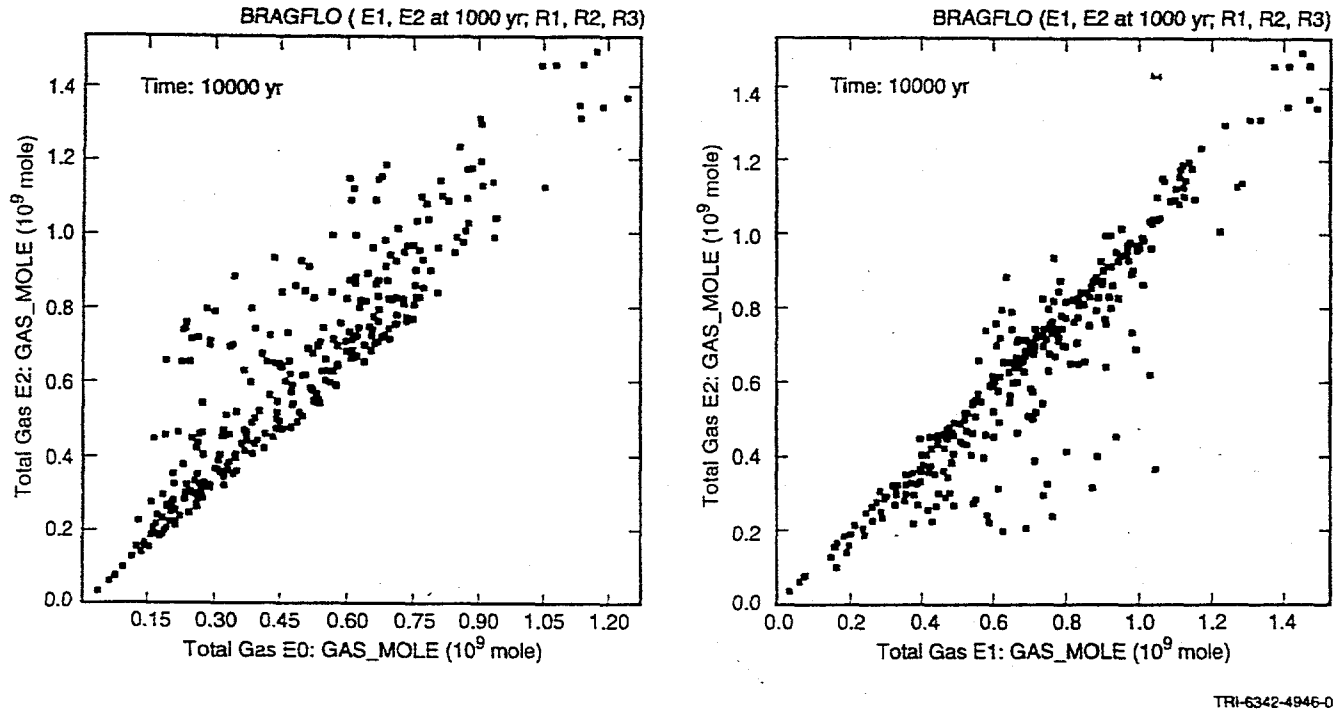

Fig. 17. Scatterplots for cumulative gas generation due to corrosion and microbial degradation (*GAS_MOLE*) at 10,000 yr for E0 conditions, an E1 intrusion at 1000 yr into lower waste panel, and an E2 intrusion at 1000 yr into lower waste panel.

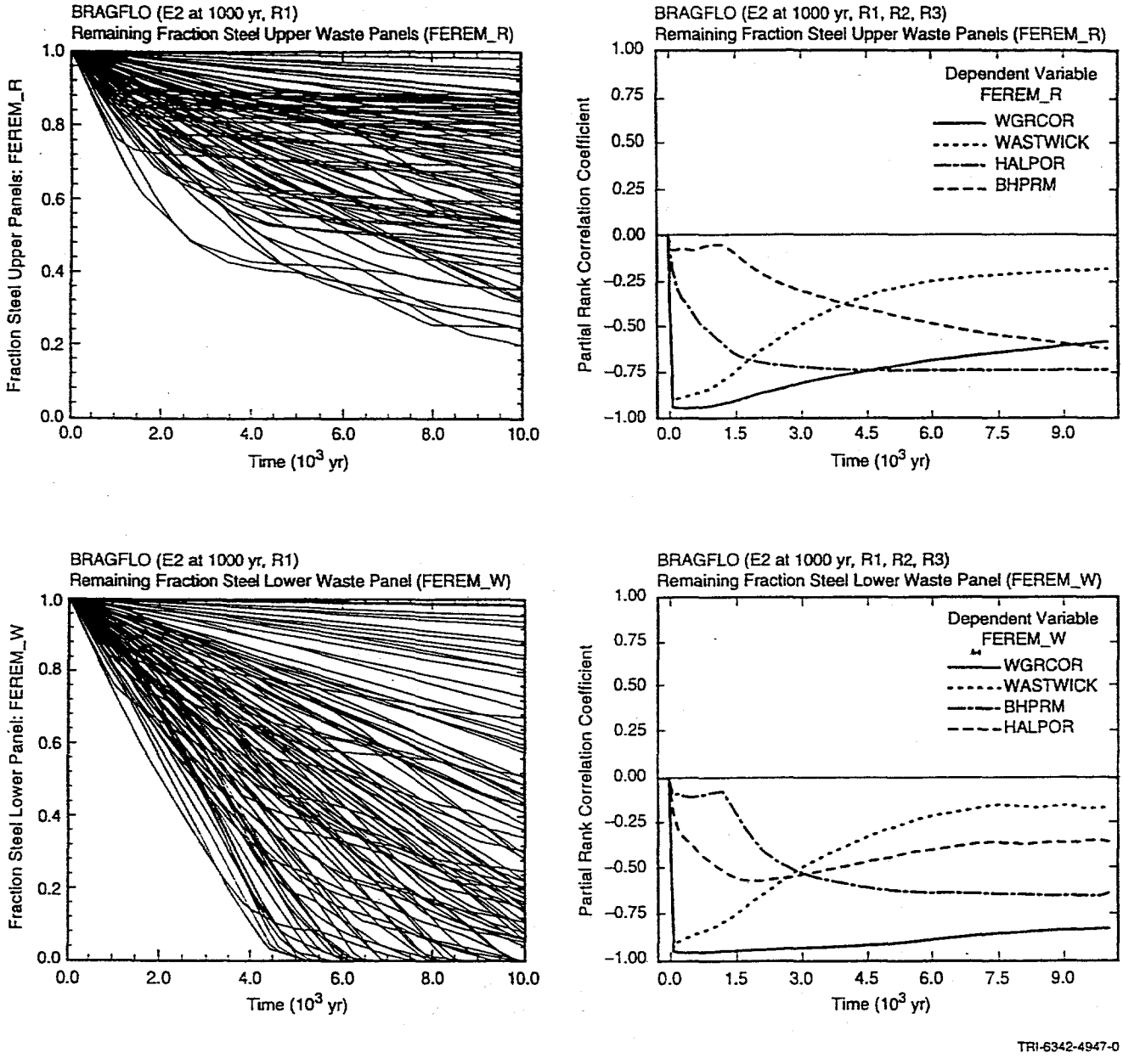

Fig. 18. Uncertainty and sensitivity analysis results for fraction of steel remaining in upper waste panels (*FEREM_R*) (upper frames) and lower waste panel (*FEREM_W*) (lower frames) for an E2 intrusion at 1000 yr into lower waste panel; similar results are obtained for an E1 intrusioin (Fig. 8.3.8, Ref. 11).

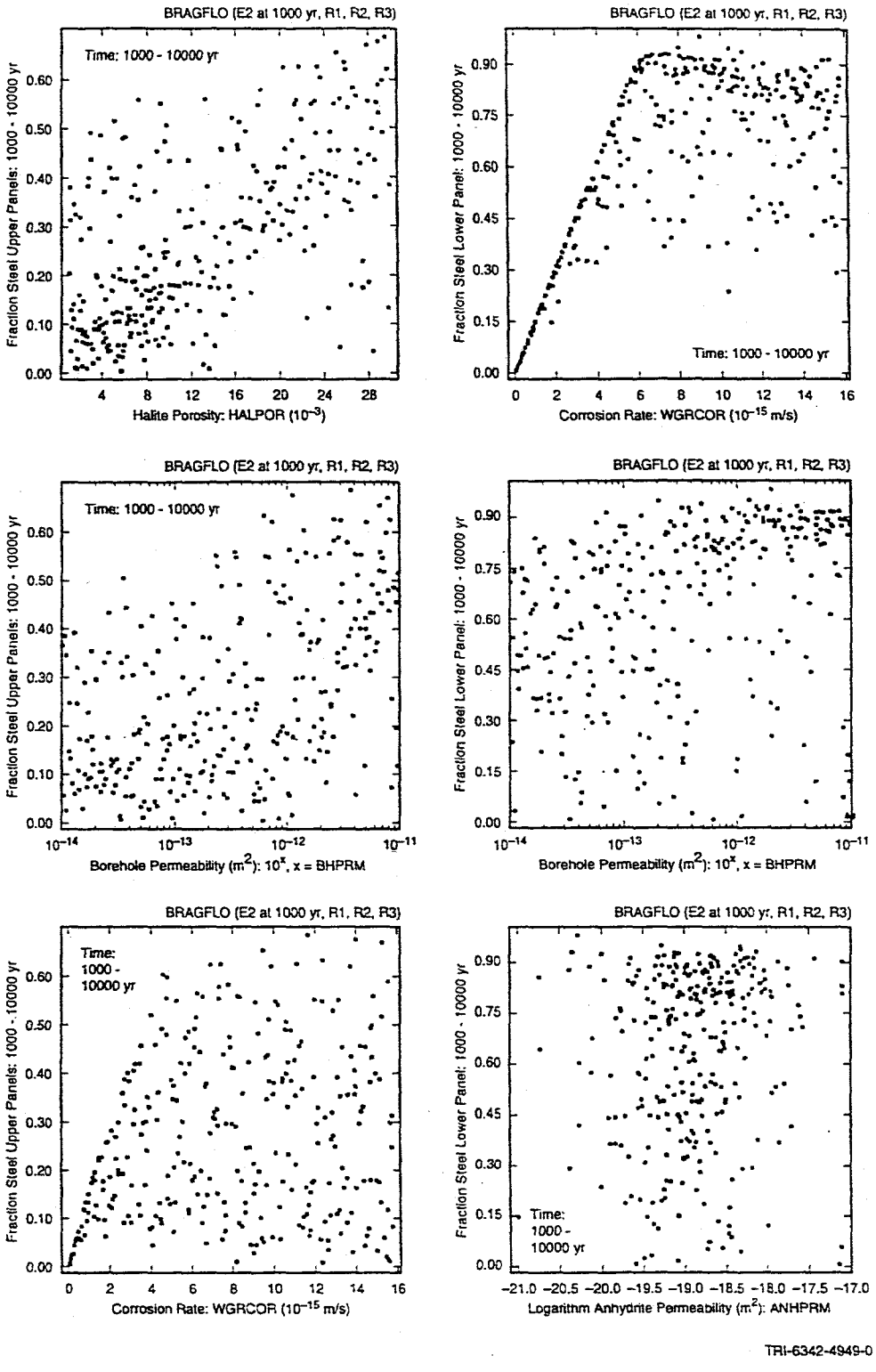

Fig. 19. Scatterplots for fraction of steel consumed in upper waste panels (1–*FEREM_R*) (left frames) and lower waste panel (1–*FEREM_W*) (right frames) between 1000 and 10,000 yr for an E2 intrusion at 1000 yr into lower waste panel versus *HALPOR*, *WGRCOR*, *BHPRM*, and *ANHPRM*.

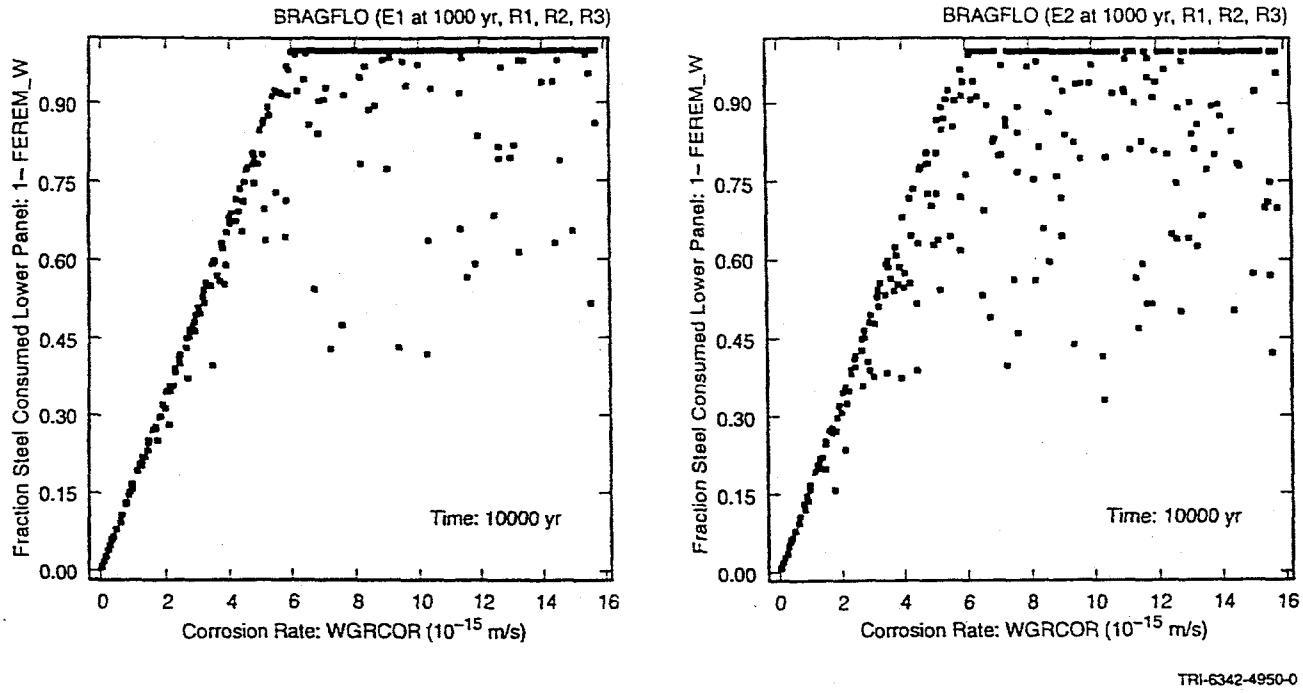

Fig. 20. Scatterplots for fraction of steel in lower waste panel consumed by corrosion (1–*FEREM_W*) over 10,000 yr for E1 and E2 intrusions at 1000 yr into lower waste panel versus *WGRCOR*.

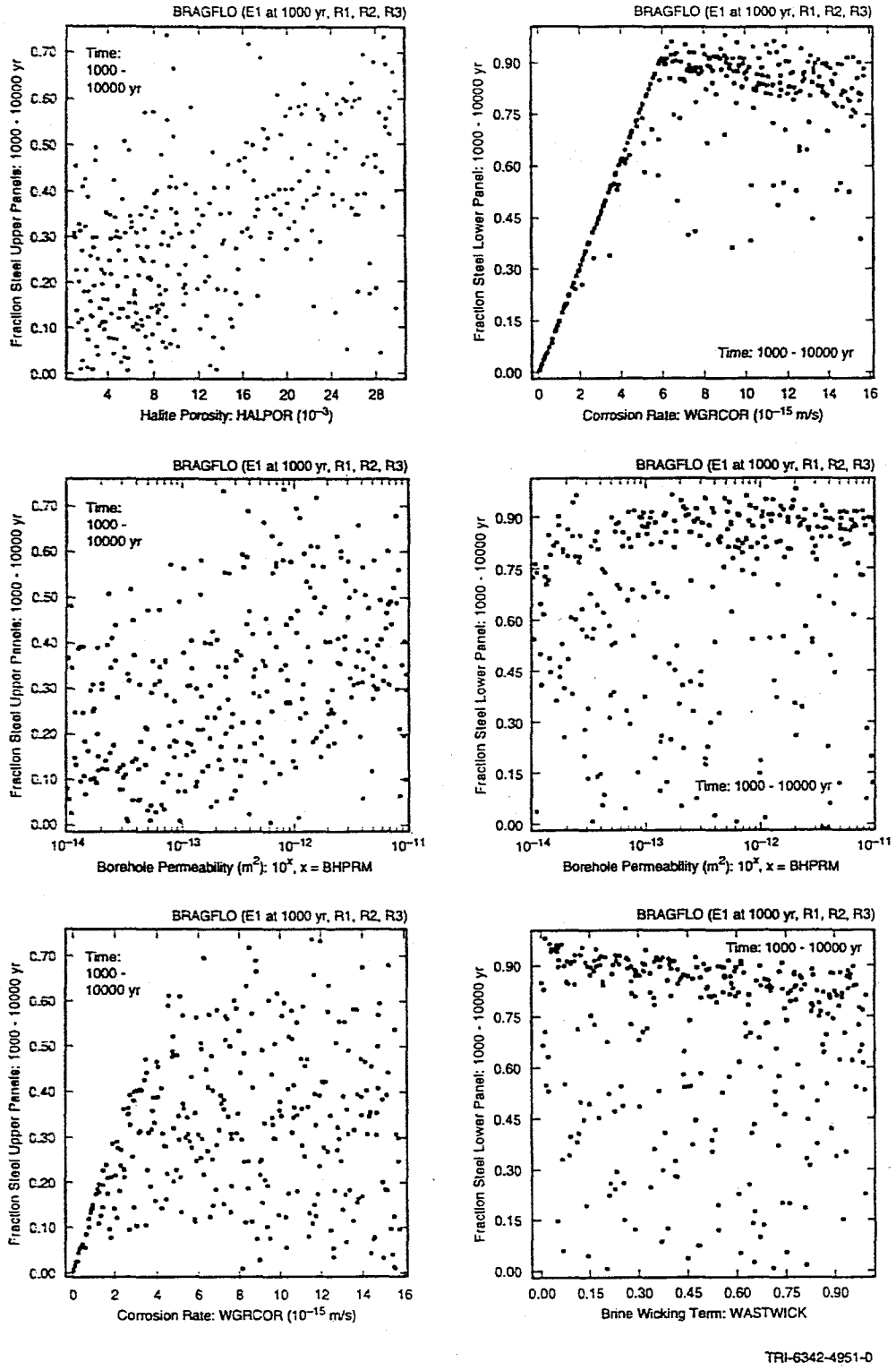

Fig. 21. Scatterplots for fraction of steel in upper waste panels (1–*FEREM_R*) (left frames) and lower waste panel (1–*FEREM_W*) (right frames) consumed by corrosion between 1000 and 10,000 yr for an E1 intrusion at 1000 yr into lower waste panel versus *HALPOR*, *WGRCOR*, *BHPRM* and *WASTWICK*.

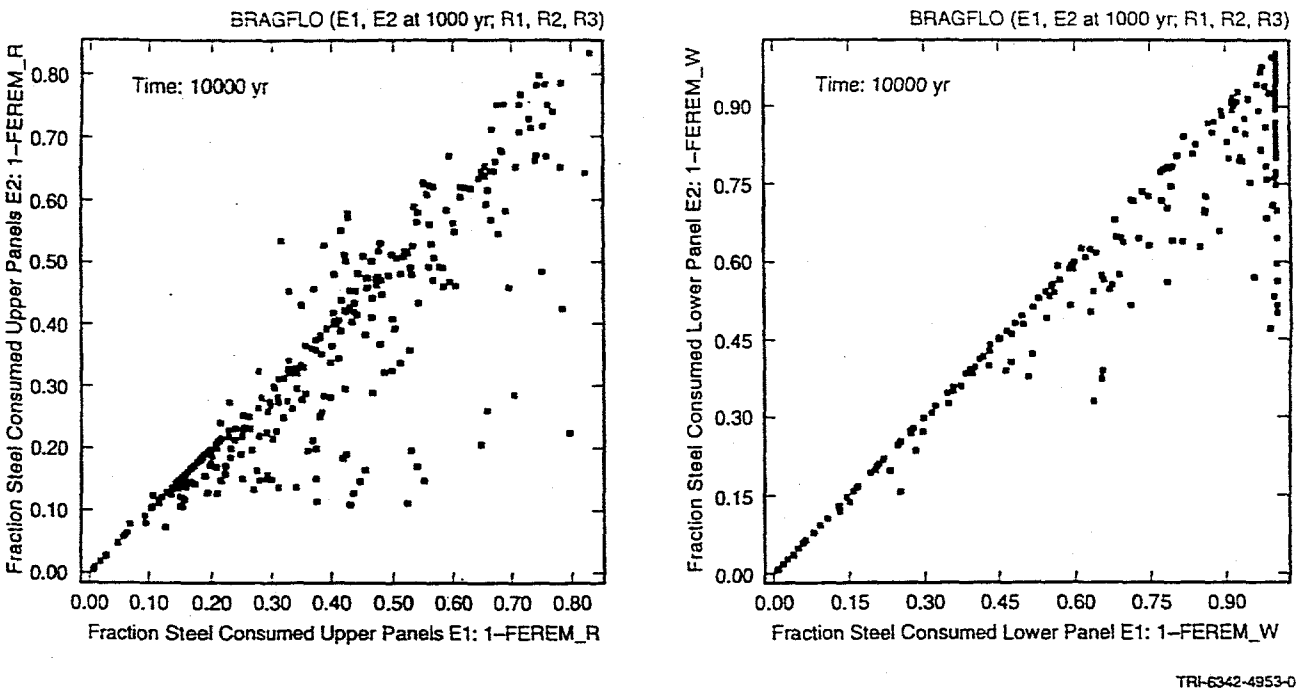

Fig. 22. Scatterplots for fraction of steel in upper (1–*FEREM_R*) and lower (1–*FEREM_W*) waste panels consumed by corrosion for E1 and E2 intrusions at 1000 yr into lower waste panel.

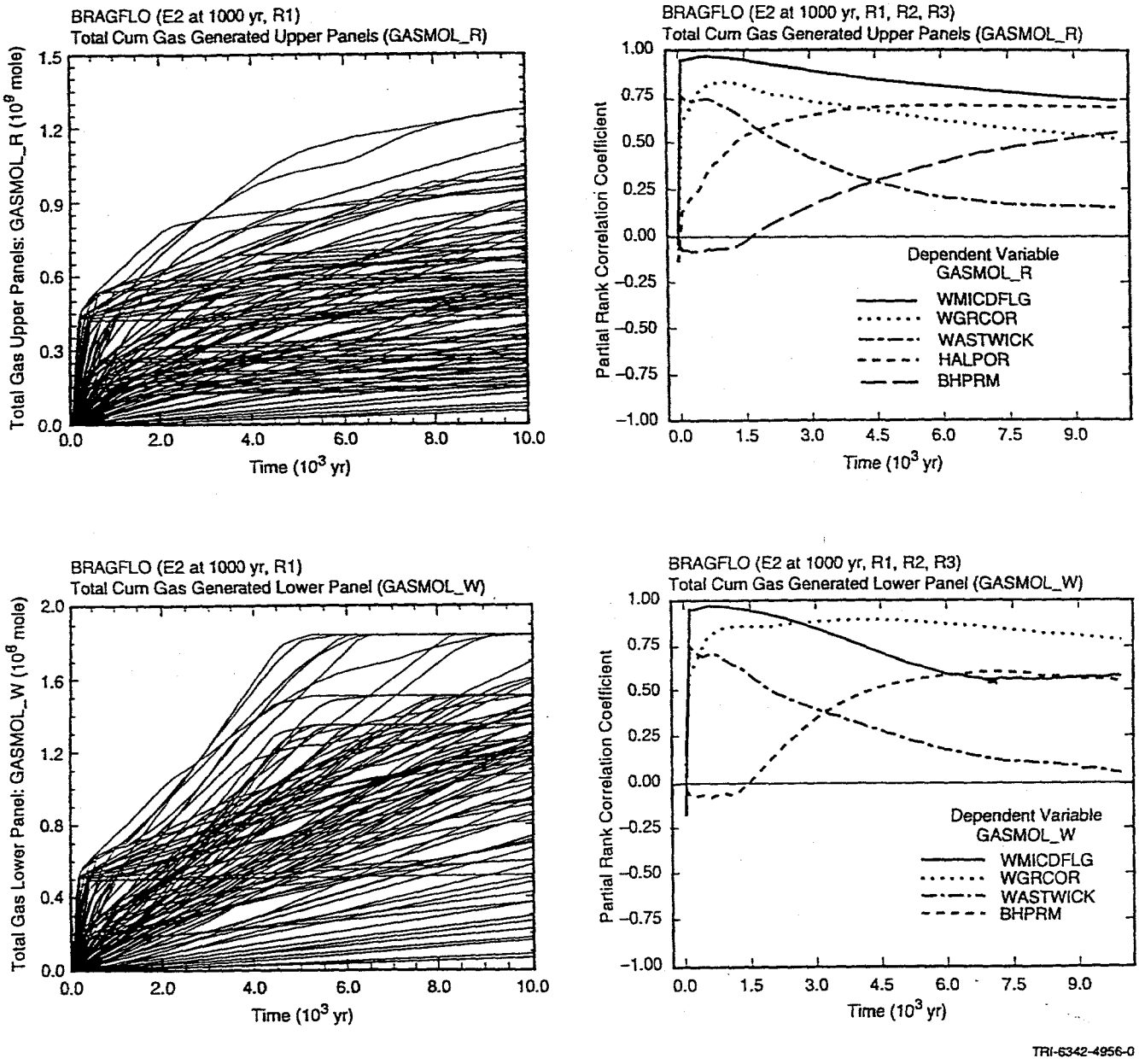

Fig. 23. Uncertainty and sensitivity analysis results for cumulative gas generation due to corrosion and microbial degradation in upper waste panels (*GSMOL_R*) (upper frames) and lower waste panel (*GASMOL_W*) (lower frames) for an E2 intrusion at 1000 yr into lower waste panel; similar results are obtained for an E1 intrusion (Fig. 8.3.17, Ref. 11).

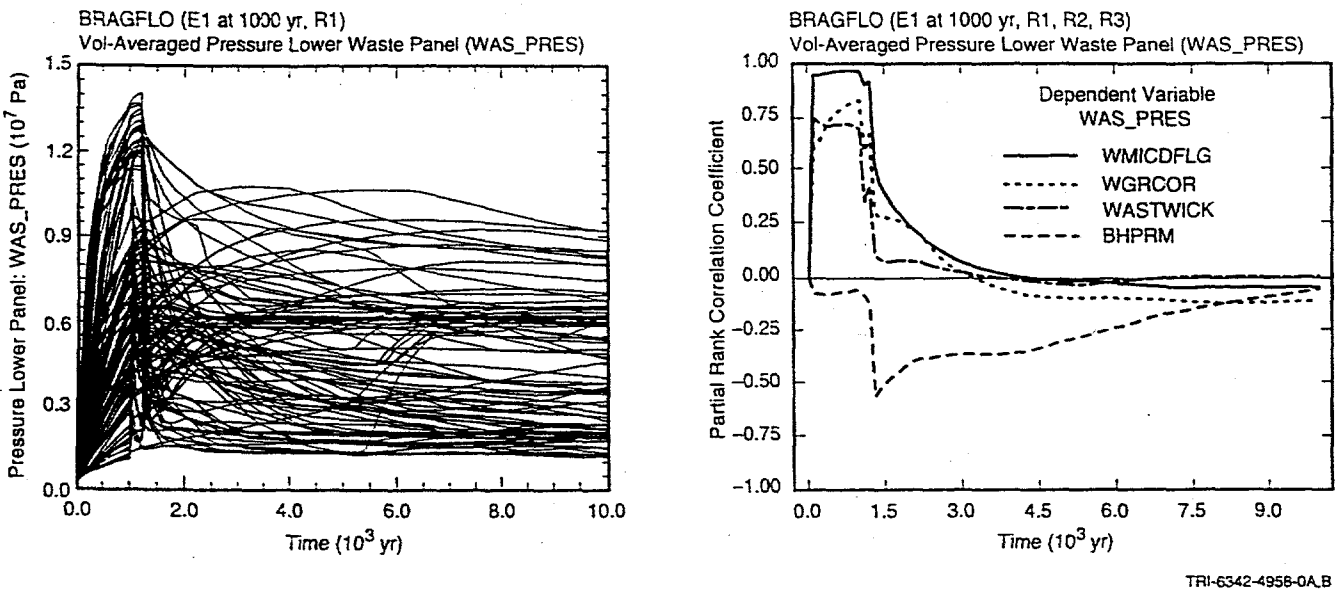

Fig. 24. Uncertainty and sensitivity analysis results for repository pressure (*WAS_PRES*) for an E1 intrusion into lower waste panel at 1000 yr; similar results are obtained for an E2 intrusion (Fig. 8.4.1, Ref. 11).

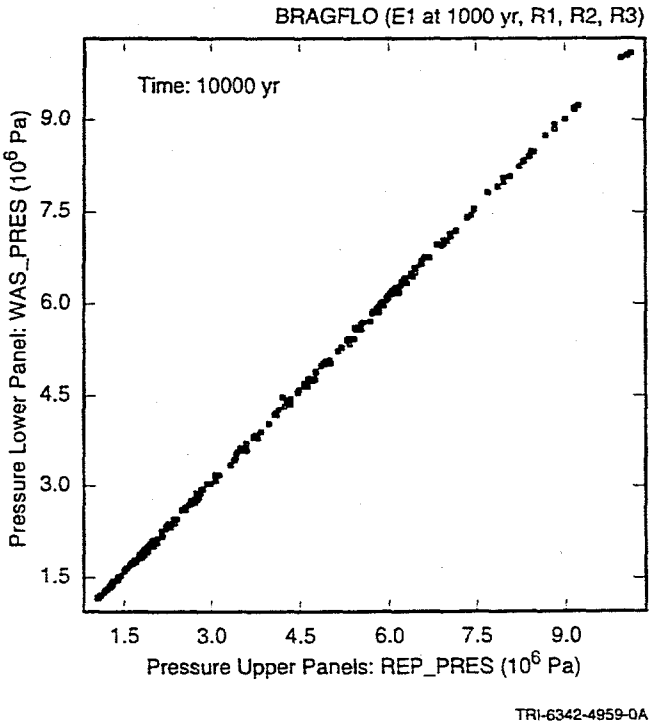

Fig. 25. Scatterplots for repository pressure in upper (*REP_PRES*) and lower (*WAS_PRES*) waste panels at 10,000 yr for E1 intrusion into lower waste panel at 1000 yr; similar results are obtained for an E2 intrusion (Fig. 8.4.2, Ref. 11).

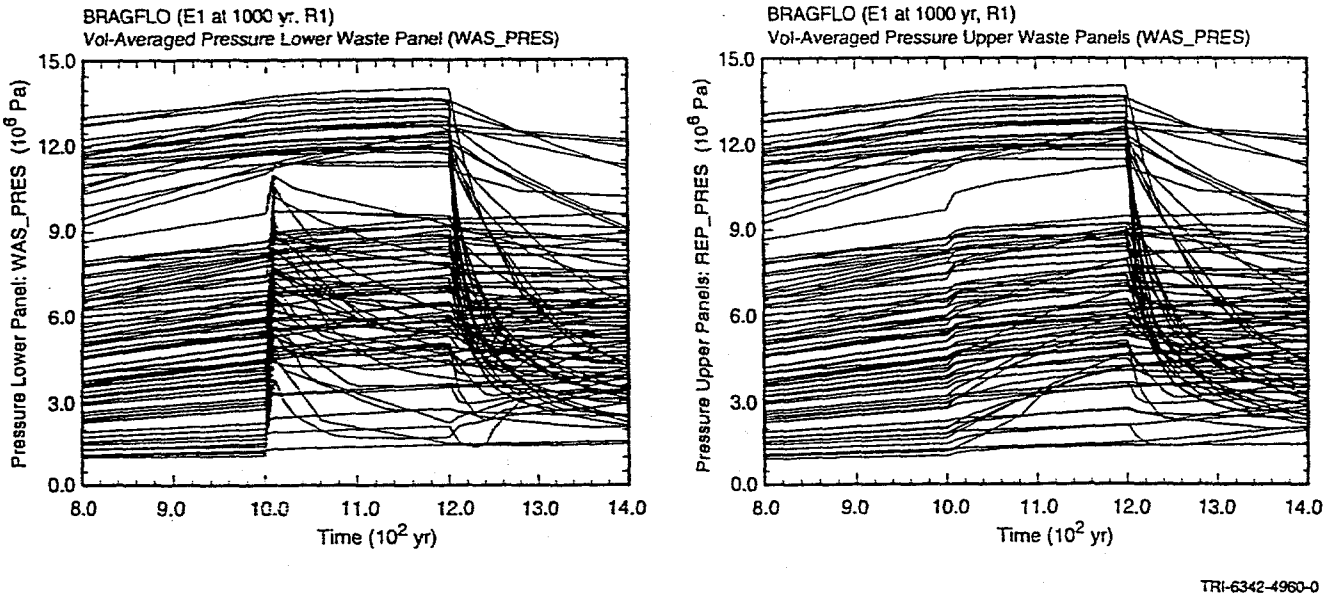

Fig. 26. Pressure in waste panel (*WAS_PRES*) penetrated by an E1 intrusion at 1000 yr (i.e., the lower waste panel) and in rest of repository (*REP_PRES*) (i.e., the upper waste panels).

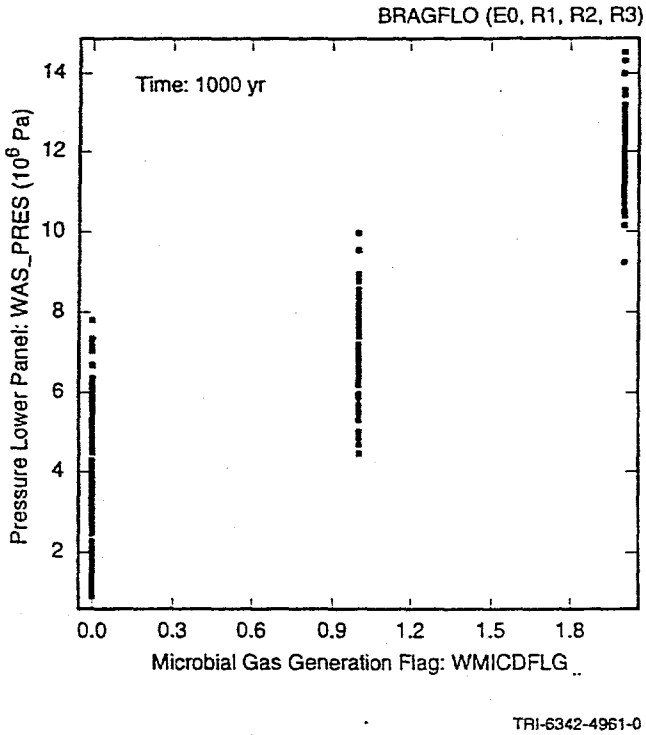

Fig. 27. Scatterplot for repository pressure (*WAS_PRES*) at 1000 yr under undisturbed conditions versus *WMICDFLG*.

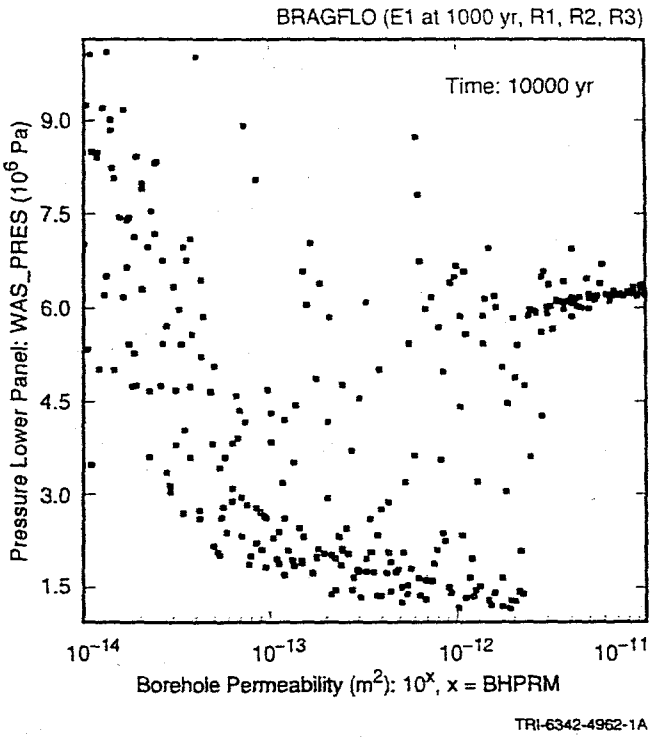

Fig. 28. Scatterplots for repository pressure (*WAS_PRES*) at 10,000 yr versus *BHPRM* for an E1 intrusion at 1000 yr into lower waste panel; similar results are obtained for an E2 intrusion (Fig. 8.4.5, Ref. 11).

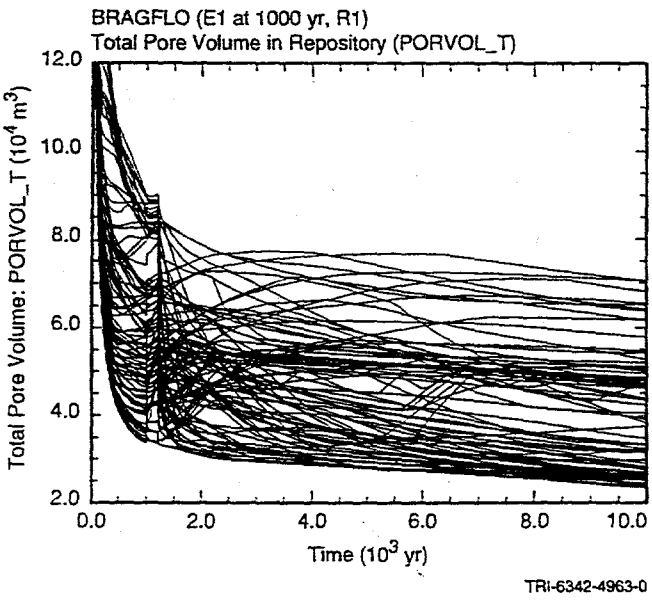

Fig. 29. Uncertainty analysis results for total pore volume in repository (*PORVOL_T*) for an E1 intrusion into lower waste panel at 1000 yr; similar results are obtained for an E2 intrusion (Fig. 8.4.6, Ref. 11).

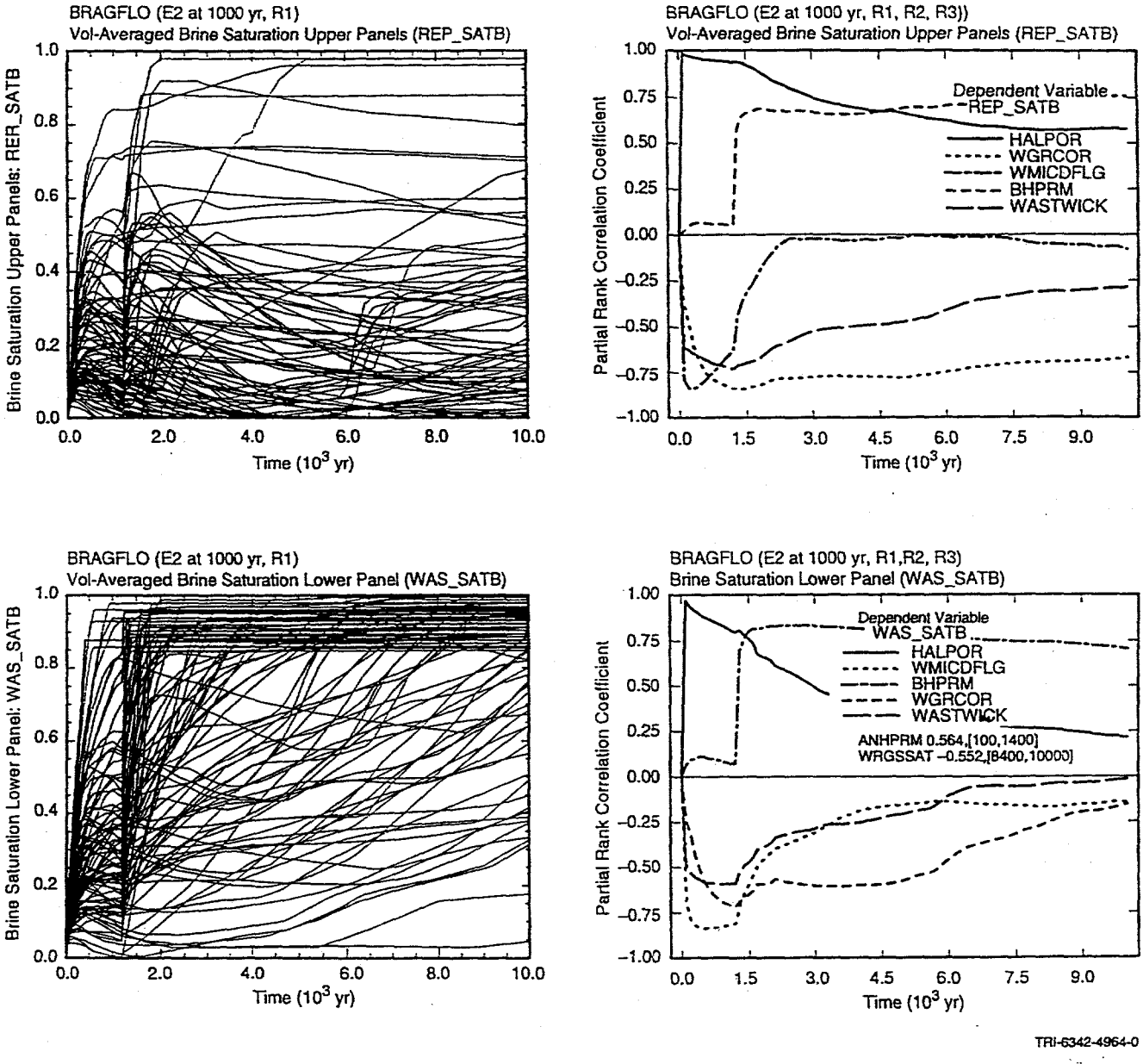

Fig. 30. Uncertainty and sensitivity analysis results for brine saturation in upper (*REP_SATB*) and lower (*WAS_SATB*) waste panels for an E2 intrusion at 1000 yr into lower waste panel (Note: Plots for PRCCs show all variables that have a PRCC that exceeds 0.5 in absolute value at some point in time, with the PRCCs for the variables with the five largest, in absolute value, PRCCs being plotted and the maximum, in absolute value, PRCCs being shown for the remaining variables together with the intervals over which the PRCCs exceed 0.5 in absolute value); similar results are obtained for an E1 intrusion (Fig. 8.5.2, Ref. 11).

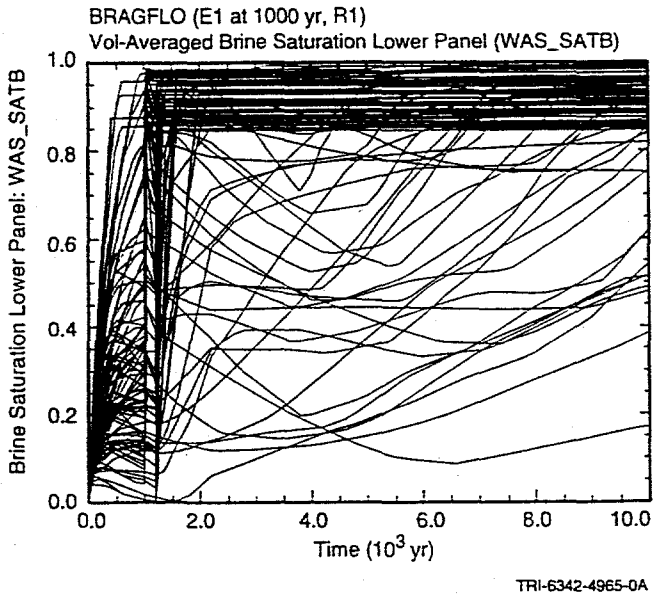

Fig. 31. Uncertainty analysis results for brine saturation in lower (*WAS_SATB*) waste panel for an E1 intrusion at 1000 yr into lower waste panel.

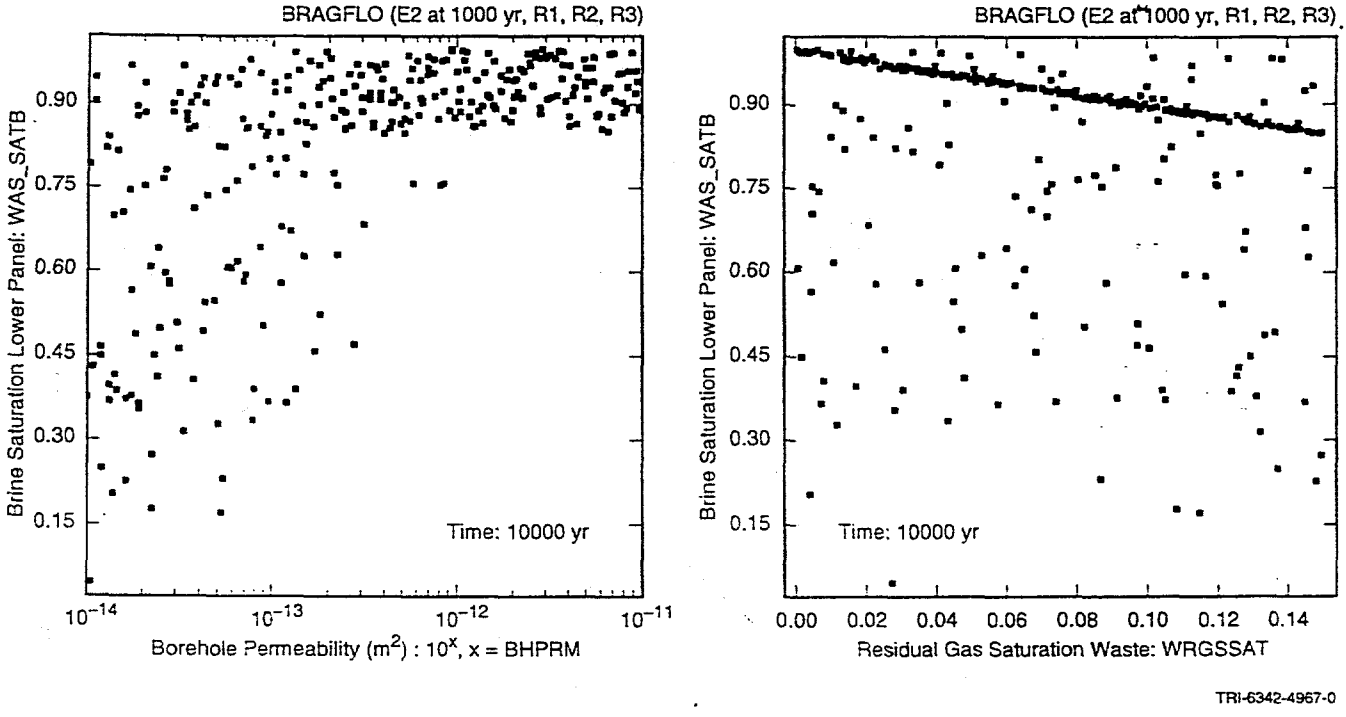

Fig. 32. Scatterplots for brine saturation in lower waste panel (*WAS_SATB*) at 10,000 yr for an E2 intrusion at 1000 yr into lower waste panel versus *BHPRM* and *WRGSSAT*.

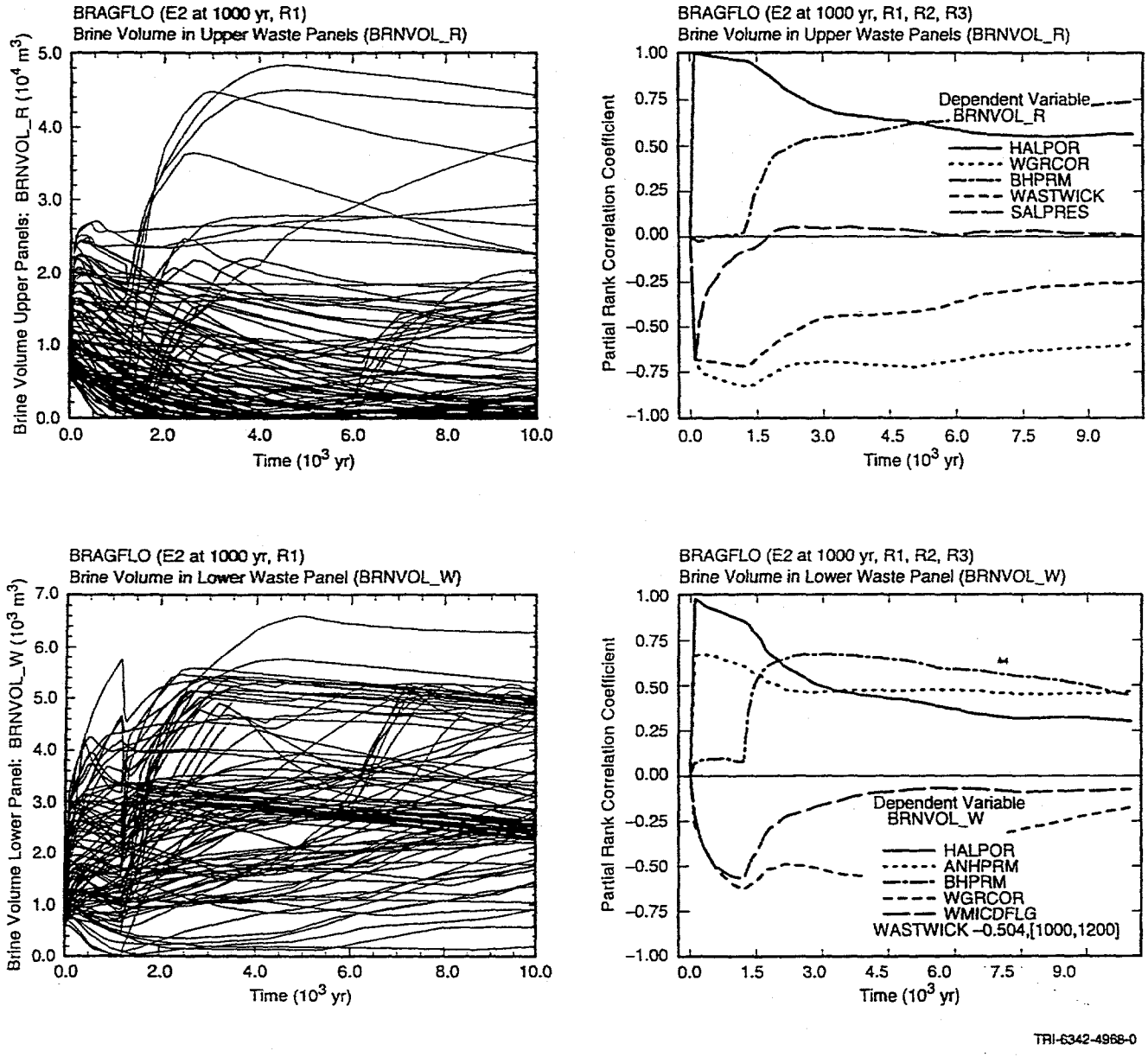

Fig. 33. Uncertainty and sensitivity analysis results for brine volume in upper (*BRNVOL_R*) and lower (*BRNVOL_W*) waste panels for an E2 intrusion at 1000 yr into lower waste panel (See Note, Fig. 30).

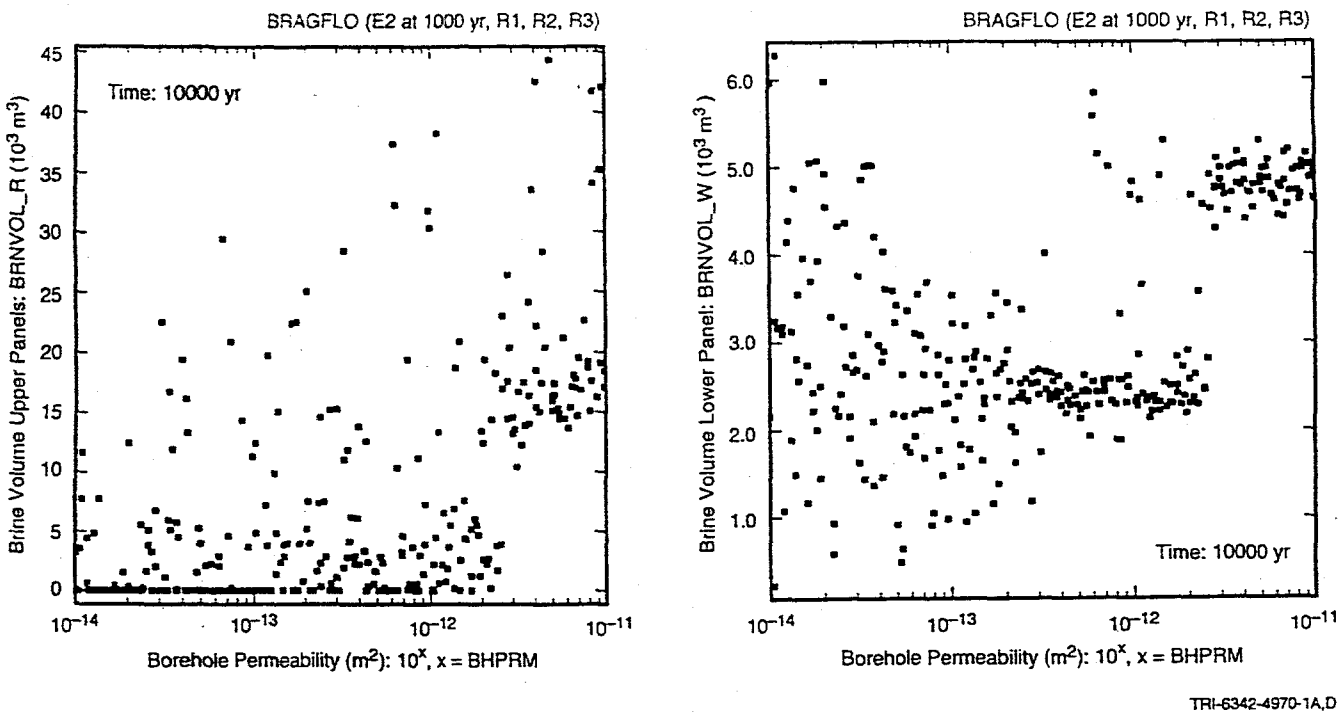

Fig. 34. Scatterplots for brine volume in upper (*BRNVOL_R*) and lower (*BRNVOL_W*) waste panels versus *BHPRM* at 10,000 yr for an E2 intrusion at 1000 yr into lower waste panel.

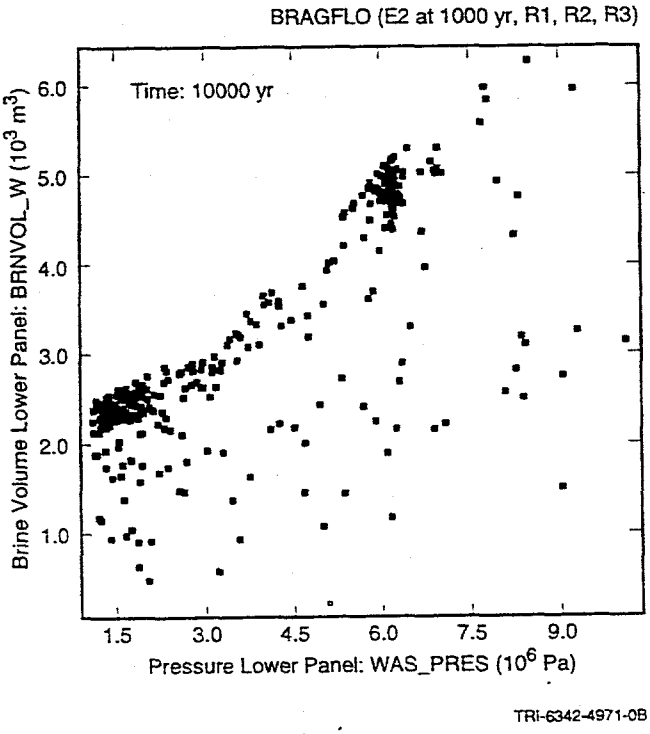

Fig. 35. Scatterplot for repository pressure (*WAS_PRES*) at 10,000 yr versus brine volume in lower waste panel (*BRNVOL_W*) for an E2 intrusion at 1000 yr into lower waste panel; similar results are obtained for an E1 intrusion (Fig. 8.5.8, Ref. 11).

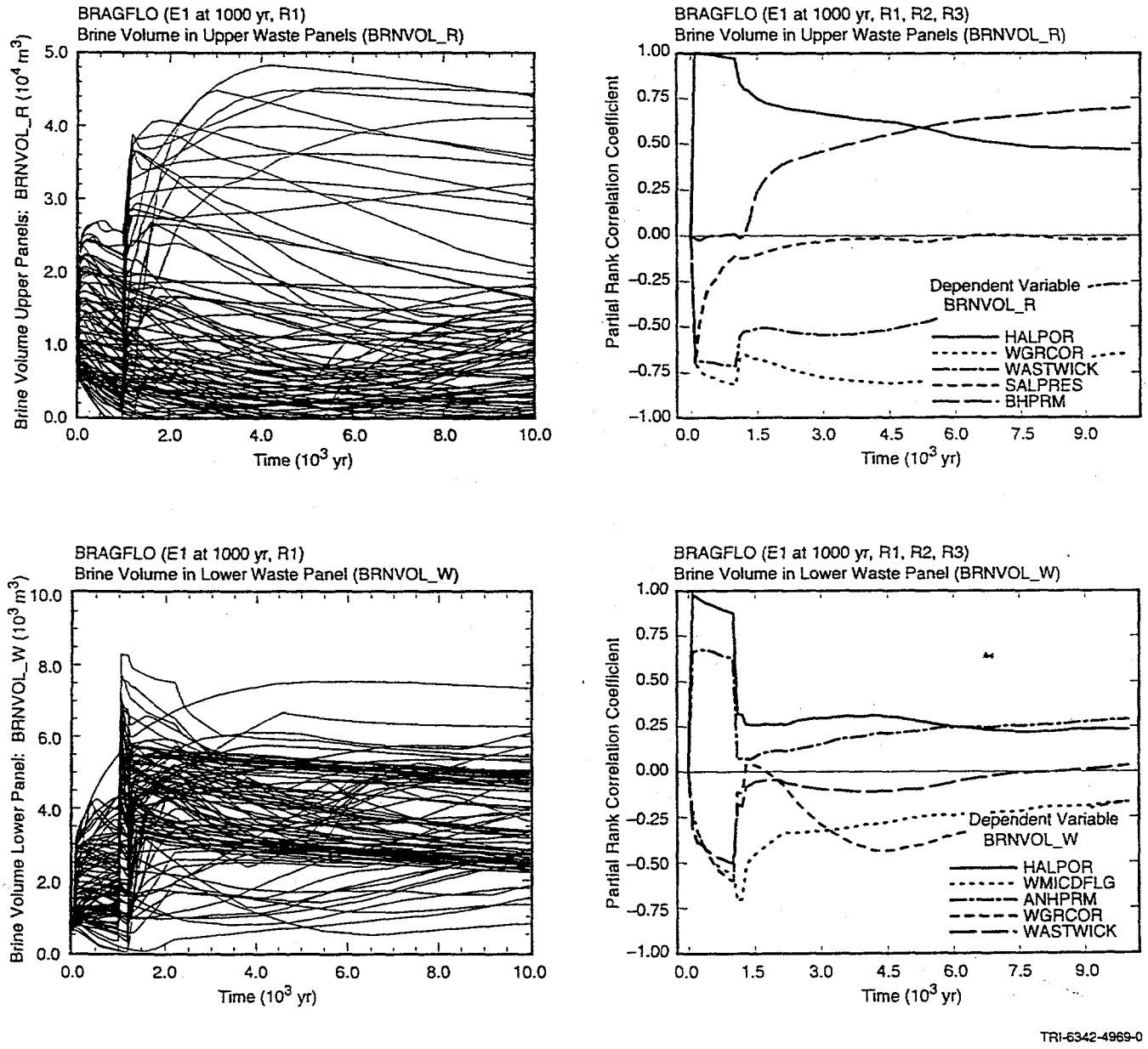

Fig. 36. Uncertainty and sensitivity analysis results for brine volume in upper (*BRNVOL_R*) and lower (*BRNVOL_W*) waste panels for an E1 intrusion at 1000 yr into lower waste panel.

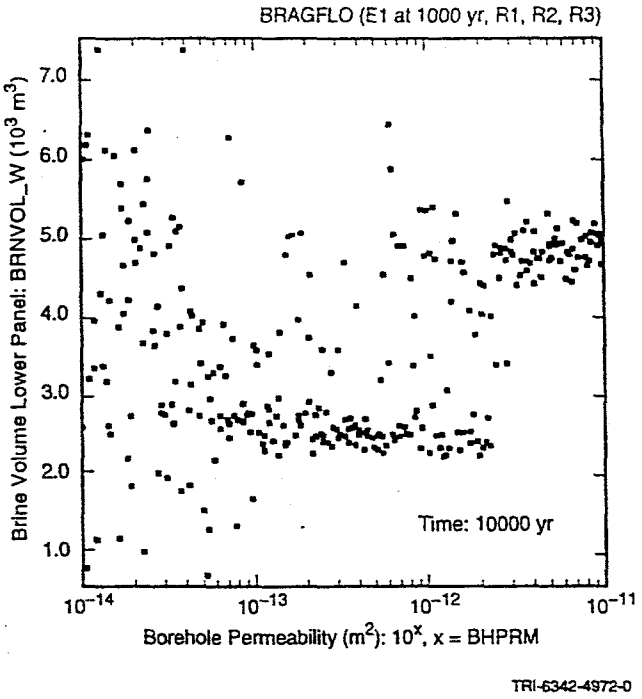

Fig. 37. Scatterplot for brine volume in lower waste panel (*BRNVOL_W*) at 10,000 yr for an E1 intrusion at 1000 yr into lower waste panel versus *BHPRM*.

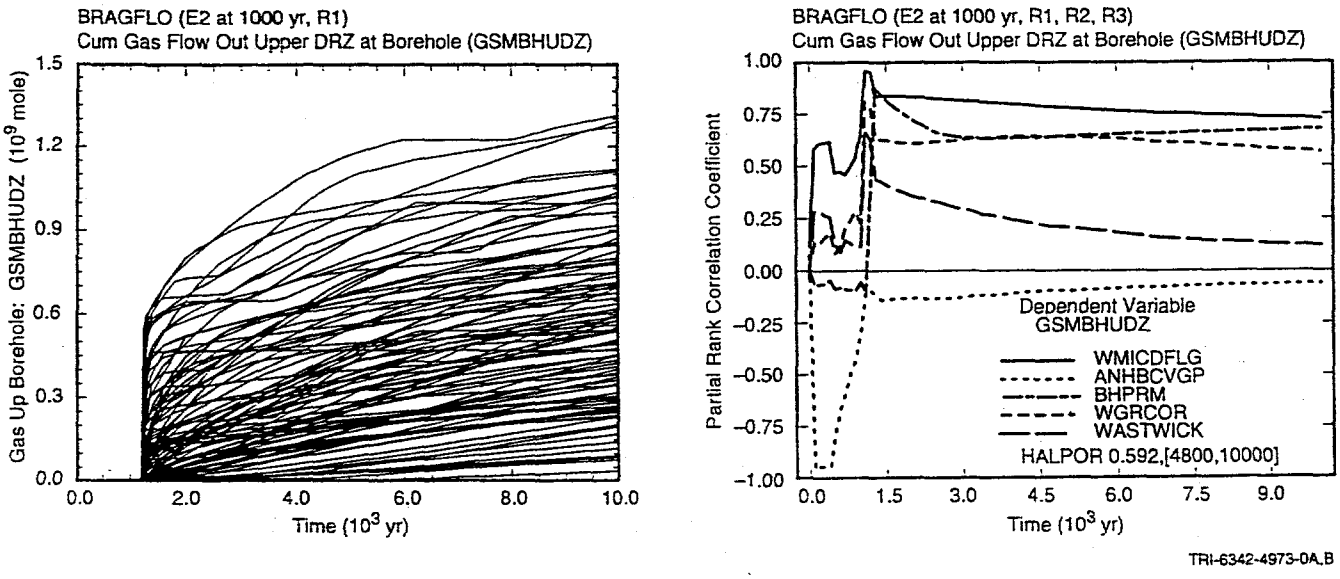

Fig. 38. Uncertainty and sensitivity analysis results for cumulative gas flow up borehole at top of DRZ (*GSMBHUDZ*) for an E2 intrusion at 1000 yr into lower waste panel (See Note, Fig. 34); similar results are obtained for an E1 intrusion (Fig. 8.6.1, Ref. 11).

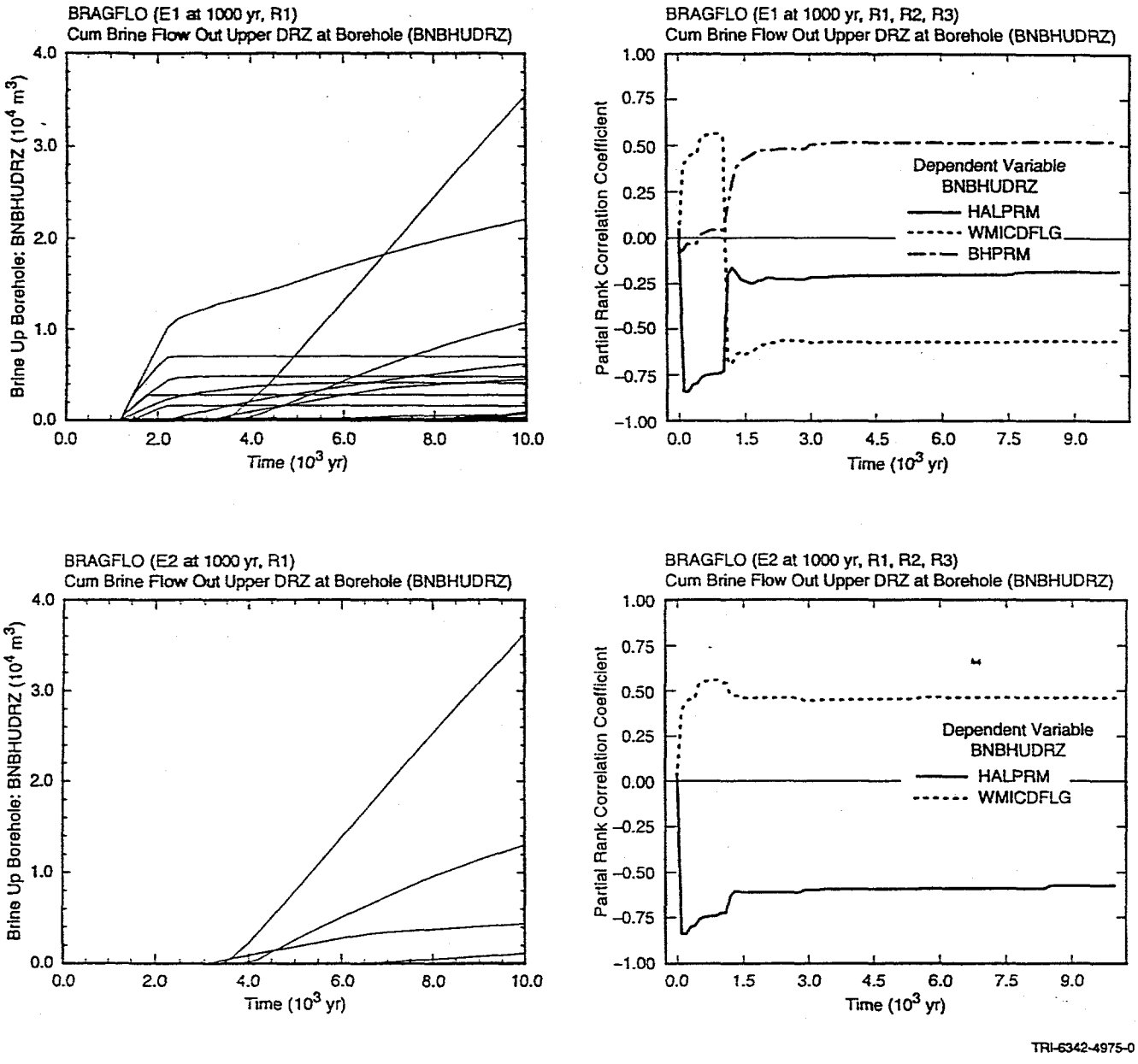

Fig. 39. Uncertainty and sensitivity analysis results for cumulative brine flow up borehole at top of DRZ (*BNBHUDRZ*) for E1 and E2 intrusions at 1000 yr into lower waste panel.

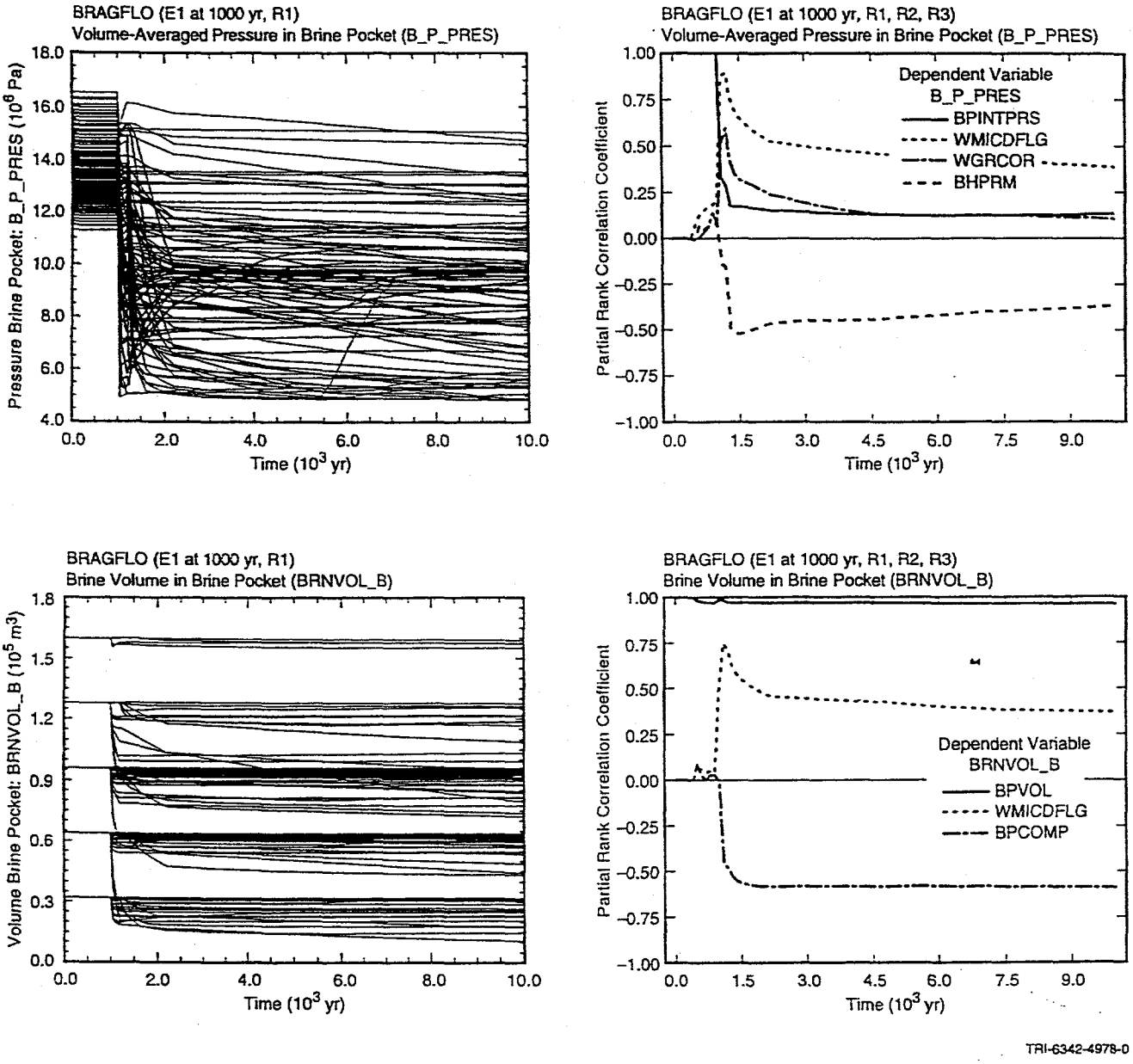

Fig. 40. Uncertainty and sensitivity analysis results for pressure (*B_P_PRES*) and brine volume (*BRNVOL_B*) in brine pocket for an E1 intrusion at 1000 yr into lower waste panel.

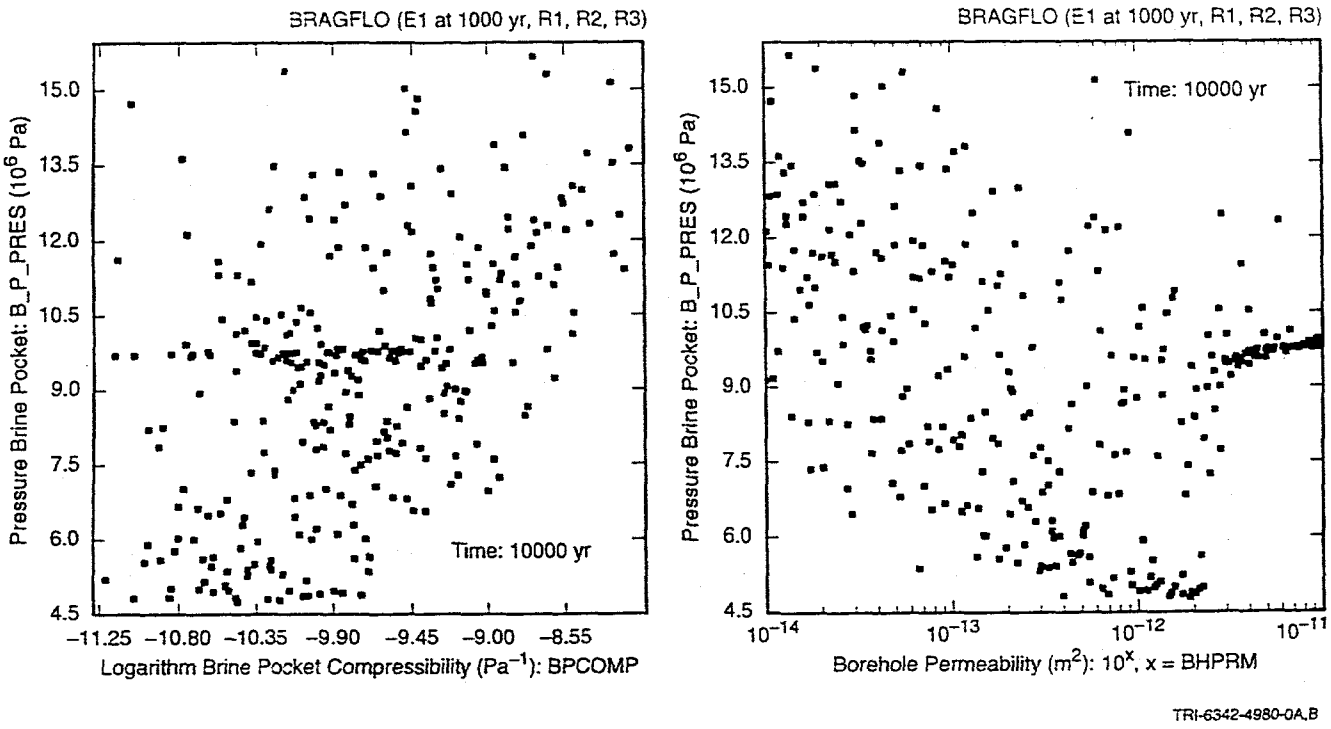

Fig. 41. Scatterplots for brine pocket pressure (*B_P_PRES*) at 10,000 yr versus *BPCOMP* and *BHPRM* for an E1 intrusion at 1000 yr into lower waste panel.

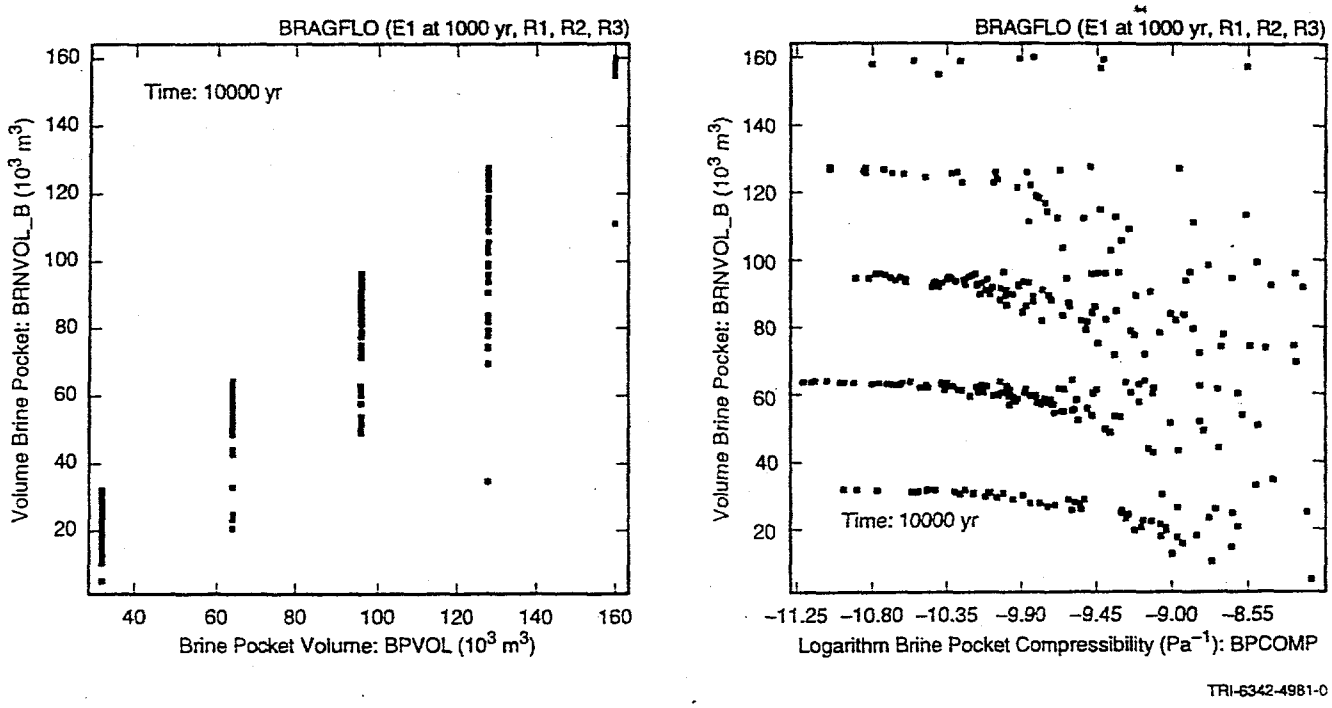

Fig. 42. Scatterplots for brine volume in pressurized brine pocket (*BRNVOL_B*) at 10,000 yr versus *BPVOL* and *BPCOMP* for an E1 intrusion at 1000 yr into lower waste panel.

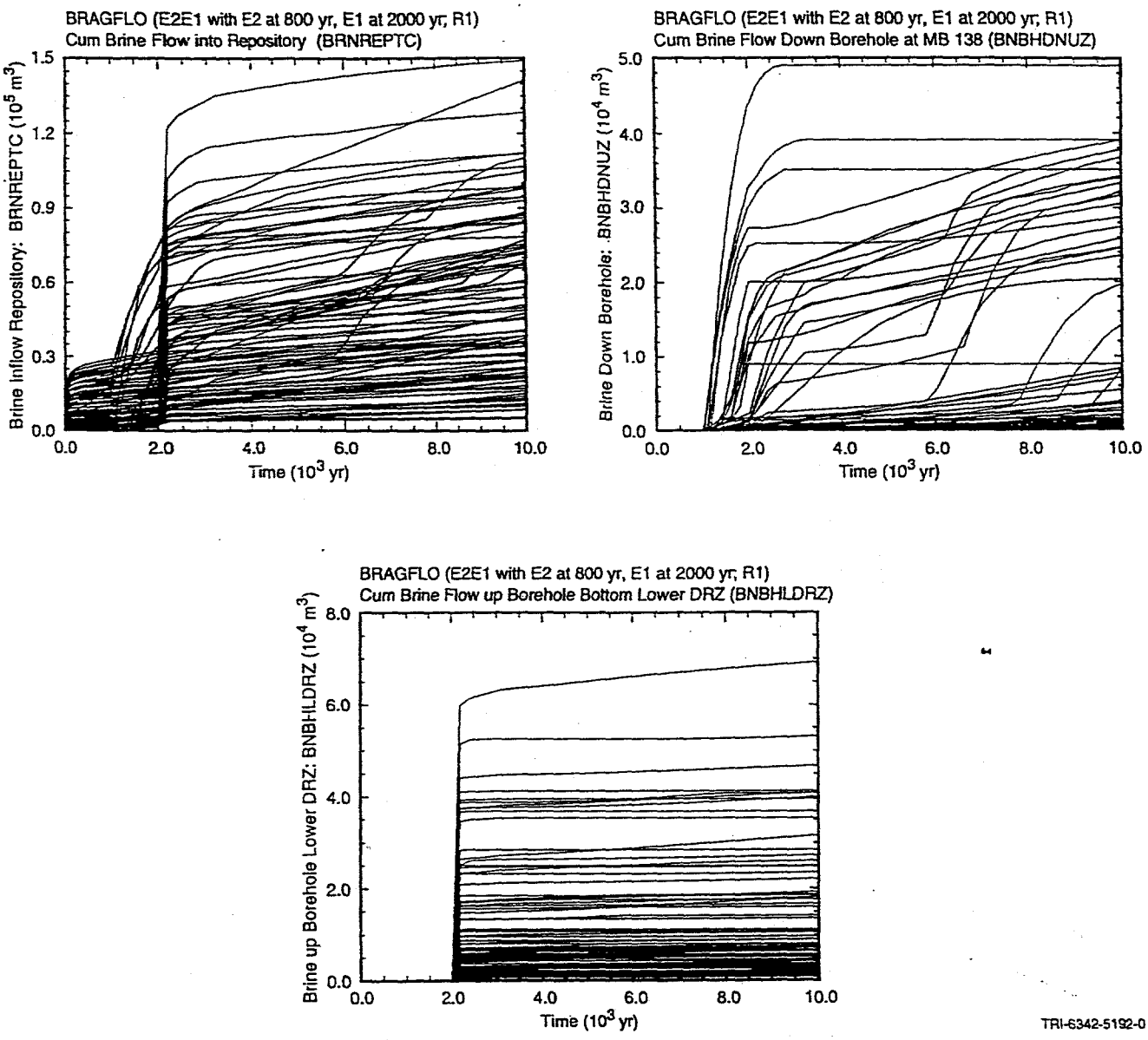

Fig. 43. Cumulative brine flow into repository (*BRNREPTC*), cumulative brine flow down intruding boreholes (*BNBHDNUZ*), and cumulative brine flow into bottom of DRZ from brine pocket (*BNBHLDRZ*) for an E2E1 intrusion into lower waste panel with the E2 intrusion at 800 yr and the E1 intrusion at 2000 yr.

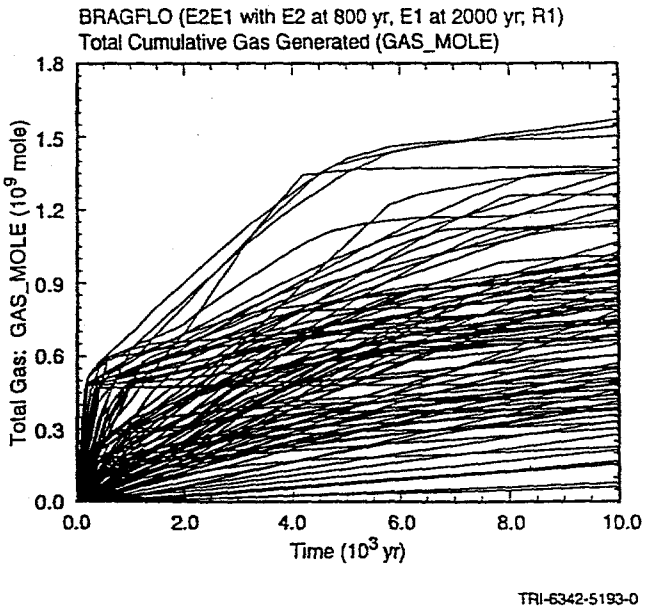

Fig. 44. Cumulative gas generation due to corrosion and microbial degradation (*GAS_MOLE*) for an E2E1 intrusion into lower waste panel with the E2 intrusion at 800 yr and the E1 intrusion at 2000 yr.

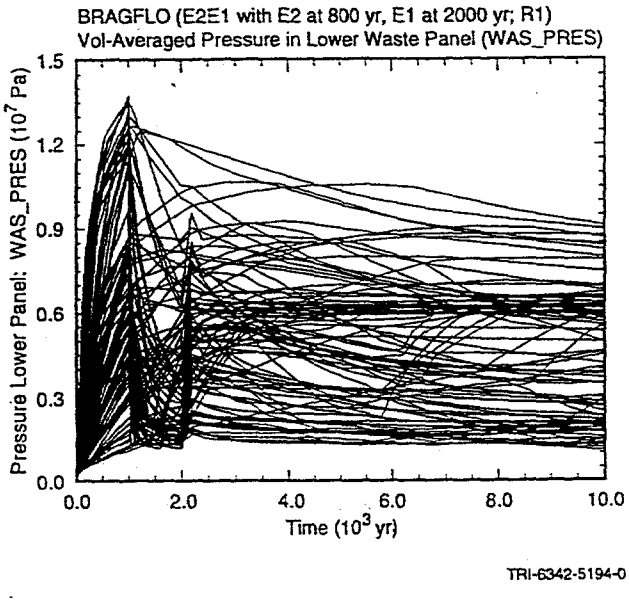

Fig. 45. Repository pressure (*WAS_PRES*) for an E2E1 intrusion into lower waste panel with the E2 intrusion at 800 yr and the E1 intrusion at 2000 yr.

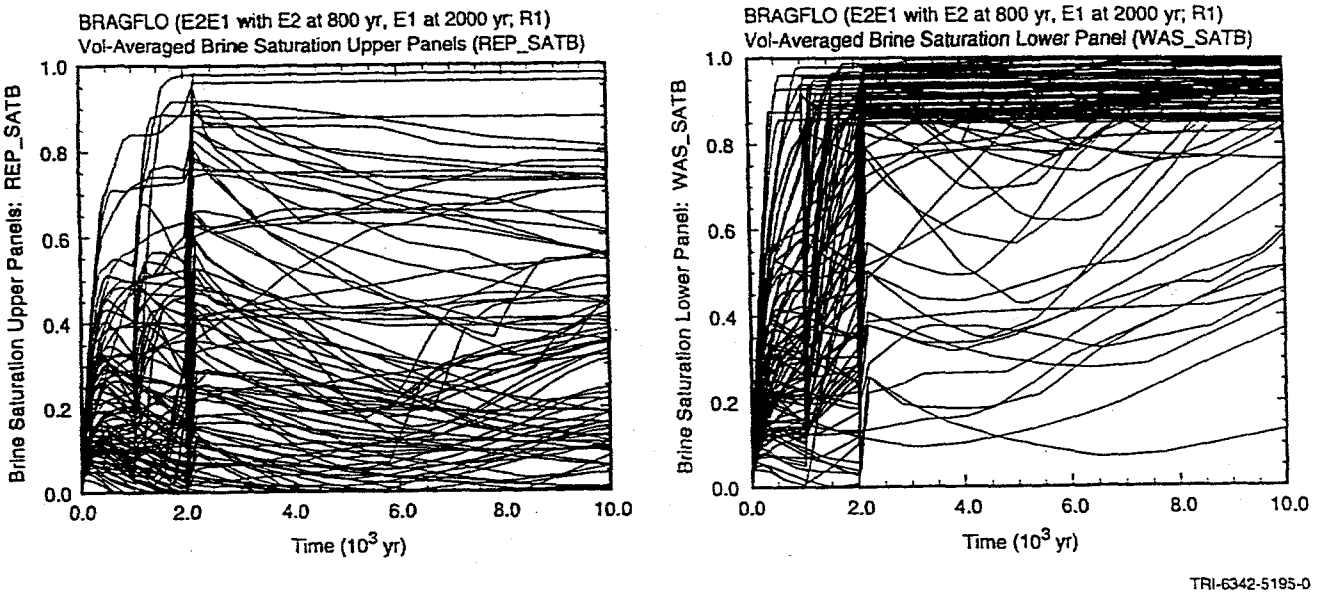

Fig. 46. Brine saturation in upper (*REP_SATB*) and lower (*WAS_SATB*) waste panels for an E2E1 intrusion into lower waste panel with the E2 intrusion at 800 yr and the E1 intrusion at 2000 yr.

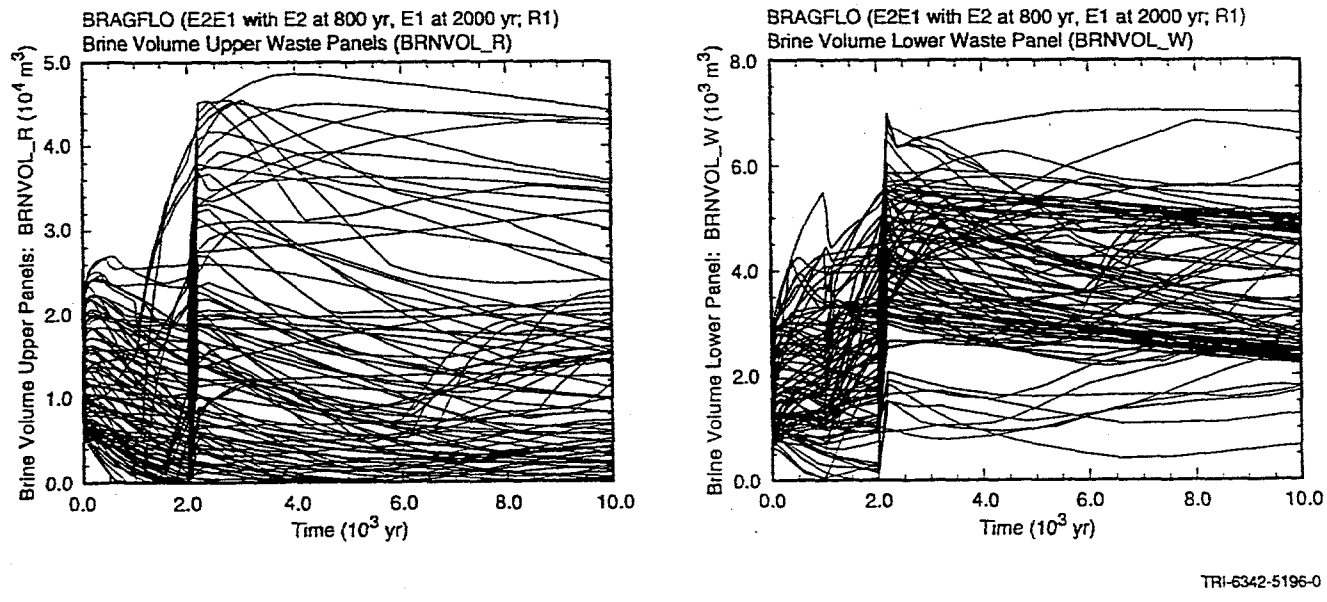

Fig. 47. Brine volume in upper (*BRNVOL_R*) and lower (*BRNVOL_W*) waste panels for an E2E1 intrusion into lower waste panel with the E2 intrusion at 800 yr and the E1 intrusion at 2000 yr.

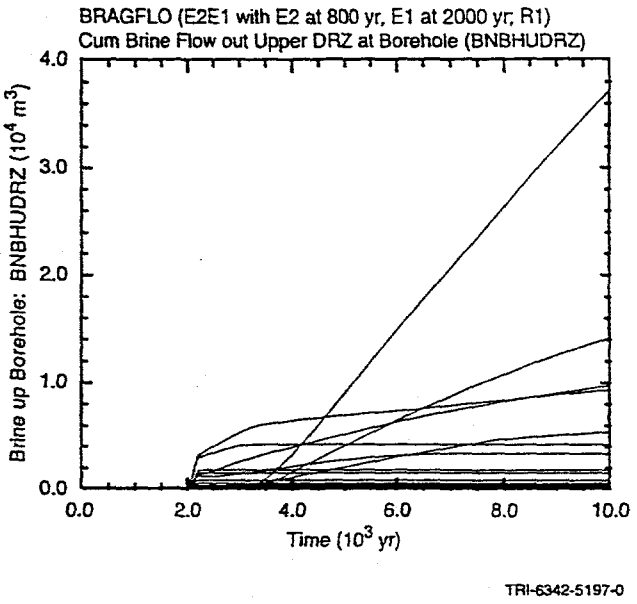

Fig. 48. Cumulative brine flow up borehole at top of DRZ (*BNBHUDRZ*) for an E2E1 intrusion into lower waste panel with the E2 intrusion at 800 yr and the E1 intrusion at 2000 yr.

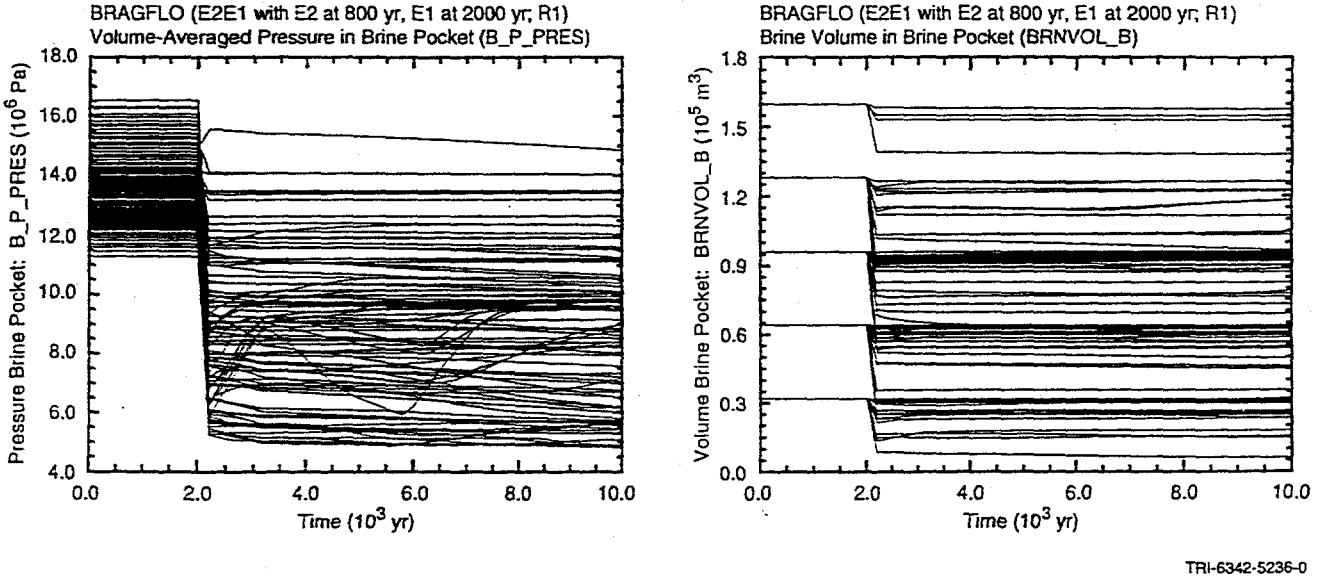

Fig. 49. Pressure (*B_P_PRES*) and brine volume (*BRNVOL_B*) in brine pocket for an E2E1 intrusion into lower waste panel with the E2 intrusion at 800 yr and the E1 intrusion at 2000 yr.

Table 1. Results Calculated by BRAGFLO Considered in Uncertainty and Sensitivity Analyses for Fluid Flow in the Vicinity of the Repository Under Disturbed (i.e., E1, E2, E2E1) Conditions in Addition to the Results in Table 1 of Ref. 1

B_P_PRES—Volume-averaged pressure (Pa) in brine pocket (i.e., in Cells 1007-1023 in Fig. 3, Ref. 2)

BNBHDNUZ—Cumulative brine flow (m^3) down borehole at MB 138 (i.e., from Cell 223 to Cell 575 in Fig. 3, Ref. 2)

BNBHLDRZ—Cumulative brine flow (m^3) up borehole at bottom of lower disturbed rock zone (DRZ) (i.e., from Cell 78 to Cell 439 in Fig. 3, Ref. 2)

BNBHUDRZ—Cumulative brine flow (m^3) up borehole at top of DRZ (i.e., from Cell 513 to Cell 575 in Fig. 3, Ref. 2)

BRNVOL_B—Brine volume (m^3) in brine pocket (i.e., in Cells 1007-1023 in Fig. 3, Ref. 2)

GASBHUDZ—Cumulative gas flow (m^3 at standard temperature and pressure; *GASBHUDZ* = 0.02463 m^3/mol * *GSMBUDZ*) up borehole at top of DRZ (i.e., from Cell 513 to Cell 575 in Fig. 3, Ref. 2)

GSMBHUDZ—Cumulative gas flow (mol) up borehole at top of DRZ (i.e., from Cell 513 to Cell 575 in Fig. 3, Ref. 2)

Table 2. Stepwise Regression Analyses with Rank-Transformed Data for Cumulative Brine Flow from Anhydrite Marker Beds (*BRAALIC*) for E1 and E2 Intrusions at 1000 yr into Lower Waste Panel

	E0: 0 - 1000 yr			E2: 1000 - 10,000 yr			E2: 0 - 10,000 yr			E1: 1000 - 10,000 yr		
Step[a]	Variable[b]	SRRC[c]	R^{2d}	Variable	SRRC	R^2	Variable	SRRC	R^2	Variable	SRRC	R^2
1	*ANHPRM*	0.73	0.58	*ANHPRM*	0.90	0.81	*ANHPRM*	0.91	0.83	*ANHPRM*	0.89	0.80
2	*WMICDFLG*	–0.45	0.79	*BHPRM*	0.16	0.84	*WMICDFLG*	–0.15	0.85	*BHPRM*	0.14	0.82
3	*HALPRM*	0.29	0.88	*WMICDFLG*	–0.10	0.85	*BHPRM*	0.13	0.87	*SALPRES*	0.12	0.83
4	*WASTWICK*	–0.11	0.89	*SALPRES*	0.10	0.86	*HALPRM*	0.12	0.88	*BPCOMP*	–0.10	0.84
5	*SALPRES*	0.08	0.90	*HALPRM*	0.08	0.86	*SALPRES*	0.10	0.89	*HALPRM*	0.08	0.85
6	*WGRCOR*	–0.07	0.90				*WGRCOR*	–0.05	0.90			
7	*WGRMICI*	–0.07	0.91									

	E1: 0 - 10,000 yr			(E2: 0 - 10,000 yr) – (E0: 0 - 10,000 yr)			(E1: 0 - 10,000 yr) – (E0: 0 - 10,000 yr)			(E2: 0 - 10,000 yr) – (E1: 0 - 10,000 yr)		
Step	Variable	SRRC	R^2	Variable	SRRC	R^2	Variable	SRRC	R^2	Variable	SRRC	R^2
1	*ANHPRM*	0.91	0.83	*ANHPRM*	0.74	0.55	*ANHPRM*	0.64	0.43	*BPCOMP*	0.57	0.32
2	*HALPRM*	0.12	0.84	*WMICDFLG*	0.27	0.63	*WMICDFLG*	0.32	0.54	*ANHPRM*	0.32	0.41
3	*BHPRM*	0.12	0.86	*WGRCOR*	0.16	0.65	*WGRCOR*	0.22	0.58	*BHPRM*	0.25	0.48
4	*SALPRES*	0.12	0.87	*BHPRM*	0.13	0.67	*BPCOMP*	–0.15	0.61	*WMICDFLG*	–0.27	0.54
5	*WMICDFLG*	–0.12	0.88	*HALPOR*	0.12	0.68	*HALPOR*	0.12	0.62	*BPINTPRS*	0.14	0.56
6	*BPCOMP*	–0.09	0.89				*BHPRM*	0.10	0.63	*BPVOL*	0.11	0.57
							BPVOL	–0.09	0.64			
							WASTWICK	0.08	0.65			

[a] Steps in stepwise regression analysis.

[b] Variables listed in order of selection in regression analysis with *ANHCOMP* and *HALCOMP* excluded from entry into regression model.

[c] Standardized rank regression coefficients in final regression model.

[d] Cumulative R^2 value with entry of each variable into regression model.

Table 3. Stepwise Regression Analyses with Rank-Transformed Data for Cumulative Brine Flow into Repository (*BRNREPTC*) for E1 and E2 Intrusions at 1000 yr into Lower Waste Panel

	E0: 0 - 1000 yr			E2: 1000 - 10,000 yr			E2: 0 - 10,000 yr			E1: 1000 - 10,000 yr		
Step[a]	Variable[b]	SRRC[c]	R^{2d}	Variable	SRRC	R^2	Variable	SRRC	R^2	Variable	SRRC	R^2
1	*HALPOR*	0.98	0.96	*BHPRM*	0.79	0.62	*BHPRM*	0.66	0.44	*BHPRM*	0.66	0.43
2	*WMICDFLG*	−0.10	0.97	*ANHPRM*	0.32	0.73	*HALPOR*	0.51	0.70	*BPCOMP*	0.42	0.60
3	*ANHPRM*	0.08	0.97	*HALPOR*	0.24	0.78	*ANHPRM*	0.24	0.76	*WMICDFLG*	−0.27	0.67
4	*HALPRM*	0.05	0.97	*HALPRM*	0.16	0.81	*HALPRM*	0.15	0.78	*BPVOL*	0.16	0.70
5	*WRBRNSAT*	−0.04	0.98	*WRBRNSAT*	−0.08	0.82	*WRBRNSAT*	−0.07	0.79	*ANHPRM*	0.14	0.72
6	*WASTWICK*	−0.04	0.98							*BPINTPRS*	0.09	0.72
7	*SALPRES*	−0.04	0.98							*WGRCOR*	−0.08	0.73
8	*WGRCOR*	−0.03	0.98									

	E1: 0 - 10,000 yr			(E2: 0 - 10,000 yr) − (E0: 0 - 10,000 yr)			(E1: 0 - 10,000 yr) − (E0: 0 - 10,000 yr)			(E1: 0 - 10,000 yr) − (E2: 0 - 10,000 yr)		
Step	Variable	SRRC	R^2	Variable	SRRC	R^2	Variable	SRRC	R^2	Variable	SRRC	R^2
1	*BHPRM*	0.58	0.34	*BHPRM*	0.83	0.69	*BHPRM*	0.68	0.46	*BPCOMP*	0.46	0.21
2	*BPCOMP*	0.38	0.49	*ANHPRM*	0.27	0.76	*BPCOMP*	0.45	0.67	*WMICDFLG*	−0.34	0.32
3	*HALPOR*	0.34	0.61	*WMICDFLG*	0.20	0.80	*WMICDFLG*	−0.18	0.70	*BHPRM*	−0.16	0.34
4	*WMICDFLG*	−0.27	0.68	*HALPRM*	0.11	0.81	*BPVOL*	0.15	0.72	*BPINTPRS*	0.15	0.36
5	*BPVOL*	0.17	0.70	*WGRCOR*	0.10	0.82	*BPINTPRS*	0.11	0.73	*BPVOL*	0.13	0.38
6	*ANHPRM*	0.12	0.72	*WASTWICK*	0.06	0.82	*ANHPRM*	0.10	0.74	*WASTWICK*	−0.11	0.39
7	*BPINTPRS*	0.09	0.72									
8	*HALPRM*	0.08	0.73									

[a] Steps in stepwise regression analysis.

[b] Variables listed in order of selection in regression analysis with *ANHCOMP* and *HALCOMP* excluded from entry into regression model.

[c] Standardized rank regression coefficients in final regression model.

[d] Cumulative R^2 value with entry of each variable into regression model.

Table 4. Stepwise Regression Analyses with Rank-Transformed Data for Cumulative Brine Flow Through Borehole into DRZ (*BNBHDNUZ*, *BNBHLDRZ*) over 10,000 yr for E1 and E2 Intrusions at 1000 yr into Lower Waste Panel

	E2: Upper DRZ			E1: Upper DRZ			(E2: Upper DRZ) − (E1: Upper DRZ)			E1: Lower DRZ		
Step[a]	Variable[b]	SRRC[c]	R^{2d}	Variable	SRRC	R^2	Variable	SRRC	R^2	Variable	SRRC	R^2
1	*BHPRM*	0.95	0.90	*BHPRM*	0.90	0.81	*BHPRM*	0.69	0.48	*BPCOMP*	0.72	0.52
2	*HALPRM*	0.13	0.92	*BPCOMP*	−0.11	0.82	*BPCOMP*	0.20	0.52	*BHPRM*	0.34	0.64
3	*HALPOR*	−0.06	0.92	*HALPRM*	0.10	0.83	*HALPOR*	−0.11	0.53	*WMICDFLG*	−0.28	0.71
4	*ANHPRM*	−0.06	0.92	*HALPOR*	−0.08	0.84	*SHPRMASP*	−0.10	0.54	*BPVOL*	0.16	0.74
5	*WRGSSAT*	−0.04	0.93	*BPINTPRS*	−0.06	0.84				*BPINTPRS*	0.12	0.75
6										*SHRBRSAT*	−0.07	0.76
										ANHPRM	−0.07	0.76

[a] Steps in stepwise regression analysis.

[b] Variables listed in order of selection in regression analysis with *ANHCOMP* and *HALCOMP* excluded from entry into regression model.

[c] Standardized rank regression coefficients in final regression model.

[d] Cumulative R^2 value with entry of each variable into regression model.

Table 5. Stepwise Regression Analyses with Rank-Transformed Data for Gas Generation Due to Corrosion (*FE_MOLE*) and Total (i.e., Corrosion and Microbial) Gas Generation (*GAS_MOLE*) for E1 and E2 Intrusions at 1000 yr into Lower Waste Panel

	Gas, Corrosion E2: 0 - 10,000 yr			Gas, Corrosion E1: 0 - 10,000 yr			Gas, Corrosion (E2: 0 - 10,000 yr) – (E0: 0 - 10,000 yr)			Gas, Corrosion (E1: 0 - 10,000 yr) – (E0: 0 - 10,000 yr)		
Step[a]	Variable[b]	SRRC[c]	R^{2d}	Variable	SRRC	R^2	Variable	SRRC	R^2	Variable	SRRC	R^2
1	*HALPOR*	0.52	0.29	*HALPOR*	0.47	0.23	*BHPRM*	0.73	0.54	*BHPRM*	0.56	0.31
2	*WGRCOR*	0.45	0.49	*WGRCOR*	0.47	0.45	*WGRCOR*	0.37	0.68	*WGRCOR*	0.39	0.46
3	*BHPRM*	0.42	0.67	*BHPRM*	0.34	0.57	*ANHPRM*	0.19	0.71	*BPCOMP*	0.27	0.53
4	*ANHPRM*	0.13	0.69	*WMICDFLG*	–0.19	0.61	*WMICDFLG*	0.10	0.72	*HALPOR*	–0.15	0.55
5	*WASTWICK*	0.09	0.70	*BPPRM*	–0.16	0.63				*WMICDFLG*	–0.11	0.57
6	*SHRGSSAT*	0.08	0.70	*BPINTPRS*	0.10	0.64				*BPINTPRS*	0.10	0.58
7	*WMICDFLG*	–0.08	0.71									

	Gas, Corrosion (E1: 0-10,000 yr) – (E2: 0 - 10,000 yr)			Gas, Total E2: 0 - 10,000 yr			Gas, Total E1: 0 - 10,000 yr		
Step	Variable	SRRC	R^2	Variable	SRRC	R^2	Variable	SRRC	R^2
1	*BPCOMP*	0.32	0.10	*WMICDFLG*	0.53	0.28	*WMICDFLG*	0.44	0.22
2	*BHPRM*	–0.29	0.18	*HALPOR*	0.44	0.48	*WGRCOR*	0.41	0.40
3	*WMICDFLG*	–0.28	0.25	*WGRCOR*	0.36	0.61	*HALPOR*	0.41	0.57
4	*HALPRM*	–0.17	0.28	*BHPRM*	0.34	0.72	*BHPRM*	0.28	0.64
5	*HALPOR*	–0.15	0.30	*ANHPRM*	0.13	0.74	*BPCOMP*	0.13	0.66
6	*ANHPRM*	–0.13	0.32	*HALPRM*	0.07	0.75	*BPINTPRS*	0.09	0.67
7	*BPINTPRS*	0.13	0.34				*ANHPRM*	0.08	0.68
8	*WGRCOR*	0.12	0.35						
9	*WASTWICK*	–0.11	0.36						

[a] Steps in stepwise regression analysis.

[b] Variables listed in order of selection in regression analysis with *ANHCOMP* and *HALCOMP* excluded from entry into regression model.

[c] Standardized rank regression coefficients in final regression model.

[d] Cumulative R^2 value with entry of each variable into regression model.

Table 6. Stepwise Regression Analyses with Rank-Transformed Data for Fraction of Steel Consumed in Upper and Lower Waste Panels (1–*FEREM_R*, 1–*FEREM_W*) for E1 and E2 Intrusions at 1000 yr into Lower Waste Panel

	Upper Waste Panels E2: 0 - 1000 yr			Upper Waste Panels E2: 1000 - 10,000 yr			Upper Waste Panels E2: 0 - 10,000 yr			Upper Waste Panels E1: 1000 - 10,000 yr		
Step[a]	Variable[b]	SRRC[c]	R^{2d}	Variable	SRRC	R^2	Variable	SRRC	R^2	Variable	SRRC	R^2
1	*WGRCOR*	0.81	0.64	*HALPOR*	0.59	0.35	*HALPOR*	0.58	0.35	*HALPOR*	0.51	0.27
2	*WASTWICK*	0.46	0.85	*BHPRM*	0.47	0.58	*BHPRM*	0.42	0.52	*BHPRM*	0.38	0.42
3	*HALPOR*	0.20	0.89	*WGRCOR*	0.17	0.60	*WGRCOR*	0.38	0.67	*WGRCOR*	0.22	0.47
4	*WMICDFLG*	–0.09	0.90	*ANHPRM*	0.12	0.62	*ANHPRM*	0.12	0.68	*WMICDFLG*	–0.20	0.50
5	*SHRGSSAT*	0.05	0.90	*HALPRM*	0.09	0.63	*WASTWICK*	0.09	0.69	*BPPRM*	–0.18	0.54
6							*HALPRM*	0.08	0.70	*BPINTPRS*	0.11	0.55
7							*SHRGSSAT*	0.08	0.70			

	Upper Waste Panels E1: 0 - 10,000 yr			Upper Waste Panels (E1: 0 - 10,000 yr) – (E2: 0 - 10,000 yr)			Lower Waste Panel E2: 0 - 1000 yr			Lower Waste Panel E2: 1000 - 10,000 yr		
Step	Variable	SRRC	R^2	Variable	SRRC	R^2	Variable	SRRC	R^2	Variable	SRRC	R^2
1	*HALPOR*	0.51	0.27	*BPCOMP*	0.31	0.09	*WGRCOR*	0.85	0.71	*WGRCOR*	0.55	0.31
2	*WGRCOR*	0.40	0.43	*WMICDFLG*	–0.30	0.17	*WASTWICK*	0.40	0.86	*BHPRM*	0.45	0.50
3	*BHPRM*	0.35	0.56	*BHPRM*	–0.22	0.22	*HALPOR*	0.15	0.89	*ANHPRM*	0.14	0.52
4	*WMICDFLG*	–0.20	0.59	*HALPRM*	–0.17	0.25	*WMICDFLG*	–0.14	0.91	*WASTWICK*	–0.12	0.54
5	*BPPRM*	–0.17	0.62	*WASTWICK*	–0.13	0.26	*ANHPRM*	0.09	0.91	*SHRGSSAT*	0.10	0.55
6	*BPINTPRS*	0.10	0.63	*BPINTPRS*	0.12	0.28	*SHRGSSAT*	0.04	0.92	*SHPRMCON*	–0.10	0.55
7										*BPVOL*	–0.09	0.56

	Lower Waste Panel E2: 0 - 10,000 yr			Lower Waste Panel E1: 1000 - 10,000 yr			Lower Waste Panel E1: 0 - 10,000 yr			Lower Waste Panel (E1: 0 - 10,000 yr) – (E2: 0 - 10,000 yr)		
Step	Variable	SRRC	R^2	Variable	SRRC	R^2	Variable	SRRC	R^2	Variable	SRRC	R^2
1	*WGRCOR*	0.71	0.51	*WGRCOR*	0.57	0.33	*WGRCOR*	0.79	0.62	*BHPRM*	–0.43	0.19
2	*BHPRM*	0.39	0.66	*BHPRM*	0.28	0.41	*BHPRM*	0.26	0.68	*HALPOR*	–0.37	0.32
3	*HALPOR*	0.18	0.70	*WASTWICK*	–0.22	0.45	*WMICDFLG*	–0.18	0.71	*ANHPRM*	–0.30	0.42
4	*ANHPRM*	0.17	0.72				*WASTWICK*	0.13	0.73	*BPINTPRS*	0.14	0.44
5	*WMICDFLG*	–0.11	0.74				*HALPOR*	0.12	0.75	*HALPRM*	–0.12	0.45
6	*WASTWICK*	0.08	0.74				*SHRGSSAT*	0.08	0.75	*WMICDFLG*	–0.11	0.46
7							*BPINTPRS*	0.08	0.76			
8							*ANHPRM*	0.07	0.76			

[a] Steps in stepwise regression analysis.

[b] Variables listed in order of selection in regression analysis with *ANHCOMP* and *HALCOMP* excluded from entry into regression model.

[c] Standardized rank regression coefficients in final regression model.

[d] Cumulative R^2 value with entry of each variable into regression model.

Table 7. Stepwise Regression Analyses with Rank-Transformed Data for Amount of Gas Generated over 10,000 yr Due to Corrosion and Microbial Degradation in Upper (*GASMOL_R*) and Lower (*GASMOL_W*) Waste Panels for E1 and E2 Intrusions at 1000 yr into Lower Waste Panel

	Upper Waste Panels E2: 0 - 1000 yr			Upper Waste Panels E2: 1000 - 10,000 yr			Upper Waste Panels E2: 0 - 10,000 yr			Upper Waste Panels E1: 1000 - 10,000 yr		
Step[a]	Variable[b]	SRRC[c]	R^{2d}	Variable	SRRC	R^2	Variable	SRRC	R^2	Variable	SRRC	R^2
1	*WMICDFLG*	0.86	0.76	*HALPOR*	0.58	0.35	*WMICDFLG*	0.54	0.30	*HALPOR*	0.51	0.27
2	*WGRCOR*	0.34	0.88	*BHPRM*	0.47	0.57	*HALPOR*	0.47	0.52	*BHPRM*	0.38	0.41
3	*WASTWICK*	0.23	0.93	*WGRCOR*	0.17	0.60	*BHPRM*	0.33	0.63	*WGRCOR*	0.23	0.47
4	*HALPOR*	0.11	0.94	*ANHPRM*	0.12	0.61	*WGRCOR*	0.30	0.72	*BPPRM*	–0.17	0.50
5	*WGRMICI*	0.04	0.94				*ANHPRM*	0.12	0.74	*WMICDFLG*	–0.18	0.53
6	*ANHBCUGP*	–0.03	0.94				*HALPRM*	0.08	0.74	*BPINTPRS*	0.12	0.54
7	*ANHPRM*	0.03	0.94				*WASTWICK*	0.07	0.75			

	Upper Waste Panels E1: 0 - 10,000 yr			Upper Waste Panels (E1: 0 - 10,000 yr) – (E2: 0 - 10,000 yr)			Lower Waste Panel E2: 0 - 1000 yr			Lower Waste Panel E2: 1000 - 10,000 yr		
Step	Variable	SRRC	R^2	Variable	SRRC	R^2	Variable	SRRC	R^2	Variable	SRRC	R^2
1	*WMICDFLG*	0.45	0.22	*BPCOMP*	0.31	0.09	*WMICDFLG*	0.84	0.73	*WGRCOR*	0.55	0.31
2	*HALPOR*	0.45	0.43	*WMICDFLG*	–0.30	0.17	*WGRCOR*	0.39	0.88	*BHPRM*	0.44	0.51
3	*WGRCOR*	0.35	0.55	*BHPRM*	–0.22	0.22	*WASTWICK*	0.21	0.93	*ANHPRM*	0.14	0.53
4	*BHPRM*	0.28	0.63	*HALPRM*	–0.17	0.25	*HALPOR*	0.09	0.93	*WASTWICK*	–0.12	0.54
5	*BPCOMP*	0.13	0.65	*WASTWICK*	–0.13	0.26	*ANHPRM*	0.07	0.94	*SHRGSSAT*	0.10	0.55
6	*BPINTPRS*	0.09	0.66	*BPINTPRS*	0.12	0.28	*WGRMICI*	0.03	0.94			

	Lower Waste Panel E2: 0 - 10,000 yr			Lower Waste Panel E1: 1000 - 10,000 yr			Lower Waste Panel E1: 0 - 10,000 yr			Lower Waste Panel (E1: 0 - 10,000 yr) – (E2: 0 - 10,000 yr)		
Step	Variable	SRRC	R^2	Variable	SRRC	R^2	Variable	SRRC	R^2	Variable	SRRC	R^2
1	*WGRCOR*	0.63	0.42	*WGRCOR*	0.58	0.34	*WGRCOR*	0.70	0.50	*BHPRM*	–0.43	0.19
2	*WMICDFLG*	0.38	0.56	*BHPRM*	0.28	0.42	*WMICDFLG*	0.39	0.66	*HALPOR*	–0.36	0.32
3	*BHPRM*	0.33	0.68	*WASTWICK*	–0.22	0.46	*BHPRM*	0.22	0.71	*ANHPRM*	–0.30	0.42
4	*ANHPRM*	0.15	0.70	*SHRGSSAT*	0.11	0.47	*ANHBCVGP*	–0.08	0.71	*BPINTPRS*	0.13	0.44
5	*HALPOR*	0.13	0.72				*BPPRM*	–0.07	0.72	*HALPRM*	–0.12	0.45
6	*SHRGSSAT*	0.08	0.72				*SHRGSSAT*	0.07	0.72	*WMICDFLG*	–0.11	0.46
										ANRGSSAT	0.10	0.47

[a] Steps in stepwise regression analysis.

[b] Variables listed in order of selection in regression analysis with *ANHCOMP* and *HALCOMP* excluded from entry into regression model.

[c] Standardized rank regression coefficients in final regression model.

[d] Cumulative R^2 value with entry of each variable into regression model.

Table 8. Stepwise Regression Analyses with Rank-Transformed Data for Pressure in Lower Waste Panel (*WAS_PRES*) for E1 and E2 Intrusions into Lower Waste Panel at 1000 yr

	E2: 1000 yr			E2: 10,000 yr			E1: 10,000 yr		
Step[a]	Variable[b]	SRRC[c]	R^{2d}	Variable	SRRC	R^2	Variable	SRRC	R^2
1	*WMICDFLG*	0.87	0.78	*HALPRM*	0.36	0.13	*HALPRM*	0.36	0.12
2	*WGRCOR*	0.33	0.89	*ANHPRM*	0.24	0.19	*BPCOMP*	0.22	0.17
3	*WASTWICK*	0.21	0.94	*HALPOR*	0.14	0.20	*ANHPRM*	0.18	0.20
4	*HALPOR*	0.08	0.94				*BPVOL*	0.17	0.23
5	*ANHPRM*	0.05	0.95				*HALPOR*	0.15	0.25
6	*WGRMICI*	0.04	0.95						

[a] Steps in stepwise regression analysis.

[b] Variables listed in order of selection in regression analysis with *ANHCOMP* and *HALCOMP* excluded from entry into regression model.

[c] Standardized rank regression coefficients in final regression model.

[d] Cumulative R^2 value with entry of each variable into regression model.

Table 9. Stepwise Regression Analyses with Rank-Transformed Data for Brine Saturations in Upper (*REP_SATB*) and Lower (*WAS_SATB*) Waste Panels at 10,000 yr for an E2 Intrusion at 1000 yr into Lower Waste Panel; similar results are obtained for an E1 intrusion (Table 8.5.1, Ref. 11)

	E2: Upper Waste Panel			E2: Lower Waste Panel		
Step[a]	Variable[b]	SRRC[c]	R^{2d}	Variable	SRRC	R^2
1	*BHPRM*	0.58	0.34	*BHPRM*	0.59	0.36
2	*WGRCOR*	–0.44	0.52	*WRGSSAT*	–0.40	0.52
3	*HALPOR*	0.35	0.64	*ANHPRM*	0.23	0.57
4	*ANHPRM*	0.20	0.68	*HALPOR*	0.13	0.59
5	*WASTWICK*	–0.15	0.70	*SHPRMHAL*	–0.12	0.60
6	*HALPRM*	0.14	0.72	*WGRCOR*	–0.10	0.61
7	*SHRGSSAT*	–0.08	0.73			

[a] Steps in stepwise regression analysis.

[b] Variables listed in order of selection in regression analysis with *ANHCOMP* and *HALCOMP* excluded from entry into regression model.

[c] Standardized rank regression coefficients in final regression model.

[d] Cumulative R^2 value with entry of each variable into regression model.

Table 10. Stepwise Regression Analyses with Rank-Transformed Data for Brine Volumes in Upper (*BRNVOL_R*) and Lower (*BRNVOL_W*) Waste Panels at 10,000 yr for E1 and E2 Intrusions at 1000 yr into Lower Waste Panel

	E2: Upper Waste Panel			E2: Lower Waste Panel			E1: Upper Waste Panel			E1: Lower Waste Panel		
Step[a]	Variable[b]	SRRC[c]	R^{2d}	Variable	SRRC	R^2	Variable	SRRC	R^2	Variable	SRRC	R^2
1	*BHPRM*	0.58	0.33	*ANHPRM*	0.38	0.15	*BHPRM*	0.52	0.27	*BPCOMP*	0.28	0.08
2	*WGRCOR*	–0.38	0.47	*BHPRM*	0.37	0.28	*WGRCOR*	–0.44	0.45	*HALPRM*	0.28	0.15
3	*HALPOR*	0.36	0.60	*HALPRM*	0.26	0.35	*HALPOR*	0.28	0.53	*ANHPRM*	0.23	0.20
4	*ANHPRM*	0.21	0.64	*HALPOR*	0.23	0.40	*BPCOMP*	0.28	0.60	*BHPRM*	0.21	0.25
5	*HALPRM*	0.17	0.67	*WGRCOR*	–0.13	0.42	*WMICDFLG*	–0.16	0.63	*HALPOR*	0.18	0.28
6	*WASTWICK*	–0.14	0.69	*WRGSSAT*	–0.11	0.43	*WASTWICK*	–0.14	0.65	*WRGSSAT*	–0.15	0.30
7	*WRBRNSAT*	–0.08	0.70	*WRBRNSAT*	–0.11	0.44	*BPVOL*	0.15	0.67	*BPVOL*	0.15	0.32
8							*ANHPRM*	0.13	0.69	*WMICDFLG*	–0.14	0.34
9							*SHRGSSAT*	–0.10	0.70	*BPINTPRS*	0.13	0.36
10							*HALPRM*	0.10	0.70	*WGRCOR*	–0.12	0.37

[a] Steps in stepwise regression analysis.

[b] Variables listed in order of selection in regression analysis with *ANHCOMP* and *HALCOMP* excluded from entry into regression model.

[c] Standardized rank regression coefficients in final regression model.

[d] Cumulative R^2 value with entry of each variable into regression model.

Table 11. Stepwise Regression Analyses with Rank-Transformed Data for Cumulative Gas (*GSMBHUDZ*) and Brine (*BNBHUDRZ*) Flow over 10,000 yr up Borehole at Top of DRZ for E1 and E2 Intrusions at 1000 yr into Lower Waste Panel

	E2: Gas Flow			E1: Gas Flow			E2: Brine Flow			E1: Brine Flow		
Step[a]	Variable[b]	SRRC[c]	R^{2d}	Variable	SRRC	R^2	Variable	SRRC	R^2	Variable	SRRC	R^2
1	*WMICDFLG*	0.53	0.29	*WMICDFLG*	0.46	0.22	*HALPRM*	–0.48	0.25	*BPCOMP*	0.48	0.21
2	*BHPRM*	0.44	0.49	*WGRCOR*	0.39	0.37	*WMICDFLG*	0.35	0.36	*WMICDFLG*	–0.42	0.38
3	*HALPOR*	0.35	0.62	*BHPRM*	0.37	0.52	*HALPOR*	0.25	0.42	*BHPRM*	0.36	0.51
4	*WGRCOR*	0.33	0.73	*HALPOR*	0.31	0.61	*ANHBCVGP*	0.22	0.46	*BPINTPRS*	0.18	0.54
5	*ANHPRM*	0.11	0.74	*BPPRM*	–0.11	0.62	*BHPRM*	0.13	0.48	*WGRCOR*	–0.19	0.58
6	*SHRGSSAT*	0.08	0.75	*HALPRM*	–0.10	0.63	*WGRCOR*	–0.13	0.50	*HALPRM*	–0.12	0.59
7										*WASTWICK*	–0.12	0.60
8										*ANHBCVGP*	0.11	0.61
9										*HALPOR*	0.10	0.62

[a] Steps in stepwise regression analysis.

[b] Variables listed in order of selection in regression analysis with *ANHCOMP* and *HALCOMP* excluded from entry into regression model.

[c] Standardized rank regression coefficients in final regression model.

[d] Cumulative R^2 value with entry of each variable into regression model.

Table 12. Stepwise Regression Analyses with Rank-Transformed Data for Pressure (*B_P_PRES*) and Brine Volume (*BRNVOL_B*) Associated with a Pressurized Brine Pocket at 10,000 yr for an E1 Intrusion at 1000 yr into Lower Waste Panel

	Pressure			Volume		
Step[a]	Variable[b]	SRRC[c]	R^{2d}	Variable	SRRC	R^2
1	*BPCOMP*	0.43	0.20	*BPVOL*	0.92	0.82
2	*WMICDFLG*	0.31	0.30	*BPCOMP*	−0.29	0.90
3	*BHPRM*	−0.27	0.37	*WMICDFLG*	0.11	0.91
4	*BPVOL*	0.24	0.42	*BHPRM*	−0.07	0.92
5	*HALPRM*	0.15	0.44	*BPINTPRS*	−0.06	0.92
6				*WASTWICK*	0.05	0.92
7				*ANHPRM*	0.04	0.93

[a] Steps in stepwise regression analysis.

[b] Variables listed in order of selection in regression analysis with *ANHCOMP* and *HALCOMP* excluded from entry into regression model.

[c] Standardized rank regression coefficients in final regression model.

[d] Cumulative R^2 value with entry of each variable into regression model.

Table 13. Permeabilities Used with BRAGFLO Calculations for E2E1 Intrusions with the E2 Intrusion Occurring at 800 yr and the E1 Intrusion Occurring at 2000 yr

800 - 1000 yr: Concrete plugs assumed to be emplaced at the Santa Rosa Fm (i.e., a surface plug with a length of 15.76 m; corresponds to Cells 905, 937 in Fig. 3, Ref. 2) and the Unnamed Mbr of the Rustler Fm (i.e., a plug at top of Salado Fm with a length of 36 m; corresponds to Cell 681 in Fig. 3, Ref. 2). Concrete plugs assumed to have a permeability of $k = 5 \times 10^{-17}$ m^2; remainder of borehole (i.e., to bottom of DRZ) assumed to have a permeability of 1×10^{-9} m^2.

1000 - 2000 yr: Concrete plugs are assumed to fail after 200 yr (Ref. 13) and entire borehole is assigned a permeability typical of silty sand, i.e., $k = 10^x$ m^2, $x = BHPRM$, where *BHPRM* is an uncertain input to the analysis (see Table 1, Ref. 4).

2000 - 2200 yr: Permeability above repository left at $k = 10^x$, $x = BHPRM$, and corresponds to permeability in borehole associated with original E2 intrusion. Permeability below repository set to 1×10^{-9} m^2 and corresponds to permeability in borehole associated with E1 intrusion at 2000 yr. Concrete plugs emplaced at the Santa Rosa Fm and the Unnamed Mbr of the Rustler Fm are assumed to prevent flow above the repository in the borehole associated with the E1 intrusion.

2200 - 3200 yr: Permeability above repository set to $k = 2 \bullet 10^x$, $x = BHPRM$, to incorporate effects of both boreholes after failure of concrete plugs at 2200 yr in borehole associated with E1 intrusion. Permeability below repository set to $k = 10^x$, $x = BHPRM$, to incorporate effects of E1 intrusion.

> 3200 yr: Permeability reduced by one order of magnitude in Salado Fm beneath repository due to creep closure of borehole (Ref. 14) (i.e., $k = 10^x/10$, $x = BHPRM$, in Cells 1010, 985, 12, 45, 78 of Fig. 3, Ref. 2). No changes are made within and above the lower DRZ.